STRUCTURE AND FUNCTION OF THE *HELICOBACTER PYLORI* VACA P33 DOMAIN

By

Christian González-Rivera

Dissertation

Submitted to the Faculty of

the Graduate School of Vanderbilt University

in partial fulfillment of the requirements

for the degree of

DOCTOR OF PHILOSOPHY

in

Microbiology and Immunology

May, 2013

Nashville, Tennessee

Professor Timothy L. Cover

Professor Eric P. Skaar

Professor Borden D. Lacy

Professor Eric Sebzda

Professor Mark Denison

Professor Richard Peek

To my wife Bernice, my sons Leandro and Armando, my grandparents Santos y Rosalia, my mom Rosa, and my dad Guillermo

ACKNOWLEDGMENTS

My journey through the graduate school has been like climbing up a steep muddy mountain. One of the biggest challenges of climbing a steep muddy mountain is that the path is slippery, and it is very easy to fall down. Fortunately, you can depend on trees and branches along the way, to pull yourself up. Everyone that has contributed to the completion of my Ph.D. has been like one of those trees.

One tree that has always had his branches extended to help me, has been my thesis advisor Dr. Timothy L. Cover. I feel very fortunate to have been part of Dr. Cover's laboratory and I am very thankful for all of his support during the past several years. Not only has he been a great scientific mentor, but he has also been a great counselor, teacher, and friend. Thank you Tim for everything you have done!

I would also like to thank the current and former members of the Cover lab. It has been a great pleasure working with them, and thanks to their support my journey has been enjoyable. Everyone in Dr. Cover's lab has been very special to me, but I would like to give a special thanks to Dr. Mark McClain, Dr. Holly Algood, and Dr. Jana Radin for directly working with me at the bench and taking the time to teach me laboratory techniques. I appreciate what you have taught me!

The collaborative environment in which I have been trained has been one of my greatest experiences at Vanderbilt University. I have had the chance to work with many talented scientists, and more importantly, learn from them. I would like to thank Dr. Borden Lacy for helping throughout my whole training and for becoming a great mentor to me. When my structural project was dragging me down the slippery mountain, Dr.

Lacy would extend her hand, and like the branches of the trees, pull me up. I would like to thank the members of the Lacy lab for sharing their equipment, reagents, and providing advice; especially, Dr. Kelly Gangwer for helping me with structural studies of the VacA toxin, and for making Chapter II possible. Thanks to Dr. Benjamin Spiller and Dr. Melanie Ohi for assistance in structural studies; Melissa Chamber and Tasia Pyburn in Dr. Ohi's lab for assistance in electron microscopy; and Dr. Spyros Kalams for assistance with T cells. I would also like to thank my thesis committee (Dr. Eric P. Skaar, Dr. Borden Lacy, Dr. Eric Sbezda, Dr. Mark Denison and Dr. Richard Peek) for all their support and advice. For me it has been an honor to have such great scientists and such great persons in my thesis committee.

My journey through the mountain would not have been possible without the Initiative for Maximizing Student Diversity Program. This great program recruited me to Vanderbilt University, believed in me, and supported me during the early stages of my career. Thanks to the directors Dr Roger Chalkley and Dr. Linda Sealy, and the staff Dr. Bharati Mehrotra and Ms. Cathleen Williams.

The work presented in my thesis was financially supported by the National Institute of Health (R01 AI039657) and by the Molecular Microbial Pathogenesis Training Grant (Meharry Medical Center).

Finally I would like to thank the people that supported me before, during, and after climbing the mountain. I especially would like to thank my beautiful wife Bernice for supporting me since we met in High School. "Mi pupuchungi, thank you for your love, sacrifice, and support"! I would also like to thank my two sons Leandro and Armando for becoming my distraction when the journey started to wear me down.

“Leandro and Armando, I love you guys very much and I also thank you for your love and sacrifice”!

Everything that I used to survive my journey through the mountain was given to me by two special individuals in my life, my grandparents Santos and Rosalia. “Mama y Papa todo lo que tengo a ustedes se lo debo!” To accomplish my journey through the mountain, I was also given very special tools by my mom Rosa and my dad Guillermo. “Mami y Papi, Gracias por su apoyo!” I would also like to thank my sister (Charlotte) for becoming my best friend. Thanks to my sister Mileisha, my brother Owen, my stepmom Mily, and my stepdad Mario for their support.

I would like to thank my undergraduate mentor, Dr. Jose M. Planas for showing me that there was a mountain waiting for me to climb, and for supporting me during my journey. I will always remember the day Dr. Planas called me to his office, and showed me the path. Thank you for believing in me, and for believing I could become a scientist! Finally, I would like to thank Dr. Gregory Buck for telling me that perseverance would make me succeed.

TABLE OF CONTENTS

LIST OF TABLES

Table

LIST OF FIGURES

LIST OF ABBREVIATIONS

H. pylori	*Helicobacter pylori*
cagPAI	Cag pathogenicity island
VacA	Vacuolating cytotoxin A
m-region	Middle region
i-region	Intermediate region
d-region	Deletion region
kDa	Kilodaltons
BAM	β-barrel assembly machine
E. coli	*Escherichia coli*
ss	Signal sequence
WT	Wild type
TOM	Translocase of the outer membrane of mitochondria
RPTP	Receptor-like tyrosine phosphatase
EGF	Epidermal growth factor
GPI	Glycosylphosphatidylinositol
LRP1	Low-density lipoprotein receptor-related protein-1
ATF2	Transcription factor 2
Git1	G -protein coupled receptor kinase interactor
CD2AP	CD2-associated molecule protein
Drp1	Dynamin-related protein 1
NFAT	Nuclear factor of activated T cells
IL-2	Interleukin-2
Lab	Laboratory
6X His	Hexahistidine
TB-KAN	Terrific broth supplemented with kanamycin

A_{600}	Absorbance at 600 nm
IPTG	Isopropyl β-D-thiogalactopyranoside
h	Hours
min	Minutes
s	Seconds
FBS	Fetal bovine serum
PMA	Phorbol 12-myristate 13-acetate
EMS	Copper mesh grids
DDM	*n*-dodecyl β-D-maltoside
SDS-PAGE	Sodium dodecyl sulfate polyacrylamide gel electrophoresis
mrc	Mixed raster content
ELISA	Enzyme-linked immunosorbent assay
PCR	Polymerase chain reaction
cat	Chloramphenicol acetyltransferase
PBS	Phosphate-buffered saline
SDS	Sodium dodecyl sulfate
BSA	Bovine serum albumin
MOI	Multiplicity of infection
MFI	Mean fluorescence intensity
BB-cholesterol	Brucella broth supplemented with 1X cholesterol
MBP	Maltose binding protein

CHAPTER 1

INTRODUCTION

Helicobacter pylori: History

For many years, the human stomach was considered an inhospitable environment for bacterial growth. In the 1980's, Robin Warren and Barry Marshall challenged this dogma by cultivating the Gram-negative bacterium known as *Helicobacter pylori* (*H. pylori*) from gastric biopsies (*1*). This discovery led to a Nobel Prize in Medicine in 2005. Currently, *H. pylori* is considered the dominant microbiota of the human stomach, and it is estimated that it persistently colonizes about 50% of the population worldwide (*2-3*).

Infection is usually acquired in early childhood, and it has been hypothesized that transmission occurs via fecal-oral and oral-oral routes (*4-5*). Most *H. pylori*-infected individuals remain asymptomatic. However, about 5% of infected persons develop peptic ulcer disease, <1% develop gastric adenocarcinoma and about 0.1% develop gastric lymphoma (*6-9*), making *H. pylori* the most common etiologic agent of infection-related cancers and the only known bacterial carcinogen (type 1 carcinogen) (*10*). Further, gastric cancer remains the second leading cause of cancer-related deaths worldwide (*11*). For the past few decades, antibiotics have been used to treat *H. pylori*-infected patients, but the bacterium is becoming resistant to several antibiotics (*12-15*).

H. pylori: Microbiological characteristics

H. pylori is a spiral-shaped, microaerophilic bacterium that contains polar flagella. Once the bacterium colonizes the stomach, it mainly localizes to the gastric mucus layer, but some bacteria adhere to gastric epithelial cells (*16*). The helical shape and the presence of flagella help the organism move within the viscous environment of the stomach (*17-19*). Interestingly, it has been shown that *H. pylori* swims faster than rod-shaped bacteria in low viscosity media, and maintains this velocity in high viscosity media (*19-21*). To survive the harsh environment of the stomach, *H. pylori* metabolizes urea to ammonia using a protein known as urease (*22-23*). This reaction generates a neutral environment around the organism, and protects it from gastric acid (*24*).

H. pylori virulence factors

Why certain individuals develop *H. pylori*-related disease and others remain unaffected remains an important unanswered question. The high level of genetic variability in *H. pylori* strains has hindered the identification of specific bacterial factors that link *H. pylori* to disease outcome. The genome sequences of several strains have been analyzed, and these studies have shown that there is extensive variation in *H. pylori* gene content (presence/absence of complete genes and pseudo-genes), and extensive variation in nucleotide sequences (92%-99% nucleotide identity in conserved genes) (*25-30*). Nevertheless, various virulence factors that link *H. pylori* to disease have been identified. These include several outer membrane proteins, the *cag* pathogenicity island (*cag* PAI), and vacuolating cytotoxin A (VacA).

Several H. *pylori* outer membrane proteins function as adhesins that mediate the attachment of the bacterium to gastric epithelial cells, resulting in cellular alterations and allowing the delivery of bacterial effector proteins into the host cell (*31*). Two outer membrane proteins considered adhesins and categorized as virulence factors are (A) BabA, which binds to Lewis b antigen and related terminal fucose residues found on antigens of gastric epithelial cells (*32-34*), and (B) SabA, which binds to sialylated carbohydrates on the surface of cells (*31*). Binding of these proteins to the surface of cells has been associated with the induction of proinflammatory responses (*31*).

Another important virulence factor is the *cag* PAI. This 40 kb segment of DNA encodes multiple proteins that assemble into a type IV secretion system which includes a needle-like pilus structure (*35-36*). Pilus formation is cell contact dependent, and several Cag proteins are reportedly capable of binding to the β1-integrin receptor on host cells (*36-40*). Once a molecular bridge forms between the cell and the bacterium, the effector protein known as CagA is translocated and delivered into the eukaryotic cell (*41-42*). CagA is then phosphorylated (*43-44*) and interacts with multiple host proteins, including tyrosine phosphatase SHP-2 (*45-46*). Non-phosphorylated CagA can also interact with multiple cellular targets, including E-cadherin and Par1b/MAPK2 (*46-48*). The crystal structure of CagA was recently solved and suggests that flexibility within the 3 domains of CagA, plus the highly disordered C-terminus, is responsible for the complex array of interactions that have been reported (*49*). Overall, CagA is considered one of the most *H. pylori* important virulence factors and the only known bacterial oncoprotein.

Another very important *H. pylori* virulence factor is the VacA toxin. My thesis will focus on studies of the VacA toxin, and thus a detailed description of the toxin will

be given in the following sections. An interesting feature of *H. pylori* virulence factors is that individual strains commonly express CagA, BabA and specific VacA types (known as s1/i1/m1), whereas other strains fail to express any of these factors. *H. pylori* strains that express CagA, BabA, and have VacA (type s1/i1/m1) are associated with increased inflammation, increased cellular alterations, and an increased risk of disease in comparison to strains that lack these factors, or that have another VacA type (s2/i2/m2) (*2*).

VacA

VacA was first described in 1988, when Leunk et al added broth culture supernatants from *H. pylori* broth cultures to eukaryotic cells (*50*). Surprisingly, they observed that the cells became vacuolated , and proposed that a secreted bacterial factor was responsible for the vacuolation phenotype (*50*). VacA was later purified, characterized, and proven to be responsible for the vacuolation of cells (*51*).

The *vacA* gene is present in almost every *H. pylori* strain, but not all strains express a functional protein. Furthermore, *vacA* alleles of *H. pylori* strains from unrelated humans exhibit a high level of genetic diversity and several *vacA* types have been recognized based on sequence diversity (*52-54*). Most studies have focused on diversity at the 5' end of *vacA* in a region known as the s-region, or within the middle region (m-region) (Figure 1) (*52*). Two main families of s-region and m-region sequences have been recognized (designated types s1 and s2, m1 and m2) (*52-54*). *H. pylori* strains containing type s1 or m1 *vacA* alleles are associated with a higher incidence of gastric disease (peptic ulcereration and gastric adenocarcinoma) than are strains containing type

s2 or m2 *vacA* alleles (*52*, *55*). A third polymorphic region, known as the intermediate region (i-region), was recently identified (*56*). Similar to the s- and m-regions, two families of i-region sequences have been recognized, and these are designated type i1 and i2 (*56*). Within the i-region, there are three main clusters of sequence diversity, known as polymorphic clusters A, B, and C (*56*). Importantly, *H. pylori* strains containing i1 *vacA* alleles have been associated with a higher incidence of gastric disease (peptic ulcereration and gastric adenocarcinoma), in comparison to *H. pylori* strains containing i2 *vacA* alleles (*56-64*). Multiple combinations of type 1 and 2 *vacA* alleles have been observed (i.e. s1/i1/m2), but several alleles are relatively common (i.e. s2/i2/m2 or s1/i1/m1) (*56*, *58*). Another polymorphic region is the deletion region (d-region) (*65*). Strains containing a 69 to 81 base pair deletion between the i-region and m-region are considered d2, while strains containing no deletion in this region are considered d1 (*65*). A previous study showed that *vacA* d1 alleles were associated with neutrophil infiltration and gastric mucosal atrophy in Western *H. pylori* strains, while *vacA* d2 alleles were not associated with any alterations (*65*). Although the relationship between *vacA* alleles and *H. pylori* disease outcome has been well established, the mechanism by which the VacA protein contributes to disease is not clear.

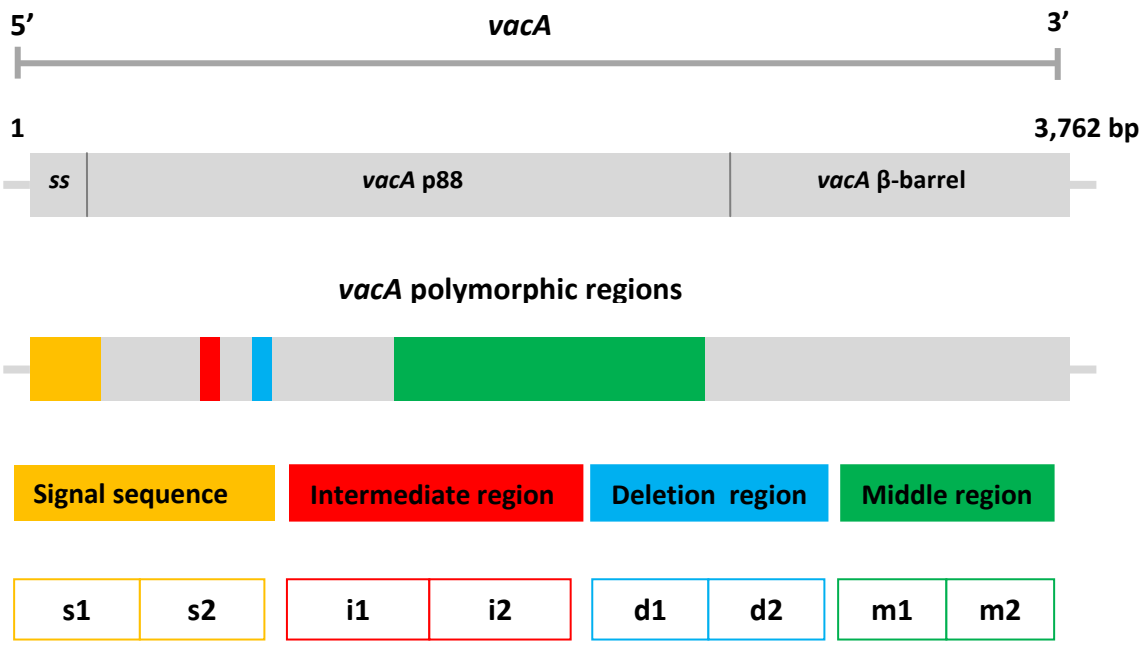

FIGURE 1: Regions of sequence diversity in *vacA*. Four major regions of sequence diversity (polymorphic regions) have been identified in the *vacA* gene. The figure illustrates the s-region, i-region, d-region and m-region, and the approximate locations of these regions within the *vacA* gene. All of these regions have been characterized as type 1 (s1, i1, d1 and m1) or type 2 (s2, i2, d2, and m2), and type 1 alleles are associated with a higher risk of *H. pylori* related disease.

VacA expression and secretion

VacA gene expression occurs via a DNA-dependent RNA polymerase (*66*). This holoenzyme recognizes a TAAAAA sequence at the -10 position and a non-conserved region at the -35 region, prior to transcription (*66*). Expression of *vacA* can be upregulated by low iron conditions in a fur-independent manner (*67-69*). After proper transcription and translation, a 140 kilodaltons (kDa) pro-toxin containing a signal peptide, passenger domain (p88), and β-barrel domain is produced (Figure 2A) (*70-72*). VacA is then secreted through a type V or autotransporter pathway as a soluble 88 kDa protein (p88) (*51*). A proportion of the toxin remains attached to the bacterial cell surface, and the remainder is released into the extracellular space (*73-74*). As a first step in the autotransporter pathway, the signal peptide is recognized by the Sec machinery in the inner membrane of the bacterium (*75-76*). This leads to the cleavage of the signal peptide, and the translocation of the p88 (passenger domain) and β-barrel domain into the periplasm (*75-76*). As a consequence, the VacA β-barrel is able to insert and form a pore in the outer membrane (*77*). Based on functional studies of pertactin (produced by *Bordetella pertussis*), it has been hypothesized that the p88 (passenger domain) is then pulled from C to N terminus in an energy-independent manner (*72, 78*). Once the toxin is exposed to the extracellular space, further cleavage events occur in the region between p88 and the β-barrel domain (*79*). This final step allows the secretion of p88 (*77, 79-80*). It is still not clear whether this final cleavage event occurs through an autoproteolytic process or through the action of a specific protease. Interestingly, in several other bacterial species, the insertion of the β-barrel domain of autotransporters requires a β-

barrel assembly machine (BAM) complex (*76, 81-85*). *H pylori* contains homologs to BAM proteins, but the functions of these proteins have not been studied in *H. pylori*.

The VacA β-barrel domain has also been studied in an *Escherichia coli* (*E. coli)* autotransporter secretion system (*86*). Specifically, Marin et al. tested whether an *E. coli* passenger domain could be translocated if its β-barrel was replaced with the VacA β-barrel. The results showed that the VacA β-barrel, in place of the *E.coli* β-barrel, was not capable of secreting *E. coli* passenger domain (*86*). On the other hand, another study by Fischer et al tested whether the passenger domain of VacA (p88) could be replaced with the B subunit of cholera toxin in *H. pylori* (*77*). The authors showed that cholera toxin was efficiently translocated, and became surface exposed, when the VacA passenger domain was replaced with cholera toxin (*77*).

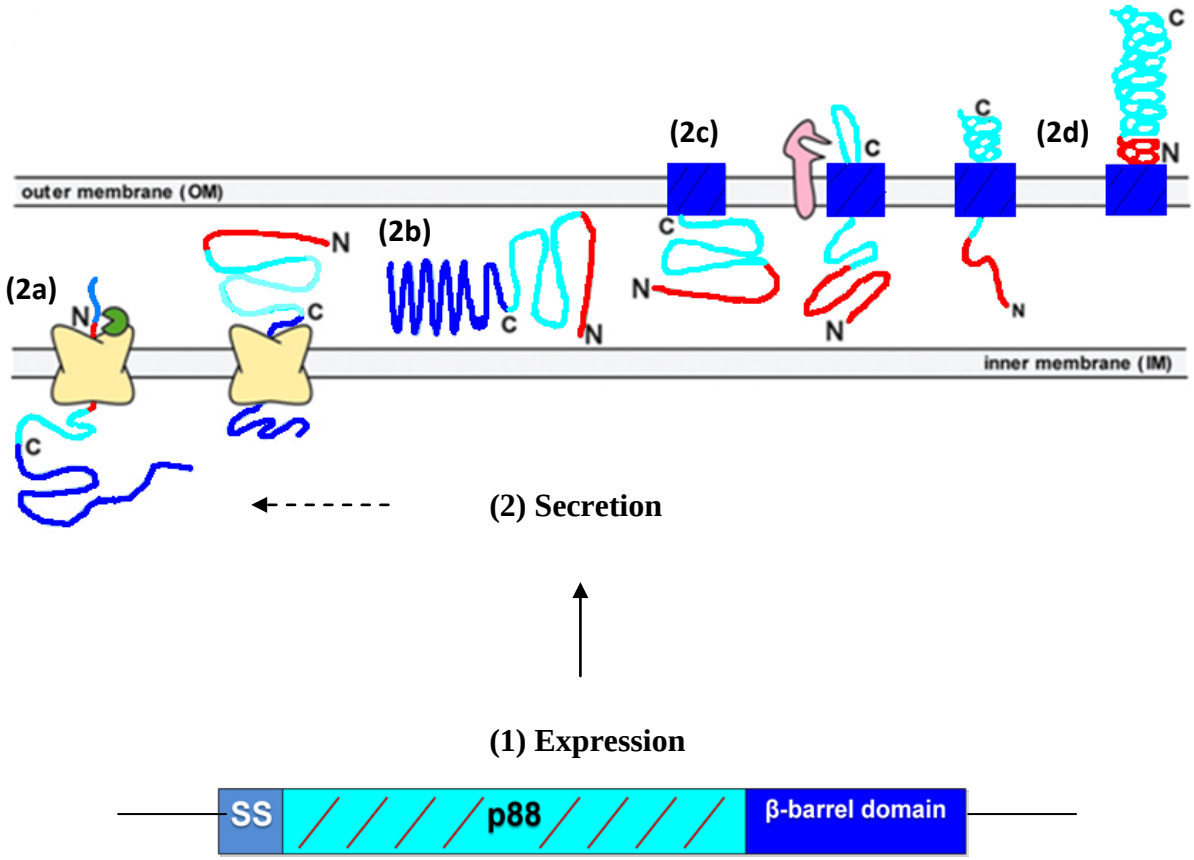

FIGURE 2: VacA expression and secretion. (1) VacA is expressed as a pro-toxin that consists of a signal sequence (SS), p88 (passenger domain), and β-barrel domain. (2) VacA is secreted through an autotransporter pathway. (2a) The signal sequence is recognized by the Sec machinery and then (2b) VacA is translocated to the periplasm. (2c) Once in the periplasm the β-barrel forms a pore in the outer membrane and (2d) VacA is translocated into the extracellular space. This figure was modified from (*78*).

VacA p33 domain

Partial proteolytic digestion *in vitro* of the 88 kDa secreted toxin yields two fragments, designated p33 and p55, which probably represent two domains of VacA (Figure 3) (*71, 87-88*). Cleavage of the p88 protein into these two fragments occurs at a site that is predicted to be a surface-exposed flexible loop (*71, 88*). The p33 domain contains part of the s-region and d-region, and the complete i-region. At the protein level, functional differences between d1 and d2 proteins have not been reported (*65*). In contrast, type s1 VacA proteins cause numerous cellular alterations *in vitro*, whereas type s2 VacA proteins lack detectable activity in most *in vitro* assays (*52, 89-91*). A 12-amino-acid amino-terminal extension has been shown to be responsible for most of the differences in activities of the s1 and s2 proteins (*91*). Although multiple studies reported that particular variants of the *vacA* i-region are markers of disease outcome, thus far there have been very few studies comparing the activities of type i1 and type i2 VacA proteins (*56*). One study reported that type i1 VacA proteins caused vacuolation of HeLa and RK13 cells (derived from human cervix and rabbit kidney, respectively), whereas type i2 VacA proteins caused vacuolation of RK13 cells but not HeLa cells (*56*). Therefore, it was concluded that the i-region is a determinant of VacA cell-type specificity (*56*). Taken together, these studies suggest that regions of sequence diversity within the p33 domain are important for functional activity of VacA.

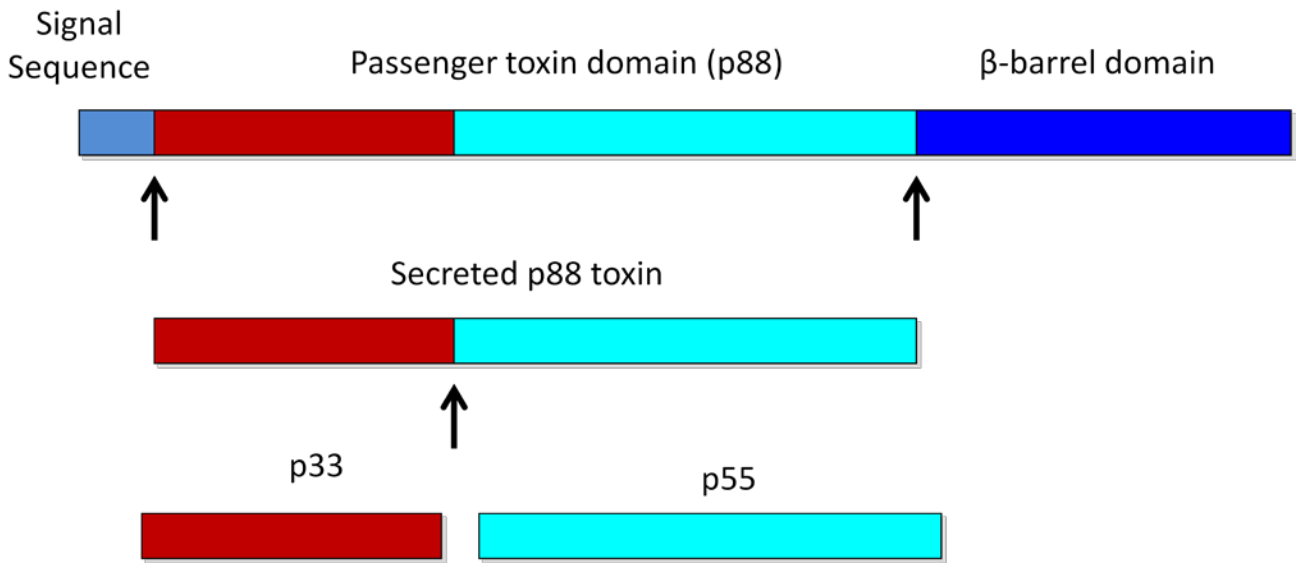

FIGURE 3: VacA domains. VacA secretion produces a p88 toxin. Proteolytic digestion of the secreted toxin yields two domains designated as p33 and p55. The arrows indicate proteolytic events that occur during VacA secretion or subsequent to secretion. This figure was modified from (*73*).

VacA p33 domain

The secreted toxin is considered a pore-forming toxin and can cause multiple cellular alterations. The identification of amino acids in the p33 domain that are important for VacA-dependent cellular effects has been an active area of VacA research. It has been determined that the p33 domain contains an amino terminal portion that is important for membrane channel formation (*92-94*). Specifically, a well characterized mutant (VacA Δ6-27) lacks three hydrophobic GXXXG motifs, lacks toxin activity and membrane channel activity, and exhibits a dominant negative phenotype when mixed with wild-type (WT) VacA (*92*). Similarly, it has been shown that amino acids located outside the amino-terminal hydrophobic region (G121 and S246 in the VacA sequence of *H. pylori* strain 60190) are important for vacuolating activity (*95*). The importance of the p33 domain in cell vacuolation has also been demonstrated by a study that expressed an approximately 422 residue VacA protein (corresponding to the p33 domain and the amino-terminal portion of the p55 domain) intracellularly in HeLa cells, and showed that this portion was sufficient to cause cell vacuolation (*96*).

Intracellular expression of p33 has been reported to result in localization of p33 to mitochondria (*97*). Additional studies of p33 domain-mitochondria interactions identified a stretch of 32 hydrophobic amino acids that seems to be a novel type of mitochondria-targeting sequence capable of interacting with the translocase of the outer membrane of mitochondria (TOM) complex (*98*). At the structural level, it has been predicted that a large portion of p33 comprises a β-helical fold (*99*); however, a detailed structure of the p33 domain has not been determined.

VacA p55 domain

The p55 domain contains the m-region, which as described previously is a region of sequence diversity. At the protein level, this region consists of approximately 280 amino acids (from approximately D455 to V735 in the VacA sequence of *H. pylori* strain 60190). Functional studies have shown that m1 and m2 VacA proteins have different cell-type specificity (*100-101*). Similar to the i-region, m1 proteins affect a wider range of cells as compared to m2 VacA proteins (*100-103*). Furthermore, it has been proposed that cell specificity is due to differences in binding to specific receptors (*102-103*). In support of this hypothesis, a phylogenetic analysis of the p55 domain showed that there is strong divergence and positive selection in the p55 domain (*54*). The crystal structure of the p55 m1 was determined, and consists predominantly of a right handed β-helical structure (Figure 4) (*99*). The β-helical structure is characteristic of passenger domains secreted by the autotransporter pathway (*75-76*).

To analyze structural differences between type m1 and m2 VacA proteins, the p55 m2 protein structure has been modeled based on comparison to the m1 crystal structure, but a detailed structure of the p55 m2 protein has not been determined (*99*). Through this analysis, various differences between the m1 and m2 structures were identified (*99*). It was also proposed that both the p55 m1 and m2 proteins contain an autochaperone domain at the C-terminal position (*99*). Interestingly, in other autotransporters it has been shown that the β-cap serves as an autochaperone important for translocation and secretion of the passenger domain (*99, 104-105*). A detailed mutagenesis study of the β-helical loops in the p55 m1 protein, showed that several coiled loops can be deleted without any adverse effects on toxin secretion or activity (*106*). Further structural and functional

studies of the p55 m2 protein will be required to allow a thorough understanding of type m2 VacA proteins.

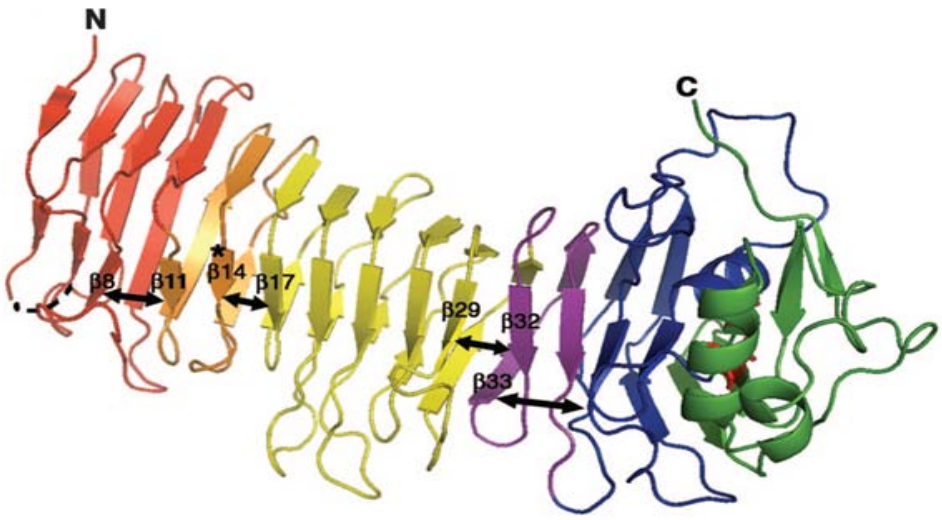

FIGURE 4: Crystal structure of the p55 domain. Structural analysis of the p55 domain shows that this domain has a β-helical structure, which is a characteristic of several other autotransporters. This figure was reprinted from (*99*).

VacA oligomerization

The 88 kDa VacA monomers secreted by *H. pylori* can assemble into large water-soluble oligomeric complexes (Figure 5) (*107-109*). These flower-shaped structures can be either single-layer (containing 6-9 subunits) or bilayer (containing 12-14 subunits) (*107-109*). Similar oligomeric structures have been visualized on the surface of VacA-treated cells or lipid bilayers (*109-111*). A current model proposes that VacA monomers interact with the plasma membrane and subsequently oligomerize, which allows the formation of VacA pores in cell membranes (*73, 112*). Amino acid sequences within both the p33 domain (residues 49-57) and the p55 domain (residues 346 and 347) are required for assembly of VacA into these oligomeric structures, and mutant proteins lacking these sequences fail to cause cell vacuolation (*113-114*). Furthermore, certain non-oligomerizing VacA mutant proteins (Δ49-57 and Δ346-347) have dominant negative inhibitory effects on the ability of WT VacA to cause cellular alterations, which supports the hypothesis that oligomeric structures are required for VacA effects on host cells (*113-115*). Water-soluble VacA oligomeric complexes lack cytotoxic activity unless they are first dissociated into monomeric components by exposure to low-pH or high-pH conditions (*107, 116*), and therefore, it is presumed that VacA monomeric components interact with host cells and subsequently reassemble into membrane channels. Although the structure of water-soluble VacA oligomeric complexes has been investigated in detail, the conditions that promote oligomerization of VacA are not well-understood.

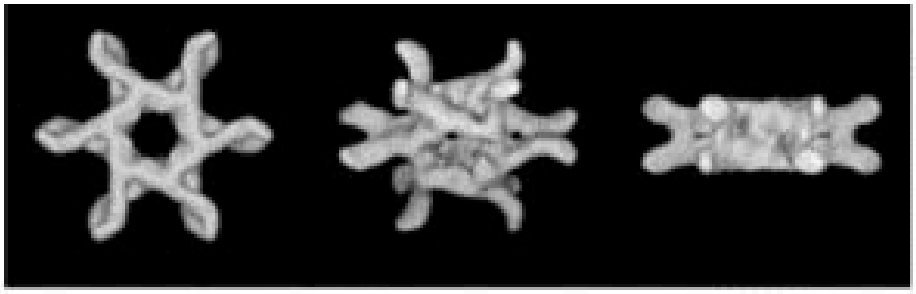

FIGURE 5: VacA oligomerization. Secreted p88 VacA can form "flower shaped" oligomeric structures. These structures are thought to mimic a pore forming state of the toxin (*108*).

VacA effects on gastric cells

VacA causes many cellular alterations and has been categorized as a multifunctional protein (*73*). In general, the toxin is considered a pore-forming toxin (*73, 117-118*), although it has also been proposed that VacA is a novel kind of AB-type toxin (*119-120*). In either case, a current model for VacA intoxication of gastric epithelial cells proposes that as a first step, the toxin binds to a host receptor. Thus far, multiple receptors have been identified and include sphingomyelin (*121-122*), receptor-like tyrosine phosphatases (RPTP-α and RPTP-β) (*123-124*), epidermal growth factor (EGF) receptor (*125*), fibronectin, heparin sulfate (*126*), glycosylphosphatidylinositol (GPI)-anchored proteins (*127-129*) and low-density lipoprotein receptor-related protein-1 (LRP1) (*130*). VacA can also associate with lipid rafts (*131-132*). Upon binding to the host cell, VacA can then (1) activate cell signaling pathways, (2) act as a pore forming toxin in the plasma membrane, and/or (3) be internalized and cause vacuolation, mitochondrial alterations, and/or cell death (*73, 117-120*).

Cell signaling occurs soon after the toxin encounters the cell, and it has been reported that VacA can activate mitogen-activated protein kinases p38, ERK1/2, and transcription factor 2 (ATF 2) in gastric epithelial cells (*133-134*). The G-protein coupled receptor kinase interactor (Git1) signaling pathway is also altered by VacA (*135*).

VacA can also act as a pore-forming toxin by causing the reduction of transepithelial electric resistance of monolayers in polarized epithelial cells (*136*). This can lead to the release of molecules such as Fe^{3+}, Ni^{2+}, sugars, and amino acids, which

affects the homeostasis of the cell (*136-139*). In addition, VacA alters nutrient acquisition in the cell by inducing apical mis-localization of transferrin receptors (*140*).

Finally, it has been shown that VacA can be internalized into the host cytoplasm through endocytosis (*128*). This process is actin-dependent, temperature-dependent, energy-dependent, and is clathrin-independent (*128-129, 131-132, 141-143*). Once in the cytoplasm, VacA first accumulates in early endosomes (*144*), and the toxin then traffics to late endosomes (*145-146*). It has been shown that GTPases like Rac1 and Cdc42, as well as the adaptor molecule CD2-associated molecule protein (CD2AP) are important for VacA internalization (*144-145, 147*). A current model proposes that once VacA is in the endosome, the toxin acts as a chloride channel (*118*). Specifically, it has been suggested that the influx of chloride ions into the endosome causes the activation of V-type ATPase (*148-149*). As a consequence, ammonium ions and other weak bases accumulate, and osmotic swelling (vacuolation) occurs (*146, 150*). The membranes of vacuoles contain late endocytic markers (Rab 7, LAMP1, and Pgp110) (*146, 151-152*). The role of vacuolation *in vivo* is not clear.

Intracellular trafficking of VacA can also lead to the localization of the toxin to the mitochondria (*73, 117-120*). It has been suggested that this occurs via juxtapositioning of endosomes with mitochondria (*153*). Once in contact with the mitochondria, the toxin causes reduction of mitochondrial transmembrane potential (*97-98, 154-155*), cytochrome c release (*97-98, 154-155*), reduction of cellular ATP and cell cycle progression (*156-157*), PARP cleavage (*157*), and mitochondrial fragmentation (*158*). The host proapoptotic factors BAX and BAK, as well as dynamin-related protein 1 (Drp1), are important for VacA effects on the mitochondria (*153, 159-160*). VacA-

induced mitochondrial alterations can lead to cell death. Thus far it has been reported that VacA can cause both apoptosis and programmed cell necrosis in epithelial gastric cells (*73, 117-120, 157, 161-164*). VacA also is reported to cause autophagy in gastric epithelial cells (*130, 165-167*). Although this pathway has not been studied in detail, it has been proposed that it could serve as a mechanism for the regulation of toxin-mediated damage in cells. It is important to mention that VacA effects on gastric cells have mainly been studied in vitro. Therefore, in future experiments it will be necessary to determine which of these pathways are relevant in vivo.

VacA toxin effects on immune cells

VacA also has effects on cells of the immune system and has been classified as an immunomodulatory toxin (*168-170*). In macrophages, it has been reported that VacA can disrupt phagosome maturation (*171*). On the other hand, VacA selectively inhibits the invariant chain (Ii)-dependent pathway of antigen presentation (*172*). In mast cells, VacA is capable of binding to the surface of the cell, inducing the production of cytokines, and inducing cell migration (*173*). More in depth studies have been done in T cells (*169, 174-175*). Based on these studies, a model for VacA effects on T cells proposes that VacA interacts with β2-integrin on the surface of human T cells (*174*) and is then internalized through a clathrin-independent pathway (*176*). In addition to binding to β2-integrin, it has been proposed that VacA also binds to another cellular factor that has not yet been identified (*174, 176*). Once inside T cells, VacA inhibits the activation and nuclear translocation of nuclear factor of activated T cells (NFAT) by preventing the action of calcineurin (*169, 176*). As a consequence, VacA inhibits the expression and secretion of interleukin- 2 (IL-2) (Figure 6) (*169, 174*). Effects of VacA on IL-2 production have been

studied most extensively in Jurkat cells (*169, 174-175*). Interestingly, mouse T cells are VacA resistant (*175*). In addition to its effects on IL-2 production by Jurkat cells, VacA inhibits the activation-induced proliferation of primary human T cells and B cells (*170, 174, 176-177*). It has been shown that some of these effects can be NFAT independent (*170, 175*). Further studies will be required to establish the specific mechanism by which VacA intoxicates immune cells.

VacA–related cellular alterations have mainly been studied in vitro, and the number of studies using animal models to study VacA has been very limited. In vivo studies reported that *H. pylori vacA*-null mutant strains are capable of colonizing the stomach of mice, gerbils and gnotobiotic piglets, which suggests that *vacA* is not required for colonization of the stomach (*178-182*). On the other hand, it was also reported that *vacA*-producing strains outcompeted *vacA*-null strains in mouse stomach colonization studies, suggesting that *vacA* provides an advantage for colonization (*181*). Furthermore it has been reported that primary murine T cells are resistant to VacA (*175*). Further animal model experimental studies will be required to better understand the role of VacA in vivo.

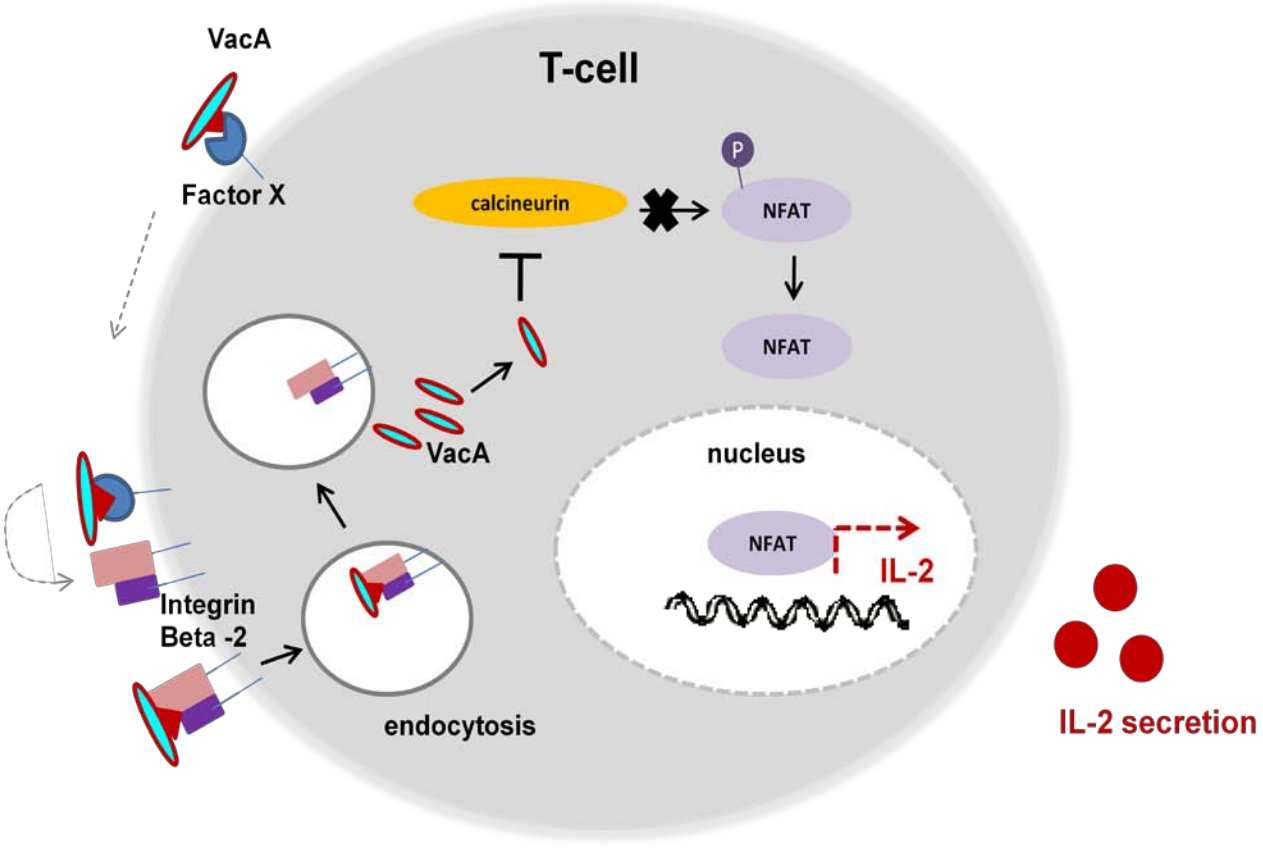

FIGURE 6: Model for VacA effects on T-cells. VacA initially binds to an uncharacterized receptor/co-receptor (factor X). This initial interaction may facilitate the binding to β2 receptor. VacA is then internalized via a clathrin-independent pathway, and once inside the cell VacA can alter the action of calcineurin. Therefore, NFAT cannot be dephosphorylated and enter the nucleus. As a consequence, IL-2 production and T-cell proliferation is disrupted. This figure was modified from (*174*).

Research objectives

Over the past decade, functional studies of the VacA toxin have demonstrated the importance of the p33 domain in toxin activity. The p33 domain is thought to be the pore-forming domain of VacA, can target mitochondria in host cells, contains various polymorphic regions that have clinical importance, and contains amino acids required for oligomerization (*73, 117-120*). The importance of the p33 domain has been well established; however, virtually nothing is known about the structural properties of this domain. Based on in silico studies, two contrasting models for the p33 domain have been proposed. The first model proposes that the p33 domain contains a β-helical structure similar to the p55 domain at the C-terminus, and a α-helical pore-forming domain (*93, 99*). In contrast, the second model proposes that the p33 domain adopts a β-barrel structure (*98*). A structural model for the p33 domain could provide important new insights into the mechanism of action of the toxin (*183-185*). Therefore, my overall research goal was to structurally and functionally analyze the p33 domain.

When I started my studies of the VacA toxin, the crystal structure of the p55 domain had been recently determined by Kelly Gangwer in Borden Lacy's laboratory (lab) (*99*). I started collaborating with Borden Lacy's lab, and as a first step we undertook studies aimed to express and purify a recombinant form of the p33 domain. In chapter 2, I will present data showing our successful purification of an active form of the p33 domain. Our experimental data showed that mixing p33 and p55 reconstituted the VacA toxin. These studies highlight the functional importance of the p33 domain, and provide a basis for structural studies of the p33 domain.

Epidemiological studies of *vacA* polymorphic regions have demonstrated that the VacA toxin can be used as a marker for *H. pylori*-disease outcome. Functional studies related to these regions have mainly focused on the s- and m-region (*52, 89-91, 100-103*). The i-region was recently described, and is present within the p33 domain (*56*). Based on previous clinical studies, the i-region was classified as either type 1 (i1) or type 2 (i2), and it was shown that strains containing i1 *vacA* alleles were associated with a higher incidence of *H. pylori* disease as compared to strains containing i2 *vacA* alleles (*56-62*). At the protein level, there has been relatively little effort to analyze possible differences in the activity of type i1 and i2 VacA proteins. To further analyze the p33 domain, I performed functional studies of the p33 i-region. In chapter 3 I will describe studies of the p33 i-region which show that i1 VacA proteins are more potent than i2 proteins in a Jurkat T cell model. This study highlights the importance of the p33 domain in T cell activity.

Structural characterization requires the efficient expression, purification, and crystallization of a protein. In chapters 2 and 3 I was able to express and purify recombinant forms of the p33 domain. As a next step in trying to structurally characterize the p33 domain, I performed crystallization studies. In chapter 4 I will summarize various approaches that I employed for these studies, and describe a current method that has led to VacA crystals. Collectively, structure and function studies of the p33 domain will (A) help elucidate mechanisms of action of VacA, and (B) help us understand the role of VacA in disease.

CHAPTER 2

EXPRESSION, PURIFICATION, AND REFOLDING OF RECOMBINANT VACA P33 DOMAIN

Introduction

H. pylori VacA is a pore-forming toxin that causes multiple alterations in human cells and contributes to the pathogenesis of peptic ulcer disease and gastric cancer. The toxin is secreted by *H. pylori* as an 88 kDa monomer (p88) consisting of two domains (p33 and p55). While an X-ray crystal structure for p55 exists and p88 oligomers have been visualized by cryo-electron microscopy, a detailed analysis of p33 has been hindered by an inability to purify this domain in an active form. In this chapter I describe the development of methods that allow the efficient purification of the p33 domain. Furthermore, through structural and functional studies, we show how p33 and p55 mixtures are able to reconstitute VacA toxin activity. These studies highlight the importance of the p33 domain in toxin activity and oligomerization, and provide a basis for structural studies of the p33 domain.

Materials and Methods

Purification of p88 VacA from the *H. pylori* broth culture supernatant

H. pylori strain 60190 (expressing WT VacA) and a strain expressing a VacAΔ6−27 mutant protein were grown in broth culture, and VacA proteins were

purified in an oligomeric form from the culture supernatant as described previously (*92, 107*). These preparations of purified VacA oligomers were acid-activated prior to use in cell culture experiments (*107, 116*).

Plasmids for expression of p33 and p55 VacA fragments

Plasmids encoding the p33 and p55 domains of VacA from *H. pylori* strain 60190 (a type s1/m1 form of VacA; GenBank accession number Q48245), as well as a c-Myc-tagged p33 protein and a p33Δ6-27 mutant protein, have been described previously (*70, 87, 99, 115*). The p33 proteins contain a C-terminal hexahistidine (6X His) tag, and the p55 protein contains an N-terminal 6X His tag.

Expression and purification of recombinant VacA proteins

VacA p55 was purified as described previously (*99*). VacA p33 was expressed in *E. coli* BL21(DE3) by culturing in Terrific broth (Fisher) supplemented with 25μg/mL kanamycin (TB-KAN) at 37°C overnight with shaking. A c-Myc-tagged form of p33 (*87*) was expressed in the same manner. Cultures were diluted 1:100 in TB-KAN and grown at 37°C until they reached an absorbance (A_{600}) of 0.6. Cultures were induced with a final isopropyl β-D-thiogalactopyranoside (IPTG) concentration of 0.5 mM and incubated at 37°C for 2 hours (h). VacA p33 proteins were purified from inclusion bodies. Briefly, IPTG-induced cultures were pelleted, washed in 0.9% NaCl, and resuspended (10 mL/L of culture) in sonication buffer [10mM Tris (pH 7.5), 100 mM NaCl, 1 mM EDTA, protease inhibitor (Roche), and 20000 units/mL lysozyme (Ready-lyse, Epicenter)]. The cells were incubated at room temperature for 15 minutes (min) with shaking and sonicated with six 20 watt bursts (45 seconds [s] per burst with 15 s cooling periods). Lysed bacterial cells were centrifuged to pellet the inclusion bodies.

The insoluble inclusion body pellet was resuspended in buffer containing 100 mM NaH_2PO_4, 10 mM Tris, and 8 M urea (pH 8.0) at 5 mL/g of wet weight and incubated for 1 h at room temperature. The samples were centrifuged, and the resulting supernatant was added to Ni-NTA beads (Novagen) at a ratio of 4 mL of supernatant/mL of beads. The protein/bead mixture was incubated for 1 h at room temperature before being loaded into a column. The column was washed with 10 column volumes of 100 mM NaH_2PO_4, 10 mM Tris, 10 mM imidazole, and 8 M urea (pH 6.3), followed by 100 mM NaH_2PO_4, 10 mM Tris, and 8 M urea (pH 5.9). The p33 protein was eluted from the column with 100 mM NaH_2PO_4, 10 mM Tris, and 8 M urea (pH 4.5). Successful expression and purification of p33 were confirmed by mass spectrometry (data not shown).

Refolding of VacA p33

The denatured VacA p33 protein was refolded via dialysis of the protein against a buffer containing 55 mM Tris, 21 mM NaCl, 0.88 mM KCl, 1.1 M guanidine, and 880 mM arginine (pH 8.2) for 24 h. The protein then was dialyzed in two other buffers, each for 24 h. The first reduced the guanidine concentration to 800 mM and the arginine concentration to 500 mM, and the second reduced the arginine concentration to 250 mM and maintained a guanidine concentration of 800 mM (*186*). Further reductions in the arginine or guanidine concentrations resulted in precipitation of p33 VacA.

Cell culture assays

HeLa cells were grown in minimal essential medium (modified Eagle's medium containing Earle's salts) supplemented with 10% fetal bovine serum (FBS) in a 5% CO_2 atmosphere at 37°C. Jurkat lymphocytes (clone E6-1) (ATCC TIB-152) were grown

in RPMI 1640 medium containing 2 mM l-glutamine, 1.5 g/L sodium bicarbonate, 4.5 g/L glucose, 10 mM HEPES, and 1.0 mM sodium pyruvate supplemented with 10% FBS.

For vacuolating assays, HeLa cells were seeded at a density of 1.2×10^4 cells/well into 96-well plates 24 h prior to the addition of VacA proteins. The recombinant p33 and p55 proteins (each at 1 mg/mL) were premixed in a 1:1 mass ratio, which corresponds to an ~1.7:1 molar ratio. The use of excess p33 on a molar basis compensated for the possibility that refolding of denatured p33 might be less than 100% efficient. Preparations of purified p33, p55, or the p33/p55 mixture were then added to the tissue culture medium overlying HeLa cells (supplemented with 10 mM ammonium chloride) and incubated overnight at 37°C. VacA-induced cell vacuolation was detected by inverted light microscopy and quantified by a neutral red uptake assay, a well-established method that is based on rapid uptake of neutral red into VacA-induced cell vacuoles (*51*, *187*). For dominant negative assays, we tested the ability of the refolded p33Δ6 protein or the purified *H. pylori* p88 Δ6–27 protein to inhibit the activity of WT VacA (*92*, *115*). To analyze VacA effects on T cells, we analyzed the capacity of VacA to inhibit IL-2 secretion by Jurkat T cells (*169*). Jurkat cells were plated at a density of 1×10^5 cells/well, and recombinant p33 and p55 were added to cells either individually or as a p33/p55 mixture (1:1 mass ratio) for 30 min at 37°C. After incubation, 0.05 μg/mL phorbol 12-myristate 13-acetate (PMA) and 0.5 μg/mL ionomycin were added for 24 h at 37°C. The cells were then centrifuged at 2000 rpm for 7 min, and the supernatants were tested for IL-2 by an enzyme-linked immunosorbent assay (ELISA), according to the manufacturer's protocol (R&D Systems Human IL-2 Immunoassay) (*175*).

Interactions of p33 and p55 with HeLa cells

Purified p55 was labeled with Alexa 488 (Molecular Probes) according to the manufacturer's instructions. HeLa cells were incubated with Alexa 488-labeled p55 alone (10 μg/mL) or a mixture of labeled p55 with purified refolded p33 (each at 5 μg/mL) at 37°C. Alternatively, cells were incubated with purified Alexa 488-labeled p55 with a c-Myc-tagged p33 protein (*87*) that was purified and refolded using the same methodology described above for p33. Cells were fixed with 4% formaldehyde. The c-Myc-tagged p33 protein was detected by indirect immunofluorescence using an anti-c-Myc antibody and an Alexa fluor-555-conjugated secondary antibody. Cells were viewed with an LSM 510 inverted confocal microscope (Carl Zeiss).

Size exclusion chromatography

Gel filtration was performed using either Superdex 200 10/300 GL high-resolution resin or Superdex 200 10/300 prep grade resin, equilibrated in 55 mM Tris (pH 8.0), 21 mM NaCl, 0.88 mM KCl, 800 mM guanidine, and arginine (either 800 or 250 mM). Protein samples were first injected onto the gel filtration column individually at a final concentration of 0.75 mg/mL for the p33 protein and 0.4 mg/mL for the p55 protein. To analyze p33/p55 mixtures, the appropriate sizing column fractions corresponding to either p33 or p55 were each concentrated to 1 mg/mL. VacA p33 was added to p55 in a 2:1 volume ratio, the mixture incubated for 45 min at 4°C, and the p33/p55 mixture then applied to a gel filtration column. Retention volumes of bovine thyroglobulin, alcohol dehydrogenase, bovine serum albumin, and carbonic anhydrase were used as standards to calculate the molecular masses of the purified VacA proteins.

Electron microscopy

To visualize the morphology of p33/p55 mixtures, appropriate gel filtration fractions containing these proteins were analyzed by electron microscopy using conventional negative staining as described previously (*188*). Protein solutions were diluted to appropriate final concentrations (25–100 μg/ mL), and 2.5 μL aliquots were spotted onto glow-discharged copper-mesh grids (EMS) for approximately 1 min. In some experiments, p33/p55 mixtures were mixed in a 9:1 (v/v) ratio with Brucella broth (*189*) or *n*-dodecyl β-D-maltoside (DDM, Anatrace) prior to electron microscopy analysis. The final concentration of DDM was 0.34 mM, which corresponds to twice the critical micelle concentration. The grids were washed in 5 drops of water followed by 1 drop of 0.7% uranyl formate. Grids were then incubated on 1 drop of 0.7% uranyl formate for 1 min, blotted against filter paper, and allowed to air-dry. Initial images of WT p88 or the p33/p55 mixture mixed with Brucella broth were collected on an FEI morgagni run at 100 kV at a magnification of 36000X. Images were recorded on an ATM 1Kx1K CCD camera. Images of p88 used for multireference alignment were collected on a FEI 120 kV electron microscope at a magnification of 67000X. Images were recorded on DITABIS (Pforzheim, Germany) digital imaging plates. The plates were scanned on a DITABIS micrometer scanner, converted to mixed raster content (mrc) format, and binned by a factor of 2, yielding final images with 4.48 Å/pixel. Images of the p33/p55 mixture in DDM purified by gel filtration were taken on a 200 kV FEI electron microscope equipped with a field emission electron source and operated at an acceleration voltage of 120 kV and magnification of 100000X. Images were collected using a Gatan 4Kx4K CCD camera. CCD images were converted to mrc format and

binned by a factor of 4, resulting in final images with 4.26 Å/pixel. Images of both p88 and the p33/p55 mixture were taken under low-dose conditions using a defocus value of −1.5 μm.

For alignment and averaging of p88 VacA and p33/p55 VacA in DDM, 9871 and 1273 images of p88 and p33/p55 VacA particles, respectively, were selected with Boxer and windowed with a 120 pixel side length (*190*). Image analysis was conducted with SPIDER and the associated display program WEB (*191*). The images were rotationally and translationally aligned and subjected to 10 cycles of multireference alignment and K-means classification. For analysis of p88 VacA, alignment particles were first classified into 20 class averages (data not shown) and seven representative classes then were chosen as references for another cycle of multireference alignment. For analysis of p33/p55 VacA, particles were first classified into 10 class averages (data not shown) and then four representative projections were chosen as references for another cycle of multireference alignment.

Results

Expression, purification, and refolding of recombinant p33 VacA

In previous studies, it has not been possible to purify a functionally active form of the p33 domain (*87*). We attempted to purify the p33 VacA fragment from *E. coli* extracts under native conditions but were unsuccessful. Therefore, we expressed and purified the recombinant p33 under denaturing conditions and then used dialysis to reduce the concentration of denaturants and allow the protein to refold. After the p33 protein was refolded, it eluted as a well-defined peak by size exclusion chromatography (Figure 7).

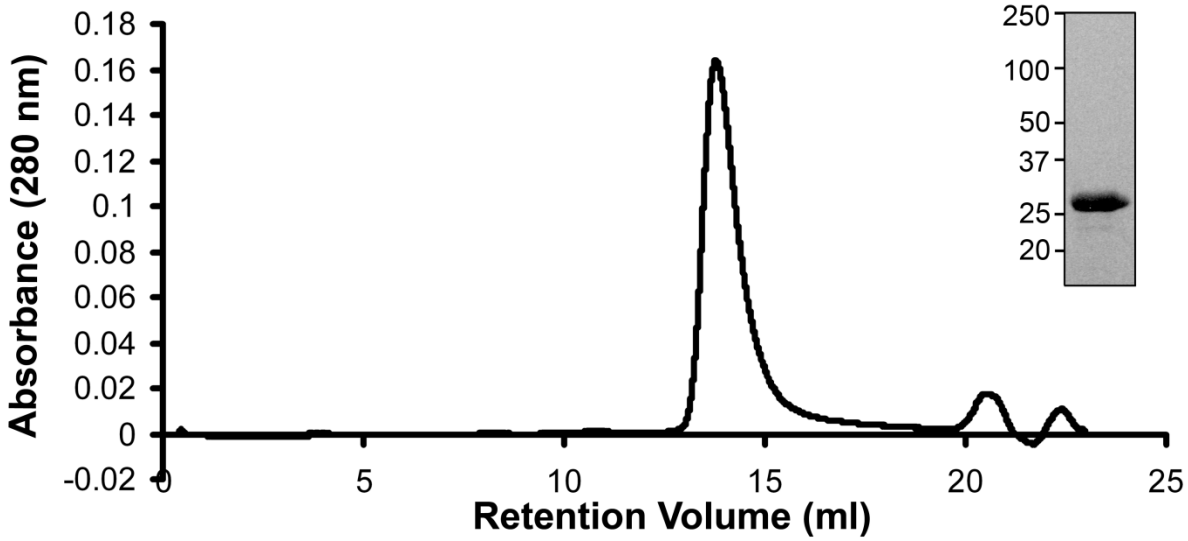

FIGURE 7: Purification of recombinant p33 VacA. Sodium dodecyl sulfate polyacrylamide gel electrophoresis (SDS-PAGE) and Coomassie blue stain of p33 VacA purified under denaturing conditions (inset). Gel filtration chromatography (Superdex 200 10/300 GL high-resolution resin) of p33 VacA after protein refolding, using buffer containing 800 mM guanidine and 800 mM arginine, as described in Experimental Procedures.

Refolded p33 mixed with purified p55 causes cellular alterations

To test the activity of the purified p33 and p55 proteins, we added these proteins individually and in combination to HeLa cells and analyzed the capacity of the proteins to cause cell vacuolation, a hallmark of VacA activity. No detectable vacuolating activity was observed when the p33 or p55 protein was added to cells individually, as demonstrated by the neutral red uptake assay and light microscopic examination of the cells (Figure 8A and data not shown). Similarly, none of the buffers alone or in combination exhibited any detectable activity (data not shown). In contrast, a mixture of the purified p33 and p55 proteins caused extensive vacuolation of HeLa cells (Figure 8A and 8B). The potency of the p33/p55 mixture was slightly lower than that of the p88 VacA protein purified from *H. pylori* broth culture supernatant (Figure 8B). A mixture of p55 and heat-denatured p33 failed to cause any detectable effects on cells (data not shown).

Previous studies have shown that VacA from *H. pylori* inhibits production of IL-2 by Jurkat cells (*169*). To test whether p33 and p55 proteins exhibit a similar activity, we incubated Jurkat cells with the purified p33 and p55 proteins individually and in combination. When added individually, neither p33 nor p55 had any effect on IL-2 secretion (Figure 8C). In contrast, the p33/p55 mixture inhibited IL-2 secretion from Jurkat cells (Figure 8C and 8D). The potency of the p33/p55 mixture was slightly lower than that of the p88 VacA protein purified from *H. pylori* (Figure 8D). Collectively, these results indicate that the refolded p33 protein, when mixed with the p55 protein, is biologically active and capable of causing alterations in eukaryotic cells.

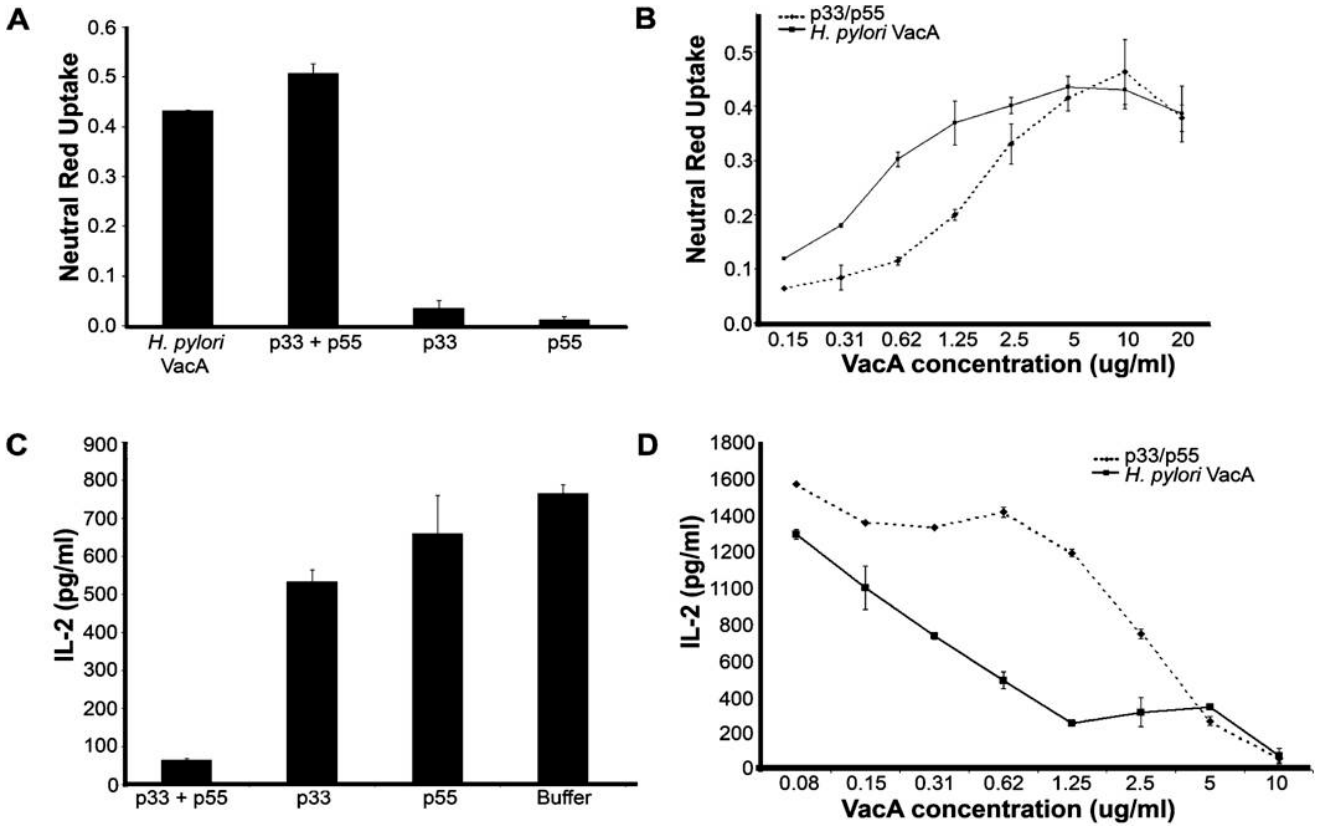

FIGURE 8: Effects of p33 and p55 VacA proteins on HeLa cells and Jurkat cells. Purified refolded p33 and purified p55 (each at 1 mg/mL) were mixed together in a 1:1 mass ratio, which ensured an excess of p33 on a molar basis. The p88 VacA protein purified from the *H. pylori* culture supernatant was acid-activated prior to contact with cells (*107, 116*), whereas the p33 and p55 preparations were not acid-activated. (A) HeLa cells were incubated with the purified VacA proteins at a final concentration of 10 μg/mL (or 5 μg/mL for each protein in the case of the p33/p55 mixture). Cell vacuolation was quantified by the neutral red uptake assay (OD_{540}). (B) HeLa cells were incubated with the indicated final concentrations of a p33/p55 mixture (20 μg/mL corresponds to 10 μg/mL p33 and 10 μg/mL p55) or the p88 form of VacA purified from the *H. pylori* broth culture supernatant. Cell vacuolation was quantified by the neutral red uptake assay. (C) Jurkat cells were incubated with the indicated purified VacA proteins at a concentration of 6 μg/mL (or 3 μg/mLfor each protein in the case of the p33/p55 mixture) for 30 min at 37˚C. The cells were then stimulated, and IL-2 secretion was measured as described in Experimental Procedures. (D) Jurkat cells were incubated with the indicated final concentrations of a p33/p55 mixture or the p88 form of VacA purified from the *H. pylori* culture supernatant. The cells were then stimulated, and IL-2 secretion was measured as described in Experimental Procedures. Results represent the mean (standard deviation, based on analysis of triplicate samples.

Refolded p33Δ6−27 exhibits a dominant negative effect

When certain mutant VacA proteins (e.g., VacAΔ6-27) are mixed with WT VacA, the mutant proteins can act as dominant negative inhibitors of WT VacA activity (*91-92*, *113-115*). To further validate the new methods for expression and refolding of p33 proteins, we expressed, purified, and refolded the p33Δ6-27 protein under the same conditions used for purification and refolding of the p33 WT protein. When added to cells individually or in combination with purified p55, the p33Δ6-27 protein did not cause detectable cell vacuolation (Figure 9A). To test for dominant negative properties of the mutant protein, we premixed the p33Δ6-27 protein with p33/p55 mixtures that were known to be active (Figure 9A). When this p33/p55/ p33Δ6-27 mixture was added to cells, no detectable vacuolation was observed, indicating that the mutant protein exhibited a dominant negative effect (Figure 9A). The purified refolded p33Δ6-27 protein, when mixed with purified p55, exhibited dominant negative inhibitory properties similar to those of the p88Δ6-27 protein purified from the *H. pylori* broth culture supernatant (Figure 9B) (*92*, *115*).

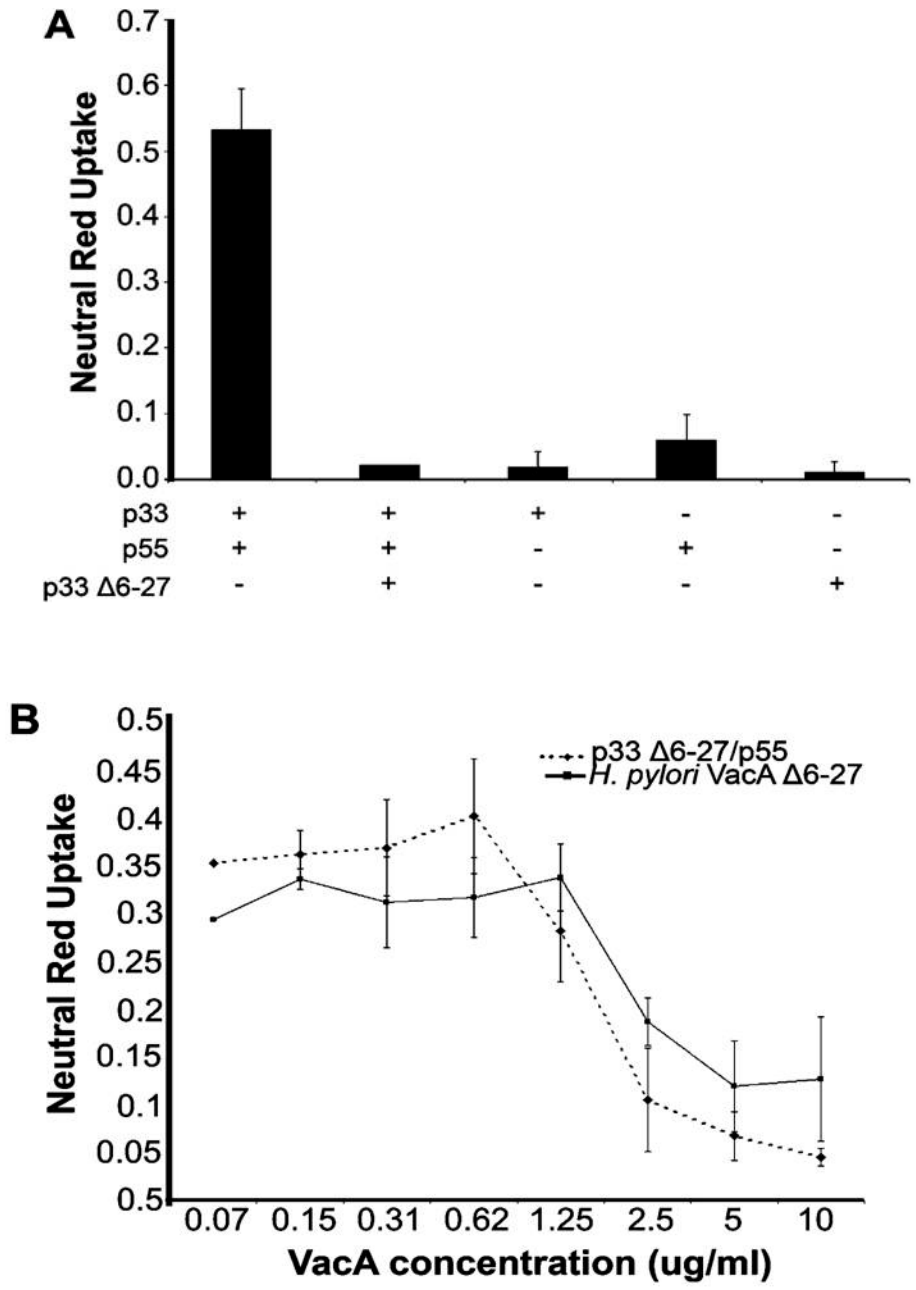

FIGURE 9: Refolded p33Δ6-27 exhibits dominant negative properties. (A) VacA p33Δ6-27 was purified and refolded as described in Experimental Procedures. Purified p33Δ6-27 was mixed with p55 and p33 (each at 1 mg/mL) at a 1:1:1 mass ratio. HeLa cells were then incubated with the indicated recombinant VacA proteins (either individually or in a mixture) at a final concentration of 10 μg/mL for 9 h at 37 C. Cell vacuolation was quantified by then neutral red uptake assay. (B) WT p88 VacA (5 μg/mL) was incubated with the indicated concentrations of the VacA p33Δ6-27/p55 mixture or the p88Δ6-27 VacA protein purified from the *H. pylori* culture supernatant. Cell vacuolation was quantified by the neutral red uptake assay. Results represent the mean standard deviation, based on analysis of triplicate samples.

Interactions of p33 and p55 with HeLa cells

Several previous studies have shown that sequences within the p55 domain contribute to the binding of p88 VacA to cells, and it has been suggested that p55 functions as a cell binding domain (*101, 192-193*). To investigate the cell binding properties of p55 in further detail, we incubated HeLa cells with purified fluorescently labeled p55. Very little if any interaction of purified p55 with HeLa cells was observed (Figure 10A). In contrast, when p55 was incubated with HeLa cells in the presence of purified refolded p33, a marked increase in the level of binding and uptake of p55 by cells was observed (Figure 10A). Thus, p33 markedly enhanced the cell binding properties of p55. Further studies indicated that when a mixture of p33 and p55 was incubated with cells, both p33 and p55 bound to the cell surface (Figure 10B). These properties of purified p33 and p55 proteins are consistent with previously observed properties of p33 and p55 proteins contained in crude *E. coli* extracts (*87*).

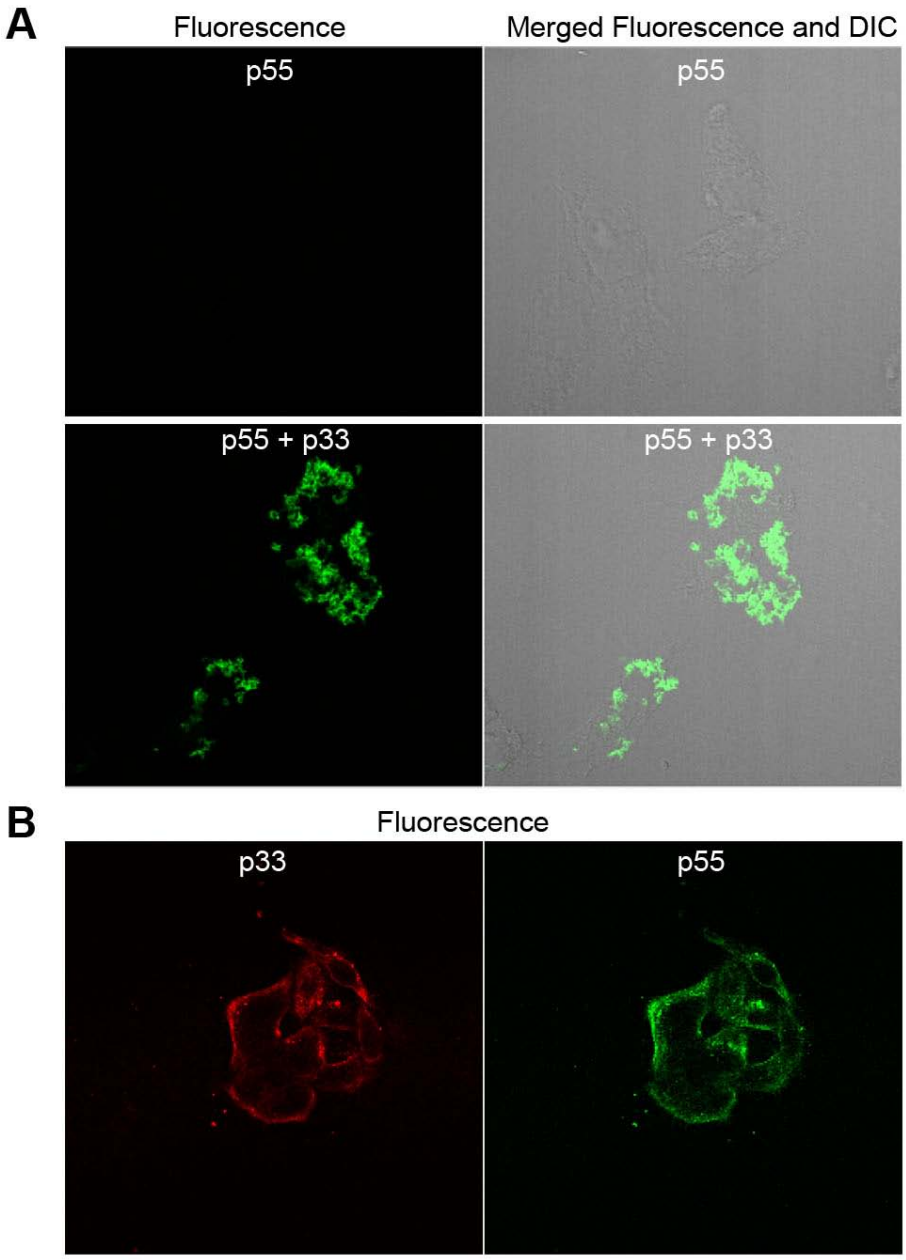

FIGURE 10: Interaction of p55 and p33 proteins with HeLa cells. (A) HeLa cells were incubated with Alexa 488-labeled p55 alone (10 μg/mL) or a mixture of labeled p55 and purified refolded p33 (5 μg/mL each) for 4 h at 37° C. Cells were imaged as described in Experimental Procedures. (B) Cells were incubated with purified Alexa 488-labeled p55 and purified refolded c-Myc-tagged p33 protein for 1 h at 37° C. The c-Myc tagged p33 protein was detected by indirect immunofluorescence.

Interaction of refolded p33 with purified p55

To investigate potential interactions among the purified p33 and p55 proteins, we performed size exclusion chromatography experiments. When the refolded WT p33 protein was analyzed, a peak with a predicted mass of ~96 kDa was observed (Figure 11, red peak with an asterisk). When the purified p55 protein was analyzed, a peak with a molecular mass of 178 kDa was observed (Figure 11, green peak with an asterisk). When the p33/p55 mixture was analyzed, a peak with a predicted mass of 86 kDa was observed (Figure 11, blue peak with an asterisk), the 96 kDa peak (corresponding to p33 alone) was lost, and the 178 kDa peak (corresponding to p55 alone) was minimized. Representative fractions were tested by SDS-PAGE and Coomassie blue staining; this revealed an approximate 33 kDa band for the VacA 96 kDa peak, a 55 kDa band for the 178 kDa peak, and two protein bands of 33 and 55 kDa for the 86 kDa peak (Figure 11B). When tested in cell culture assays, the p33/p55 mixture corresponding to the blue peak in Figure 11 caused cell vacuolation with a potency similar to that shown in Figure 8B (data not shown). Taken together, these results suggest that the refolded p33 protein interacts with the purified p55 protein to yield a p33/p55 complex. Moreover, these data suggest that p33 homo-oligomers and p55 homo-oligomers must undergo disassembly to interact with each other and form 88 kDa p33/p55 complexes.

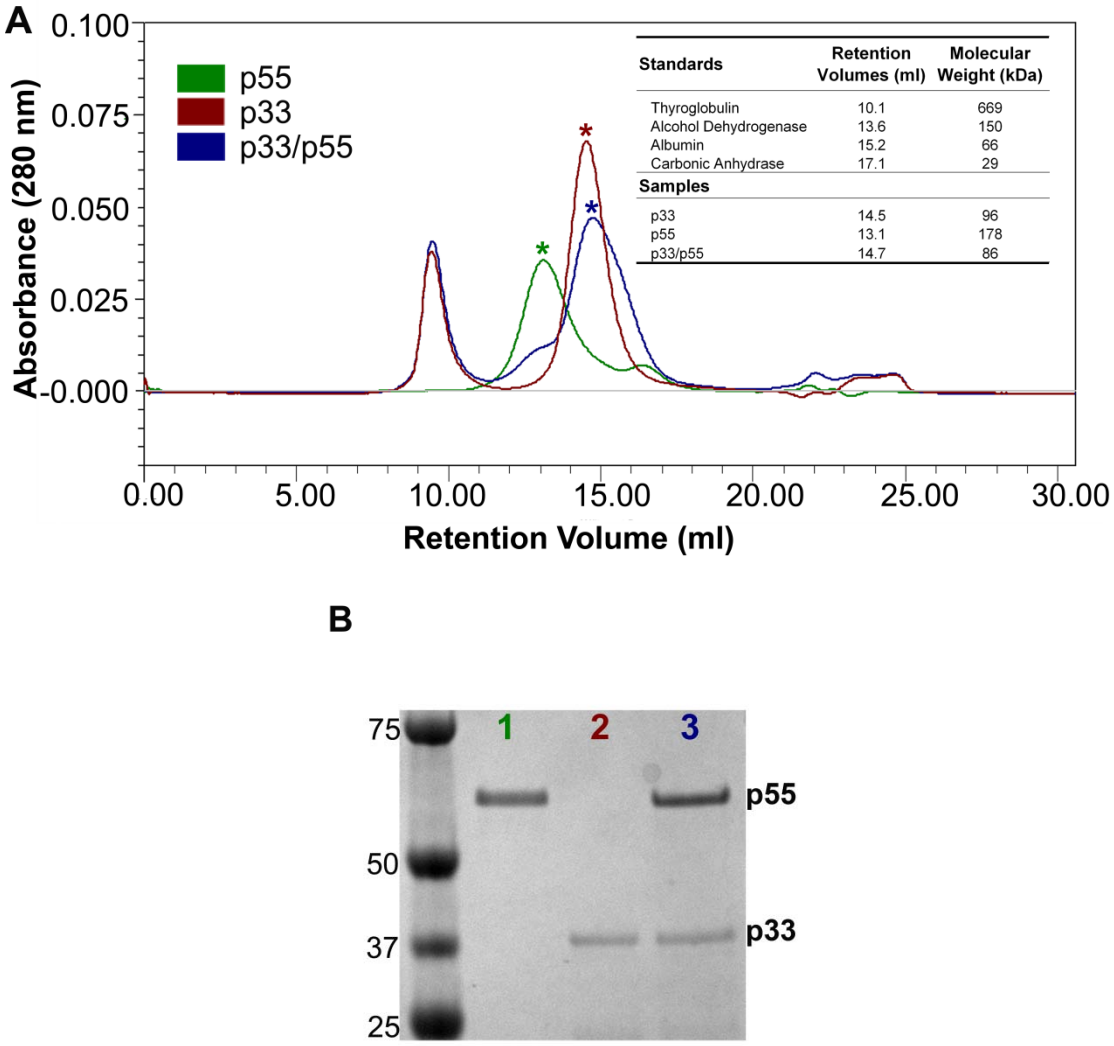

FIGURE 11: Analysis of p33 and p55 proteins by gel filtration. (A) Size exclusion chromatography (Superdex 200 10/300 prep grade resin) of refolded p33 (red peak), purified p55 (green peak), or a mixture of the two proteins (blue peak). Refolded p33 and purified p55 (each 1 mg/mL) were mixed at a 2:1 mass ratio and injected into the sizing column, as described in Experimental Procedures. The buffer contained 800 mM guanidine and 250 mM arginine, which were required to maintain the solubility of the p33 protein. The inset shows retention volumes of p33, p55, and the p33/p55 mixture in comparison to those of standard proteins. (B) The lower-molecular mass peaks (asterisks) from each of the size exclusion chromatography experiments shown in panel A were analyzed by SDS-PAGE and Coomassie blue staining.

Assembly of p33/p55 complexes into oligomeric structures

The p88 VacA protein secreted by *H. pylori* can assemble into water-soluble oligomers (*107-109, 194*). To investigate the possibility that p33 and p55 domains might assemble into similar structures, we visualized the p33/p55 mixture (purified by gel filtration as a monomeric complex) by electron micrsocopy. VacA p88 oligomers purified from the *H. pylori* culture supernatant (and exchanged into guanidine- and arginine-containing buffer by gel filtration) were analyzed as a control. As expected, large flowerlike structures were visualized in preparations of *H. pylori* p88 VacA (Figure 12A). In contrast, the p33/p55 mixture consisted mainly of small rodlike particles (Figure 12B), similar to the appearance of p88 monomers produced by *H. pylori* (*107-108*).

To explain why p88 proteins in the *H. pylori* broth culture supernatant readily assemble into flowerlike oligomeric structures whereas purified p33 and p55 proteins do not, we hypothesized that the broth culture medium used for growth of *H. pylori* (a nutrient-rich medium prepared from yeast extract and animal tissue, known as Brucella broth) might contain factors that promote VacA oligomerization. To test this hypothesis, we examined the appearance of the p33/p55 mixture by electron microscopy, either in the presence or in the absence of added Brucella broth. In the presence of added Brucella broth, an increased level of formation of flower-shaped complexes was detected (Figure 12C). These experiments indicated that Brucella broth stimulates the oligomerization of p33/p55 mixtures into oligomeric structures similar to those formed by p88 VacA from *H. pylori*.

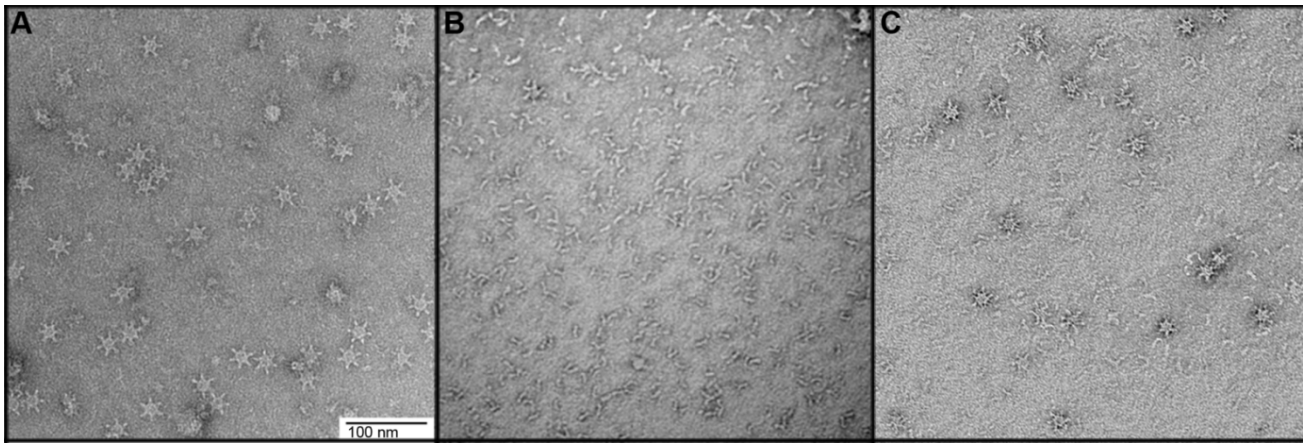

FIGURE 12: Assembly of p33 and p55 proteins into oligomeric structures. Electron microscopy analysis of (A) p88 purified from the *H. pylori* culture supernatant and then exchanged into a guanidine-containing buffer by gel filtration or (B) a mixture of refolded p33 and p55 that eluted from the sizing column (corresponding to Figure 11A, blue peak with an asterisk). (C) The p33/p55 preparation shown in panel B was mixed with Brucella broth as described in Experimental Procedures and then analyzed by electron microscopy. The images in this figure represent analysis of at least three grids for each condition and analysis of >10 fields per grid. The scale bar is 100 nm for all panels.

High resolution imaging of p33/p55 oligomeric complexes

We reasoned that the complex mixture of components in Brucella broth, including numerous membrane-derived factors, promoted the formation of flowerlike oligomers. In an effort to stimulate VacA oligomerization using more refined conditions, we incubated p33/p55 mixtures with various additives designed to create an amphipathic environment, including bovine heart total extract solubilized in chloroform, chloroform alone, and the detergent DDM. Each of these additives promoted oligomerization of the p33/p55 monomeric complexes into flowerlike oligomeric structures (data not shown). The VacA oligomers formed in the presence of bovine heart extract or chloroform had a more heterogeneous appearance than the VacA oligomers formed in the presence of DDM, and therefore, we studied the latter oligomers in further detail. To permit higher-resolution imaging, p33/p55 monomeric complexes (corresponding to the 86 kDa blue peak in Figure 11) were mixed with DDM, dialyzed, and passed over a gel filtration column in the presence of DDM and arginine and the absence of guanidine. Under these conditions, the 86 kDa peak was minimized and a high-molecular mass (>300 kDa) peak was observed (data not shown). High-molecular mass complexes containing WT p33 and p55 were isolated and analyzed further by electron micrsocopy. The appearance of these oligomers (Figure 13A) was similar to that of p88 oligomers isolated from *H. pylori* broth culture supernatant (Figure 13B). To further characterize the structural features of p33/p55 oligomers, approximately 1300 particles were classified into 10 groups and four classes were chosen as references for an additional round of reference based-alignment (Figure 13C and data not shown). To directly compare the structural organization of p33/p55 oligomers with that of p88 oligomers purified from *H. pylori* broth culture

supernatant, class averages of p88 oligomers were also generated. Because p88 oligomers seemed to adopt a larger number of conformations than p33/p55 oligomers, a larger number of p88 images were classified. Approximately 10000 particles of p88 VacA were classified into 20 class averages (data not shown), and seven classes were chosen for an additional round of reference-based alignment (Figure 13D and data not shown). The result of the p33/p55 complex alignment (Figure 13C) shows that the majority of the p33/p55 oligomers are composed of six or seven subunits [67% (Figure 13C, panels 1 and 2)], with one smaller class composed of an oligomer with 12 visible subunits [22% (Figure 13C, panel 3)] and one class representing poorly formed oligomers (Figure 13C, panel 4). The 12-subunit complex may represent a double-layer oligomer with the two layers splayed (*108-109*). The overall appearances of hexameric and heptameric p33/p55 oligomers are reminiscent of single-layer hexameric and heptameric oligomers formed by p88 VacA (Figure 13D, panels 1 and 2) (*107-109*). These single-layer oligomers exhibit a striking chirality, which suggests that one surface adsorbs preferentially to the support film. In contrast to the p33/p55 oligomers, a majority of the p88 oligomers exist as double-layer complexes containing 12–14 subunits (Figure 13D, panels 3–6) (*107-109*). Importantly, difference maps created between averages of p33/p55 and p88 single-layer heptameric and hexameric oligomers did not show any statistically relevant difference peaks (data not shown), which indicates that these oligomeric forms are structurally equivalent.

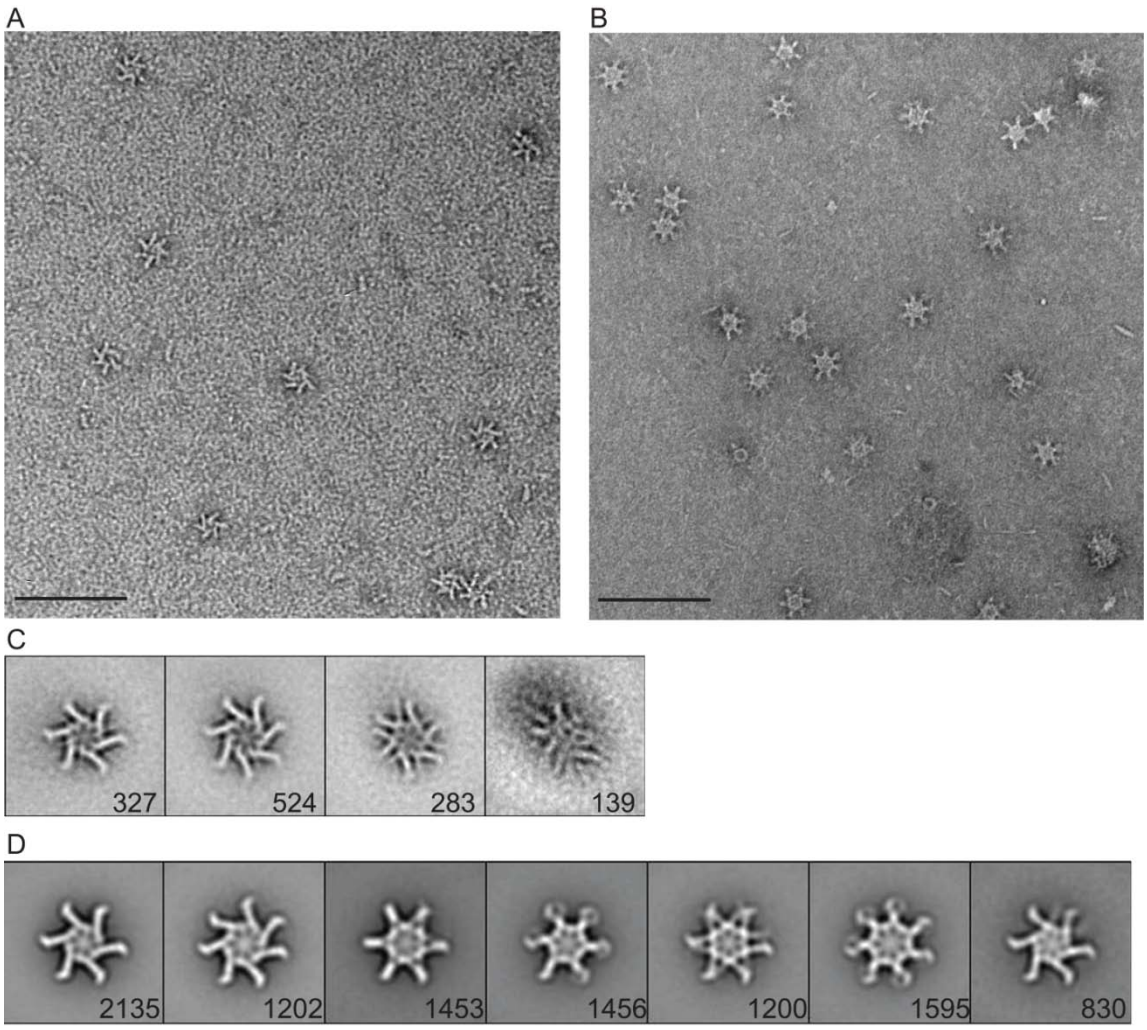

FIGURE 13: Analysis of p33/p55 VacA oligomers in negative stain. Mixtures of refolded p33 and p55 eluted from the sizing column (corresponding to Figure 11A, blue peak with an asterisk) were mixed with DDM and then dialyzed overnight in buffer containing 55 mM Tris (pH 8.0), 21 mM NaCl, 0.88 mM KCl, 250 mM arginine, and DDM. The protein was passed over a gel filtration column that was equilibrated with dialysis buffer containing DDM, and VacA oligomers eluting in a high-molecular mass fraction were then analyzed by electron microscopy. (A) Representative image of negatively stained p33/p55 VacA oligomers eluting in a high-molecular mass fraction. The scale bar is 100 nm. (B) Representative image of negatively stained p88 VacA oligomers isolated from *H. pylori* broth culture supernatant. The scale bar is 100 nm. (C) Four class averages of p33/p55 VacA particles in negative stain generated from reference-based alignment. The number of particles in each projection average is shown in the bottom right corner of each average. The side length of individual panels is 511 Å. (D) Seven representative class averages of p88 VacA particles in negative stain generated from reference-based alignment. The number of particles in each projection average is shown in the bottom right corner of each average. The side length of individual panels is 538 Å.

Discussion

In this study, we demonstrate that a functionally active form of *H. pylori* VacA can be reconstituted from two purified VacA fragments (p33 and p55). Previously, the p55 fragment was purified and its crystal structure determined (*99*), but it was not possible to purify a soluble, functionally active form of p33. In this study, we purified the p33 domain under denaturing conditions and then employed a series of steps designed to allow the protein to refold and remain soluble. We found that the refolded p33 protein was soluble in a buffer containing 800 mM guanidine and 250 mM arginine, but upon removal of these additives, the p33 protein became insoluble. Analysis of the p33 protein by circular dichroism was not feasible because of interference caused by the presence of arginine. Nevertheless, in comparison to denatured p33, the refolded p33 protein exhibited functional activity when mixed with the p55 fragment, which suggests that the p33 protein was successfully refolded.

Previous studies reported that a mixture of *E. coli* lysates containing VacA p33 and p55 can cause vacuolation of HeLa cells (*87*), and intracellular coexpression of p33 and p55 in HeLa cells results in cell vacuolation (*96*, *195*). However, there are numerous limitations associated with the use of crude *E. coli* lysates or intracellular expression systems. By using purified p33 and p55 proteins in this study, we were able to monitor the process by which p33 and p55 proteins interact to yield a functionally active VacA protein. Specifically, we demonstrate that the p33 and p55 proteins were purified with molecular masses of ~96 and ~178 kDa, respectively. The mass of the p33 protein is consistent with a trimeric form, but efforts to validate this by electron microscopy were unsuccessful. The mass of the p55 protein is consistent with a trimer as well, but the

crystal structure of p55 revealed a head-to-head packed dimer that adopts an elongated dumbbell shape (*99*). The elongated shape and the unusual buffer conditions likely account for the high apparent molecular mass of p55 on the sizing column. When the p55 and p33 preparations are mixed, the p55 and p33 homo-oligomers each dissociated to yield a p33/p55 complex with a mass of ~86 kDa, corresponding to a complex containing one p55 subunit and one p33 subunit. These p33/p55 monomeric complexes were visible by EM as elongated rods (Figure 12), similar to the appearance of p88 VacA monomers (*108*).

The ability to reconstitute a functional protein from two individually expressed component domains is somewhat unusual among bacterial protein toxins, and unusual among proteins in general. This phenomenon is probably facilitated by distinctive structural features of VacA. The VacA p55 domain consists predominantly of a β-helix, composed of multiple ~25-amino acid repeats, each of which forms a three-β-strand triangle-shaped coil (*99*). Adjacent coils are held together by backbone hydrogen bonds. The β-helix is therefore very different from globular proteins where adjacent structural elements are held together with an intricate arrangement of side chain interactions. On the basis of computer modeling, the VacA p33 domain is also predicted to comprise a β-helical structure, and it is predicted that the p88 protein comprises an elongated continuous β-helical structure (*99*). In the experiments described here, we speculate that the C-terminal coil of p33 interacts with the N-terminal coil of p55, recapitulating the structural relationship that exists between these two domains in the intact p88 VacA protein (*99*).

A distinctive property of the p88 VacA protein secreted by *H. pylori* is its ability to assemble into water-soluble, flower-shaped oligomeric structures (*107-109, 194*). In contrast, we observed that purified p33 and p55 proteins interact to form ~86 kDa complexes but do not readily assemble into oligomeric structures when maintained in buffer alone. One possible explanation is that the guanidine and arginine constituents of the buffer (required for maintenance of p33 solubility) prevent VacA oligomerization; however, we observed that these agents did not cause disassembly of p88 oligomers purified from the *H. pylori* culture supernatant. We hypothesized that the *H. pylori* broth culture supernatant might contain factors (either components of the rich Brucella broth medium used for culture of *H. pylori* or additional *H. pylori* products) that allow VacA oligomers to form. We observed that, indeed, the addition of freshly prepared Brucella broth (not previously cultured with *H. pylori*) to purified p33/p55 mixtures promoted assembly of VacA into oligomeric structures. Similarly, the addition of detergent also stimulated oligomerization. We speculate that oligomerization is stimulated by exposure to an amphipathic environment and that the oligomerization observed in these experiments mimics the process by which VacA oligomerizes when in contact with membranes of host cells.

The p88 VacA protein is typically purified in an oligomeric form from the *H. pylori* broth culture supernatant (*51, 107-109, 194*), and monomeric forms of p88 VacA have been relatively difficult to purify. When added to cultured eukaryotic cells, purified p88 VacA oligomers lack detectable activity in most assays unless the oligomers are first exposed to low-pH or high-pH conditions, which results in oligomer disassembly; oligomers have been observed to reassemble if the pH is returned to neutral (*107, 110,*

116, 123, 196-198). A current model presumes that VacA monomers interact with the cell surface and then reassemble into oligomeric complexes that function as membrane channels. In our study, we demonstrate that a mixture of purified p33 and p55 proteins is fully active in cell culture assays in the absence of low-pH or high-pH activation. Since the p33/p55 mixture predominantly consists of a p88 complex (Figures 11 and 12), this provides additional support for a model in which VacA monomers interact with the plasma membrane.

Several lines of evidence indicate that oligomerization of p88 VacA is required for VacA-induced cellular alterations (*92, 94, 113-114*). VacA oligomeric structures have been visualized on the surface of VacA-treated cells or lipid bilayers (*109-111*), and in contrast to double-layer oligomeric forms of VacA found in *H. pylori* culture supernatant, there is evidence that the VacA oligomeric complexes formed on the surface of cells are single-layer (*110*). Potentially, oligomerization of VacA occurs preferentially within lipid raft components of the plasma membrane (*111, 131, 143*). In this study, we observed that detergent promoted assembly of p33/p55 mixtures into predominantly single-layer oligomeric structures. Therefore, the complexes visualized in this study are predicted to be useful models for VacA channels that form in the context of human cells.

The reconstitution of VacA activity from purified p33 and p55 components probably involves a complex series of molecular events. An initial step involves disassembly of p33 and p55 homo-oligomers and formation of a p33/p55 complex. Potentially, the presence of p55 disrupts p33/p33 interactions, or the presence of p33 may disrupt p55/p55 interactions. An important observation is that neither p33 nor p55 bound to cells when added individually, whereas the p33/p55 mixture exhibited strong binding

to cells (Figure 10). One possible explanation is that the homo-oligomeric forms of p33 and p55 lack cell binding activity, and cell binding surfaces become exposed upon disassembly of the homo-oligomeric complexes. Alternatively, the receptor binding site(s) may span both the p33 and p55 domains. Finally, the assembly of p33/p55 complexes into higher-order flower-shaped oligomers may stabilize the interaction of VacA with the surface of eukaryotic cells, and oligomer formation is predicted to be required for insertion of VacA into membranes and channel formation.

CHAPTER 3

FUNCTIONAL STUDIES OF THE VACA P33 DOMAIN I-REGION

Introduction

The secreted VacA toxin is an important *H. pylori* virulence factor that causes multiple alterations in gastric epithelial cells and T cells. Several families of *vacA* alleles have been described, and *H. pylori* strains containing certain *vacA* types (s1, i1, and m1) are associated with an increased risk of gastric disease, compared to strains containing other *vacA* types (s2, i2, and m2). The m-region is located in the p55 domain, and has been shown to be important for cell type specificity. The s-region is located within the VacA signal peptide and the N-terminus of the p33 domain, and has been shown to be important in various in vitro assays. The i-region is located exclusively in the p33 domain, and thus far there has been relatively little study of the role of the i-region in toxin activity. We hypothesized that type 1 VacA proteins would cause increased cellular alterations in vitro as compared to type 2 VacA proteins. In this chapter I will present experimental data indicating that type i1 and i2 proteins differ in the capacity to cause alterations in T cells.

Materials and Methods

Bacterial strains and culture conditions

Bacterial strains and the plasmids used in this study are listed in Table 1. The WT *H. pylori* 60190 strain (ATCC 49503) and strain X47 (generously provided by

Douglas Berg) were grown on Trypticase soy agar plates containing 5% sheep blood at 37°C in ambient air containing 5% CO_2. *H. pylori* mutant strains were grown on Brucella agar plates containing 10% FBS, supplemented with metronidazole (3.75 μg/ml) or chloramphenicol (5 μg/ml) when indicated. *H. pylori* liquid cultures were grown in Brucella broth supplemented with either activated charcoal or 5% FBS (*51*).

Preparation of *H. pylori* broth culture supernatants and normalization of VacA concentrations

For experiments using *H. pylori* broth culture supernatant (derived from bacteria cultured in Brucella broth containing FBS), supernatants were concentrated 50-fold by ultrafiltration with a 30-kDa-cutoff membrane (Millipore). The relative concentrations of VacA in broth culture supernatant preparations from WT and mutant *H. pylori* strains were determined by Western blot analysis using anti-VacA antiserum no. 958 (prepared by immunization of a rabbit with VacA oligomers purified from *H. pylori* broth culture supernatant) (*131*). This anti-VacA antiserum reacted equally well with i1 and i2 VacA proteins in an ELISA assay (data not shown). When necessary, the concentrations of VacA in individual preparations were normalized by diluting samples with the appropriate volumes of concentrated Brucella broth containing FBS.

Purification of VacA from *H. pylori* broth culture supernatants

For experiments using purified VacA, VacA oligomers were purified from *H. pylori* culture supernatants as described previously (*107*). Prior to adding purified VacA to eukaryotic cells, the oligomeric VacA preparations were acid activated by the slow addition of 200 mM HCl until a pH of 3.0 was reached.

Mutagenesis of *vacA*

To generate unmarked *H. pylori* mutant strains, we used a negative selection method (*199*). As a first step, metronidazole-resistant forms of strains 60190 and X47, designated 60190 Δ*rdxA* and X47 Δ*rdxA*, were generated by deletion of the *rdxA* gene. Polymerase chain reaction (PCR) analysis confirmed that the *rdxA* locus was deleted from the mutant strains. As a next step, cloned *vacA* sequences were disrupted by insertion of a *cat-rdxA* cassette. This cassette confers resistance to chloramphenicol mediated by the chloramphenicol acetyltransferase (*cat*) gene from *Campylobacter coli*, and susceptibility to metronidazole is mediated by an intact *rdxA* gene (HP0954) from *H. pylori* 26695 (*199*). For mutagenesis of *vacA* in *H. pylori* strain 60190, the *cat-rdxA* cassette (described above) was ligated into an StuI site in plasmid pA178, which contains a *vacA* DNA fragment from *H. pylori* 60190 (*91*). The resulting plasmid (pCGR1), which is unable to replicate in *H. pylori*, was used to transform the *H. pylori* 60190 Δ*rdxA* strain, and single colonies resistant to chloramphenicol (5 μg/ml) but sensitive to metronidazole (3.75 μg/ml) were selected. For mutagenesis of *vacA* in *H. pylori* strain X47, a DNA fragment encoding VacA amino acids 4 to 727 was PCR amplified from this strain, and the PCR product was cloned into pGEMT-Easy (Promega). The resulting plasmid was digested with EcoRV, and the *cat-rdxA* cassette was ligated into this restriction site. The resulting plasmid (pCGR2) was transformed into the *H. pylori* X47 Δ*rdxA* strain, and single colonies resistant to chloramphenicol but sensitive to metronidazole were selected. Immunoblot analysis revealed the loss of VacA expression in these mutants, and insertion of the *cat-rdxA* cassette into the *vacA* gene was confirmed by PCR amplification and nucleotide sequence analysis of PCR products. To

introduce alterations into the i-region of the chromosomal *vacA* gene in *H. pylori* strains, we constructed various plasmids using an inverse PCR approach′ with the 5 phosphorylated primers listed in Table 2. The *vacA* sequence from each plasmid was sequenced to ensure that unintentional mutations were not introduced. These plasmids were used to transform *H. pylori* strains containing the *cat-rdxA* cassette, and transformants resistant to metronidazole were selected. The presence of the desired mutations was confirmed by PCR and nucleotide sequence analysis of PCR products.

Table 1: *H. pylori* strains and plasmids

Strains/Plasmid	Relevant characteristics	Reference
Strains		
60190	WT (ATCC 49503); *vacA* s1/i1/m1	(*50*)
60190 Δ*rdxA*	Same as 60190 except HP0954 (*rdxA*) gene deleted; metronidazole resistant	This study
60190 *cat rdxA*	Same as 60190 Δ*rdxA* except *cat* cassette and *rdxA* inserted in *vacA*; chloramphenicol resistant and metronidazole sensitive; expression of VacA is disrupted	This study
60190 i2B	Same as 60190 Δ*rdxA* except *vacA* cluster B changed to i2	This study
60190 i2C	Same as 60190 Δ*rdxA* except *vacA* cluster C changed to i2	This study
60190 i2BC	Same as 60190 Δ*rdxA* except *vacA* clusters B & C changed to i2	This study
60190 i1/i2C	Same as 60190 Δ*rdxA* except *vacA* cluster C has 4 amino acids changed to i2	This study
X47	Wild type; *vacA* s1/m2, chimeric i-region	(*200*)
X47 Δ*rdxA*	Same as X47 except HP0954 (*rdxA*) gene deleted; metronidazole resistant	This study
X47 *cat rdxA*	Same as X47 Δ*rdxA* except *cat* cassette and *rdxA* inserted in *vacA*; Chloramphenicol resistant and metronidazole sensitive; expression of VacA is disrupted	This study
X47 i1C	Same as X47 Δ*rdxA* except *vacA* cluster C changed to i1	This study
Plasmids		
pMM672	Allows deletion of *rdxA* in *H. pylori* strains	(*199*)
pCGR1	Contains *cat-rdxA* cassette on Stu1 site; derived from pA178 plasmid	This study
pCGR2	Contains cat-rdxA cassette on EcoRV site from X47 *vacA*	This study
pCGR3	60910 cluster B changed from i1 to i2 by inverse PCR using primers B1F & B1R	This study
pCGR4	60190 cluster C changed from i1 to i2 by inverse PCR using primers C1F & C1R	This study
pCGR5	60190 cluster B & C changed from i1 to i2 by inverse PCR using primers C1F & C1R and pCGR3 as template	This study
pCGR6	A portion of 60190 cluster C changed from i1 to i2 by inverse PCR using primers C2F & C2R	This study
pCGR7	X47 cluster C changed from i2 to i1 by inverse PCR using primers C3F & C3R	This study
p55	Expresses VacA p55	(*99*)
p33	Expresses VacA p33	(*201*)
p33 i2	Expresses p33 i2	This study

Table 2: PCR primers used for mutagenesis of the *vacA* i-region

Primer[a]	Sequence (5'-3')
Primer B1F	ATTACAAGCCGTGAAAATGCTGAAATTTCTCTTTATG
Primer B1R	TTTTTCTGAACTTTTCAAAGTCAAAACCGTAGAGC
Primer C1F	TATATGGTAAGGTGTGGATGGGCCGTTTGC
Primer C1R	GATCAACGCTCTGATTTGAGCTTGAAACCAAATTGAGCGTAGCGCCATC
Primer C2F	AACCAAAGCGTTAAATTAAATGGCAATGTG
Primer C2R	GCTGTTTGACACCAAATTGAGCGTAGCGCCA
Primer C3F	TTAAATGGCAATGTGTGGATGGGCCGTTTGCAATA

Cell culture

RK13 cells were obtained from the American Type Culture Collection (ATCC CCL-37) and were cultured in minimal essential medium supplemented with 10% FBS and 1 mM nonessential amino acids. Jurkat T lymphocytes (clone E6-1, ATCC TIB-152) were cultured in RPMI 1640 medium containing 2 mM L-glutamine, 1.5 g/liter sodium bicarbonate, 4.5 g/liter glucose, 10 mM HEPES, 1.0 mM sodium pyruvate, and 10% FBS. Jurkat lymphocytes containing stable luciferase reporters were cultured as described above, except that the medium was supplemented with 1 μM puromycin.

Neutral red uptake assay

To quantify VacA-induced cell vacuolation, RK13 cells were seeded at a density of 2×10^4 cells/well into 96-well plates for 24 h prior to the experiment. Serial dilutions of concentrated *H. pylori* culture supernatants containing different forms of VacA were added to serum-free tissue culture medium (supplemented with 10 mM ammonium chloride) overlying cells and incubated overnight at 37°C. VacA-induced cell vacuolation was detected by inverted light microscopy and quantified by a neutral red uptake assay, a well-established method that is based on rapid uptake of neutral red into VacA-induced cell vacuoles (*51, 187*). Background levels of neutral red uptake by untreated cells were subtracted to yield net neutral red uptake values.

Analysis of IL-2 production by Jurkat cells

Jurkat T cells were plated in 96-well plates at a density of 1×10^5 cells/well, and *H. pylori* broth culture supernatant preparations or purified VacA proteins were added to cells for 30 min at 37°C. The cells were then stimulated with PMA (50 ng/ml; Sigma) and ionomycin (500 ng/ml; Sigma) and maintained in RPMI 1640 medium

containing 10% FBS for 24 h. Cells were pelleted, and levels of IL-2 in the supernatants were quantified by ELISA, according to the manufacturer's protocol (R&D Systems; human IL-2 immunoassay). To ensure that IL-2 production was not altered by T-cell apoptosis, we monitored the viability of Jurkat cells in each experiment by using trypan blue staining and did not detect any significant effect of VacA on viability of the cells (data not shown), a result that is consistent with previous publications (*169-170*).

Expression and purification of recombinant VacA proteins

Recombinant p33 and p55 proteins, derived from *H. pylori* strain 60190, were expressed in *E. coli* and purified as described previously (*99, 201*). In addition, we modified the plasmid encoding the i1 p33 protein derived from *H. pylori* strain 60190, so that it expressed an i2 form of p33. To do this, we first changed the sequence in the *vacA* i-region polymorphic cluster B from type 1 to 2 by inverse PCR, using the WT p33 plasmid as a template and primers B1F and B1R (Table 2). The resulting plasmid, containing a type 2 cluster B and type 1 cluster C, was then used as a template to change the amino acid sequence of cluster C to type 2, using primers C1F and C1R (Table 2). The modifications in the i-region were confirmed by nucleotide sequence analysis. VacA p33 and p55 were expressed by culturing *E. coli* BL21 (DE3) in TB-KAN at 37°C overnight with shaking. Cultures were diluted 1:100 in TB-KAN and grown at 37°C until they reached an A_{600} of 0.6. Cultures were induced with a final IPTG concentration of 0.5 mM and incubated at 25°C for 16 to 18 h (p55 proteins) or at 37°C for 3 h (p33 proteins). VacA p55 was purified under native conditions by nickel affinity, ion exchange, and gel filtration chromatography (*99*). VacA p33 proteins were purified under denaturing conditions from inclusion bodies by using Ni-affinity resin (Novagen). The purified

denatured VacA p33 proteins were then refolded by dialysis and were purified further by gel filtration chromatography (*201*).

Flow cytometric analysis of VacA binding to cells

Purified p55 was labeled with Alexa 488 (Molecular Probes) according to the manufacturer's instructions (*201*). Jurkat cells (1×10^5 cells per condition) were treated with Alexa 488-labeled p55 alone (10 μg/ml) or with a mixture of Alexa 488-labeled p55 plus either purified refolded p33 i1 or p33 i2 proteins (each at 5 μg/ml) at 4°C for 1 h. Cells were then washed three times in cold phosphate-buffered saline (PBS) containing 0.5% bovine serum albumin (BSA) and fixed in 2% paraformaldehyde. The cells were collected using a flow cytometer (LSR II system; BD, San Alta, CA) and analyzed using BD Diva (*175*). Immunofluorescent microscopy experiments indicated that the VacA proteins were not internalized at 4°C (data not shown).

Immunoblot analysis of VacA binding to cells

Jurkat cells (1×10^6 cells per condition) were cultured in serum-free medium for 8 h and then incubated with preparations of *H. pylori* broth culture supernatants at 4°C for 1 h. Cells were washed three times with cold PBS, pelleted, and heated at 100°C for 5 min in sodium dodecyl sulfate (SDS) loading buffer. Samples were electrophoresed on a 4 to 20% gradient precast acrylamide gel (Bio-Rad) and transferred onto nitrocellulose membranes. Membranes were immunoblotted with rabbit anti-VacA serum (serum number 958, diluted 1:10,000) or anti-GAPDH serum (ABcam, diluted 1:1,000), followed by horseradish peroxidase-conjugated secondary antibodies (Promega, diluted 1:10,000). Immune complexes were revealed by using an enhanced chemiluminescence system (ECL Western Blotting Analysis System; GE Healthcare).

Generation of a Jurkat cell line with a stable NFAT luciferase reporter

Jurkat lymphocytes were transduced with replication-deficient lentiviral particles encoding an NFAT reporter or a negative-control reporter (Cignal Lenti NFAT reporter assay and Cignal Lenti reporter negative control; Qiagen), according to the manufacturer's protocol. Briefly, Jurkat cells (1×10^4 cells per condition) were infected with lentiviral particles carrying the desired reporter at a multiplicity of infection (MOI) of 50 viral particles per cell. After 3 days, the cell culture medium was changed and supplemented with 1 μM puromycin. After 3 additional days, surviving clones were used for further experiments.

Luciferase assay

Jurkat cells carrying a stable luciferase reporter (NFAT or negative control) were cultured (1×10^5 cells per condition) and treated with viable *H. pylori* strains (MOI of 50 bacterial cells per Jurkat cell) or *H. pylori* broth culture supernatant preparations for 1 h at 37°C. Cells were then stimulated with PMA (50 ng/ml) and ionomycin (500 ng/ml; Sigma) for 6 h. Luciferase activity was measured using the luciferase assay system with reporter lysis buffer (Promega) according to the manufacturer's protocol. Luciferase activity is expressed as relative values (luciferase activity of cells containing NFAT reporter divided by luciferase activity of cells containing the negative-control reporter), and the values for control cells (stimulated with PMA-ionomycin, without VacA treatment) are assigned a relative value of 1 (or 100%).

VacA binding to integrin

VacA binding to β2 integrin was evaluated by ELISA. The wells of microtiter plates (Immunolon IB) were coated with 50 μl of recombinant αMβ2 integrin or αVβ3

integrin derived from human CHO cells (R&D system) at 4°C for 24 h. Unbound protein was then removed and the wells were blocked with PBS containing 5% BSA at 4°C for 48 h. After blocking, serial dilutions of *H. pylori* culture supernatants containing equivalent concentrations of different forms of VacA were added to the wells at 25°C for 1 h. Wells were then washed three times with PBS-0.05% Tween 20, and bound VacA was detected by incubating the wells with anti-VacA rabbit serum (diluted 1:1,000/serum no. 958), followed by incubating with horseradish peroxidase-conjugated secondary antibody (diluted 1:1,000; Promega), each at 25°C for 1 h. Rabbit serum and secondary antibody were diluted in PBS containing 3% BSA. ELISA was developed using Strep Ultra TMB-ELISA (Thermo Scientific).

Results

Manipulation of the *vacA* i-region

The VacA proteins secreted by different WT *H. pylori* strains vary markedly in amino acid sequences, and there are also differences among strains in the levels of VacA secretion (*52, 89*). To facilitate analysis of the VacA i-region, we used an approach in which we manipulated the chromosome of reference *H. pylori* strains (60190 and X47) in a manner so that we altered the region of *vacA* encoding the i-region and maintained all other regions of *vacA* without changes. For initial studies, we altered *vacA* in strain 60190 (which contains type s1/i1/m1 *vacA*) so that two clusters of polymorphisms in the i-region (cluster B and cluster C) were changed from an i1 form to an i2 form, as described in Materials and Methods. The modified strain was designated 60190 i2BC (Table 1 and Figure 14A). Immunoblot analysis indicated that the modified *H. pylori* strain expressed and secreted VacA in a manner similar to the WT strain (data not shown). The WT strain and modified *H. pylori* strain were grown in broth cultures, and bacterial supernatants were concentrated and normalized so that they contained equivalent concentration of VacA, as described in Materials and Methods. To investigate whether there were any detectable differences in the ability of these proteins to cause alterations in gastric epithelial cells, serial dilutions of the supernatant preparations were added to RK13 cells. Consistent with results of a previous study (*56*), we did not detect any difference in the ability of the i1 and i2 forms of VacA to cause vacuolation of RK13 cells (Figure 14B). This suggests that manipulation of the VacA i-region by this approach does not result in misfolding of the protein.

A

```
                        Cluster B                       Cluster C
60190(i1)    SSTVLTLQASEGITSSKNAEISLYDGATLNLASN---SVKLNGNVWMGRLQY
60190(i2BC) SSTVLTLKSSEKITSRENAEISLYDGATLNLVSSSNQSVDLYGKVWMGRLQY
```

B

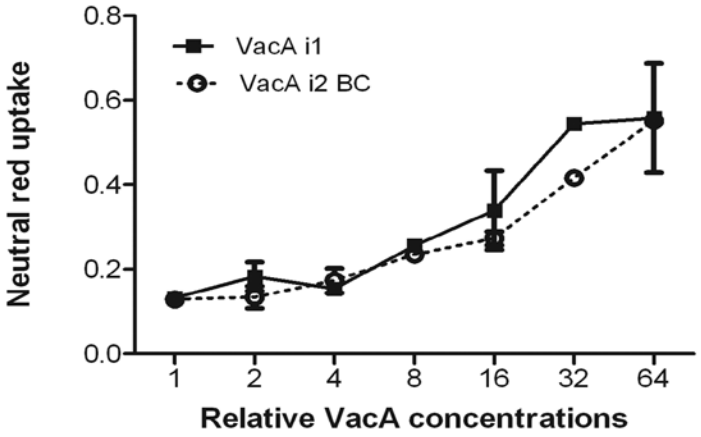

FIGURE 14: VacA-induced vacuolation of RK13 cells. (A) Amino acid sequence of the VacA i-region in WT *H. pylori* strain 60190 (type i1) and a strain expressing a modified VacA protein in which clusters B and C were changed from type i1 to type i2 (60190 i2BC). (B) Broth culture supernatants derived from the WT strain (type i1) or strain 60190 i2BC were concentrated and normalized so that they contained equivalent VacA concentrations, as described in Materials and Methods. Serial dilutions of VacA-containing preparations were then added to RK13 cells. Vacuolating activity was measured by a neutral red uptake assay. Relative VacA concentrations are indicated. Results represent the means ± standard deviations from triplicate samples.

Effects of type i1 and i2 VacA on IL-2 production by Jurkat cells

Previous studies have shown that type i1 forms of VacA can suppress IL-2 secretion from Jurkat cells (*169, 174-175*). To determine whether type i1 and i2 forms of VacA differ in this activity, we compared the ability of the WT i1 form of VacA and the i2BC form described above to suppress IL-2 secretion by Jurkat cells. We also manipulated *H. pylori* strain 60190 so that individual polymorphic regions within the *vacA* i-region (cluster B or cluster C) were changed to type i2 (Figure 15A). These modified strains are designated 60190 i2B and 60190 i2C. Cluster A was not manipulated, since sequence variation at this site has not been linked to disease outcome (*56*). Immunoblot analysis indicated that each of the modified *H. pylori* strains expressed and secreted VacA, similar to the WT strain (data not shown). The WT and modified *H. pylori* strains were grown in broth cultures, and supernatant preparations containing equivalent concentrations of VacA were prepared, as described in Materials and Methods. Jurkat cells were pretreated with broth culture supernatant preparations from the WT and modified strains and were then stimulated with PMA and ionomycin. IL-2 production by Jurkat cells was quantified by ELISA, as described in Materials and Methods. In comparison to supernatant from a *vacA*-null mutant strain, supernatant containing WT i1 VacA suppressed IL-2 secretion, as expected (Figure 15B). Supernatants containing i2 forms of VacA (i2B, i2C, or i2BC) also suppressed IL-2 secretion, but in comparison to i1 VacA, the i2 forms of VacA had a significantly reduced capacity to suppress IL-2 secretion (Figure 15B).

We next investigated the role of the VacA i-region in the context of *H. pylori* strain X47, which contains an s1/m2 type of *vacA*. The *vacA* gene in this strain contains a type i2 sequence in cluster C of the i-region, and cluster B is chimeric. A previous study (*56*) reported that polymorphisms in cluster C accounted for differences in the activity of i1 and i2 forms of VacA on epithelial cells. Therefore, we investigated whether changing cluster C of *vacA* in this strain from type i2 to type i1 would result in an increased capacity of VacA to suppress IL-2 secretion from Jurkat cells. To do this, we manipulated *H. pylori* strain X47 as described in Materials and Methods such that amino acids in cluster C of the *vacA* i-region were changed from an i2 to an i1 form, resulting in a strain designated X47 i1C (Figure 15C). The WT and modified *H. pylori* strains were grown in broth cultures, and supernatant preparations containing equivalent concentrations of VacA were prepared, as described in Materials and Methods. Jurkat cells were pretreated with the *H. pylori* culture supernatant preparations and were then stimulated with PMA and ionomycin. In comparison to VacA produced by the *H. pylori* X47 WT strain (X47 i2), VacA containing an i1 form of cluster C (X47 i1C) had an increased inhibitory effect on IL-2 secretion by Jurkat cells (Figure 15D).

A

```
                          Cluster B                          Cluster C
60190(i1)    SSTVLTLQASEGITSSKNAEISLYDGATLNLASN---SVKLNGNVWMGRLQY
60190(i2B)   SSTVLTLKSSEKITSRENAEISLYDGATLNLASN---SVKLNGNVWMGRLQY
60190(i2C)   SSTVLTLQASEGITSSKNAEISLYDGATLNLVSSSNQSVDLYGKVWMGRLQY
60190(i2BC)  SSTVLTLKSSEKITSRENAEISLYDGATLNLVSSSNQSVDLYGKVWMGRLQY
```

B

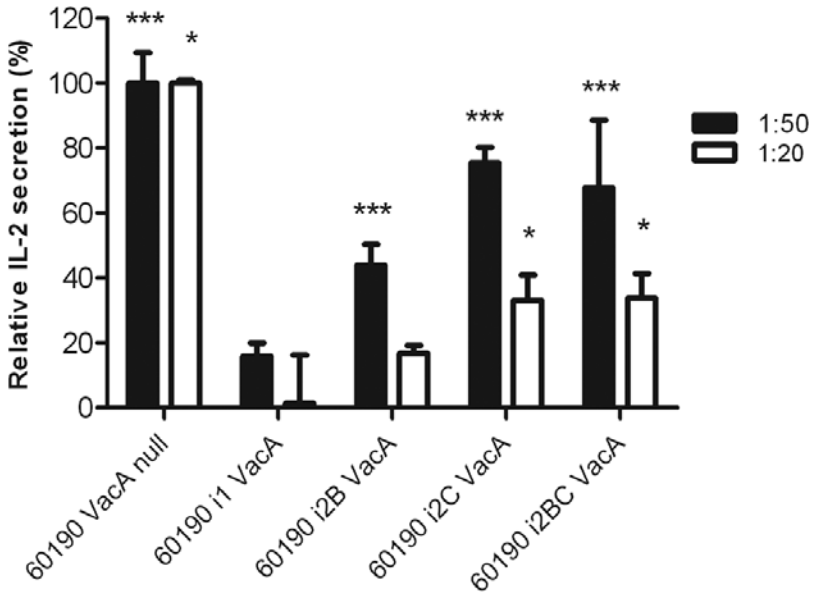

C

```
                          Cluster B                  Cluster C
X47(i2)   SSTVLTLQASEKITSSENAEISLYDGATLNLVSSSNHSVDLYGKVWMGRLQY
X47(i1C)  SSTVLTLQASEKITSSENAEISLYDGATLNLASN---SVKLNGNVWMGRLQY
```

D

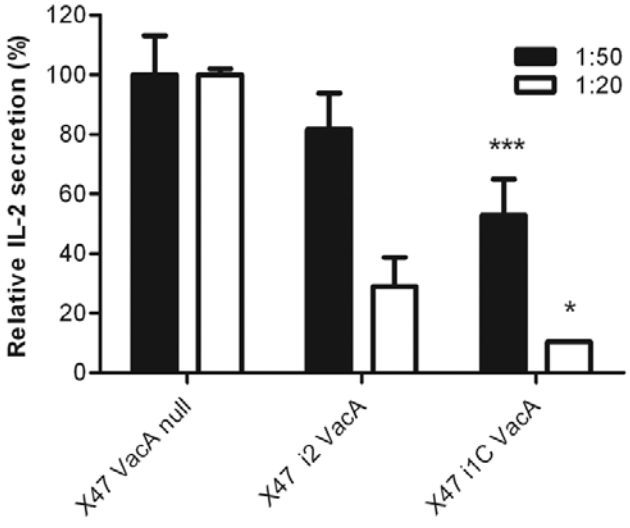

FIGURE 15: Role of the VacA i-region in inhibition of IL-2 secretion by Jurkat cells. (A) Amino acid sequence of the VacA i-region in WT *H. pylori* strain 60190 (type i1) and modified strains. Modified strains were constructed so that 60190 i2B contains an i2 sequence in polymorphic cluster B and an i1 sequence in cluster C, 60190 i2C contains an i2 sequence in cluster C and an i1 sequence in cluster B, and 60190 i2BC contains i2 sequences in both clusters B and C. (B) *H. pylori* strains were cultured in broth, and preparations of culture supernatants were standardized so that they contained equivalent concentrations of VacA, as described in Materials and Methods. Jurkat cells were pretreated with 1:20 or 1:50 dilutions of culture supernatant preparations, each containing the indicated VacA protein, and then stimulated with PMA-ionomycin. After 24 h, the cells were pelleted and the IL-2 content of supernatants was analyzed by ELISA. (C) Amino acid sequence of the VacA i-region in WT strain X47 and a modified strain. WT strain X47 contains an i2 sequence in cluster C, and the X47 i1C strain contains an i1 sequence in cluster C. (D) Jurkat cells were pretreated with 1:20 or 1:50 dilutions of culture supernatant preparations, each containing the indicated VacA protein, and cells were then stimulated with PMA-ionomycin. After 24 h, the cells were pelleted, and the IL-2 content of supernatants was analyzed by ELISA. Results represent the means ± standard deviations of triplicate samples of a single experiment. Similar results were obtained in two additional experiments. *, P value of ≤ 0.05 compared to WT i1 VacA (A) or WT VacA from strain X47 (B) at a 1:20 dilution; ***, P value of ≤ 0.05 at a 1:50 dilution (analysis of variance [ANOVA] followed by Dunnett's *post hoc* test for panel B; Student *t* test for panel D). Levels of IL-2 secretion are expressed as relative values (levels of IL-2 secreted by cells treated with WT VacA or modified VacA proteins, divided by levels of IL-2 secreted by cells treated with supernatant from the VacA-null mutant strain). Values for cells treated with supernatant from the VacA-null mutant strain are assigned a relative value of 1 (or 100%).

Effects of purified VacA proteins on IL-2 production by Jurkat cells

To further analyze the activities of type i1 and i2 VacA proteins, we purified i1 and i2 VacA proteins from broth culture supernatant of either WT *H. pylori* 60190 (expressing i1 VacA) or the 60190 i2BC strain (expressing an i2 form of VacA) (Table 1) and then tested the effects of these proteins on Jurkat cells. The purified VacA i1 protein suppressed IL-2 secretion from Jurkat cells, whereas the purified VacA i2 protein had relatively little effect (Figure 16A). To corroborate the conclusion that i1 and i2 proteins differed in activity, we generated an additional modified form of VacA and analyzed the activity of this purified protein. Specifically, we mutated the 5' end of *vacA* cluster C in *H. pylori* strain 60190 so that it contained amino acids corresponding to i2 sequences. Cluster C in this modified form of VacA, designated i1/i2C VacA, contained an A-to-V substitution and an SNQ insertion (VSNSNQSVKLNGN; for comparison, the type i1 sequence is ASNSVKLNGN and the type i2 sequence is VSSSNQSVDLYGK). We then purified the WT i1 protein and the VacA i1/i2C protein (containing i2 amino acids in the 5′ region of cluster C) from *H. pylori* supernatants and tested these proteins for their ability to inhibit IL-2 production by Jurkat cells. In comparison to the WT i1 VacA protein, the i1/i2C VacA protein was less potent in its ability to inhibit IL-2 production (Figure 16B). We also attempted to purify WT and modified VacA proteins expressed by *H. pylori* strain X47, but this was not feasible due to a failure of this strain to grow in medium free of FBS (which is essential for purification of VacA).

As another approach, we tested the activity of purified recombinant VacA i1 and i2 proteins. We have previously shown that a mixture of i1 p33 plus p55 VacA domains reconstitutes toxin activity in assays using HeLa cells (*87, 200*). Therefore, we expressed

both i1 and i2 forms of p33 as described in Materials and Methods, mixed either purified VacA p33 i1 or p33 i2 proteins with purified p55 (1:1 mass ratio), and tested the effects of these preparations on Jurkat cells. In comparison to a mixture of p33 i1 plus purified p55, a mixture of p33 i2 plus purified p55 had a significantly reduced capacity to suppress IL-2 secretion from Jurkat cells (Figure 16C). Taken together, these results indicate that the i-region is an important determinant of the capacity of VacA to inhibit IL-2 secretion.

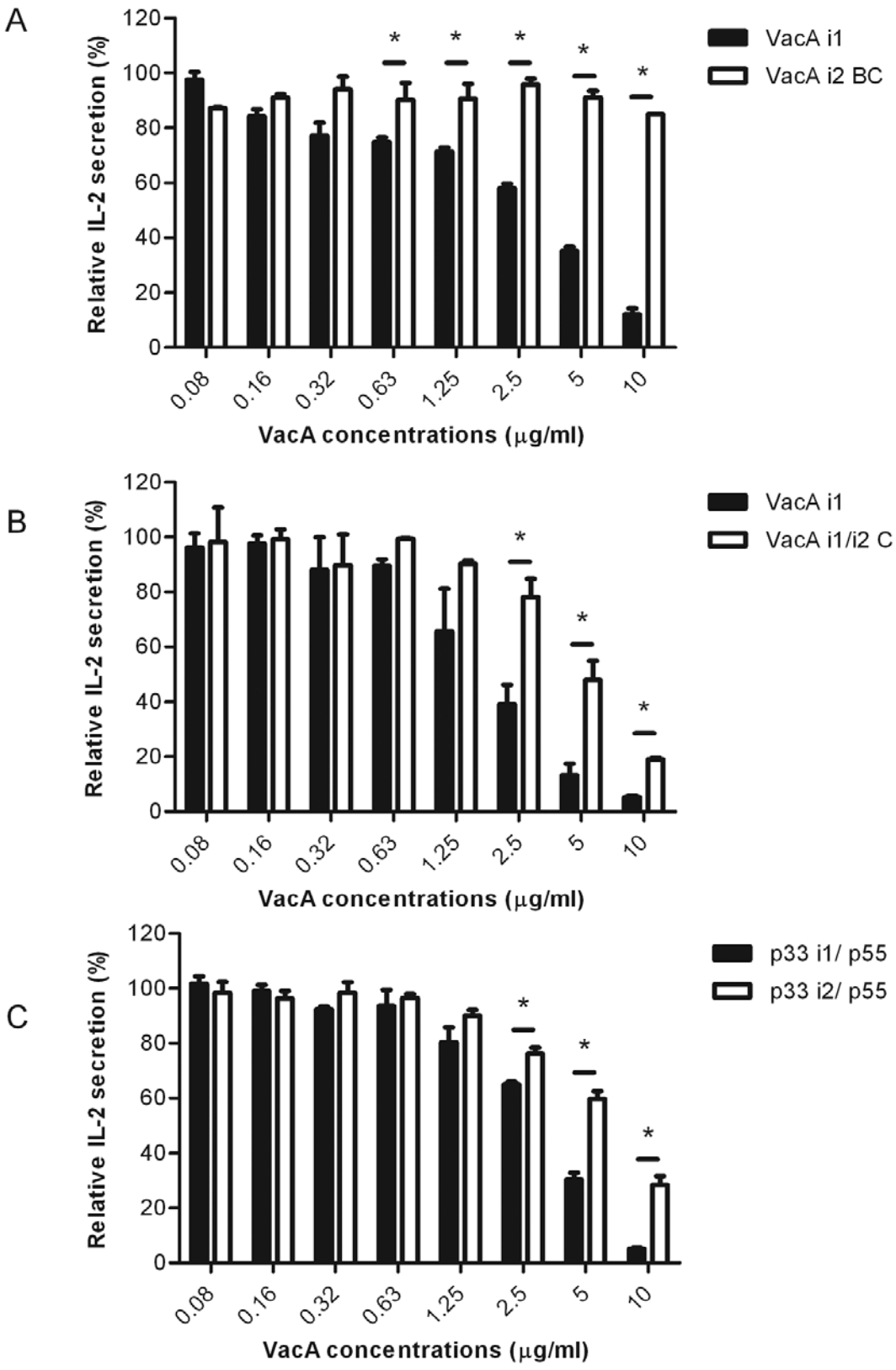
A
Relative IL-2 secretion (%)
120
100
80
60
40
20
0
*
*
*
*
*
0.08
0.16
0.32
0.63
1.25
2.5
5
10
VacA concentrations (μg/ml)
VacA i1
VacA i2 BC
B
Relative IL-2 secretion (%)
120
100
80
60
40
20
0
*
*
*
0.08
0.16
0.32
0.63
1.25
2.5
5
10
VacA concentrations (μg/ml)
VacA i1
VacA i1/i2 C
C
Relative IL-2 secretion (%)
120
100
80
60
40
20
0
*
*
*
0.08
0.16
0.32
0.63
1.25
2.5
5
10
VacA concentrations (μg/ml)
p33 i1/ p55
p33 i2/ p55

FIGURE 16: Effects of purified VacA proteins on IL-2 secretion by Jurkat cells. (A) Jurkat cells were pretreated with purified p88 VacA proteins secreted by either WT strain 60190 (expressing type i1 VacA) or a modified strain expressing i2BC VacA, which contains i2 sequences in polymorphic clusters B and C. (B) Jurkat cells were pretreated with purified *H. pylori* VacA proteins secreted by either WT strain 60190 (type i1) or a modified strain expressing an i1/i2C protein (as described in Results) at the indicated protein concentrations. Cells were then stimulated with PMA-ionomycin, and after 24 h the cells were pelleted and the IL-2 content of supernatants was analyzed by ELISA. (C) Recombinant purified p33 proteins containing either i1 or i2 (clusters BC) amino acid sequences were mixed with purified p55. The indicated protein concentrations for the VacA p33-p55 mixture (1:1 mass ratio) correspond to the total protein concentration. Jurkat cells were pretreated with the VacA preparations and were then stimulated with PMA-ionomycin. After 24 h, IL-2 production was quantified by ELISA. Results represent the means ± standard deviations of triplicate samples of a single experiment. Similar results were obtained in two additional experiments. *, *P* value of≤ 0.05 as determined by Student's *t* test. Levels of IL-2 secretion are expressed as relative values (levels of IL-2 secreted by cells treated with WT VacA or modified VacA proteins, divided by levels of IL-2 secreted by cells treated with buffer alone). Values for cells treated with buffer are assigned a relative value of 1 (or 100%).

Analysis of VacA effects on NFAT activation

Previous studies have shown that the effect of VacA on IL-2 secretion by Jurkat cells is dependent on inhibition of NFAT (*169*). We therefore investigated whether the composition of the VacA i-region influences the ability of VacA to inhibit NFAT activation. We first transduced Jurkat cells with replication-deficient lentiviral particles that carry an NFAT luciferase reporter or a negative-control reporter and selected for puromycin-resistant cells that contain the reporters, as described in Materials and Methods. We then cocultured the cells with viable *H. pylori* (60190 WT strain, 60190 *vacA*-null mutant strain, or 60190 i2BC) (Figure 17A). After 1 h of incubation, cells were stimulated with PMA-ionomycin for an additional 6 h, and luciferase was measured as described in Materials and Methods. In comparison to the WT *H. pylori* strain (expressing type i1 VacA), which inhibited NFAT activation, *H. pylori* expressing type i2 VacA (60190 i2BC) had an impaired ability to inhibit NFAT activation (Figure 17A). Similar results were obtained when analyzing *H. pylori* broth culture supernatant preparations (Figure 17B). As shown in Figure 17B, supernatant from the *vacA*-null mutant strain caused some detectable inhibition of NFAT activation, which might be attributable to actions of other factors besides VacA on NFAT activation or nonspecific effects of the preparation on the luciferase assay. In summary, the results obtained in these studies of NFAT activation were concordant with results obtained in the IL-2 assays.

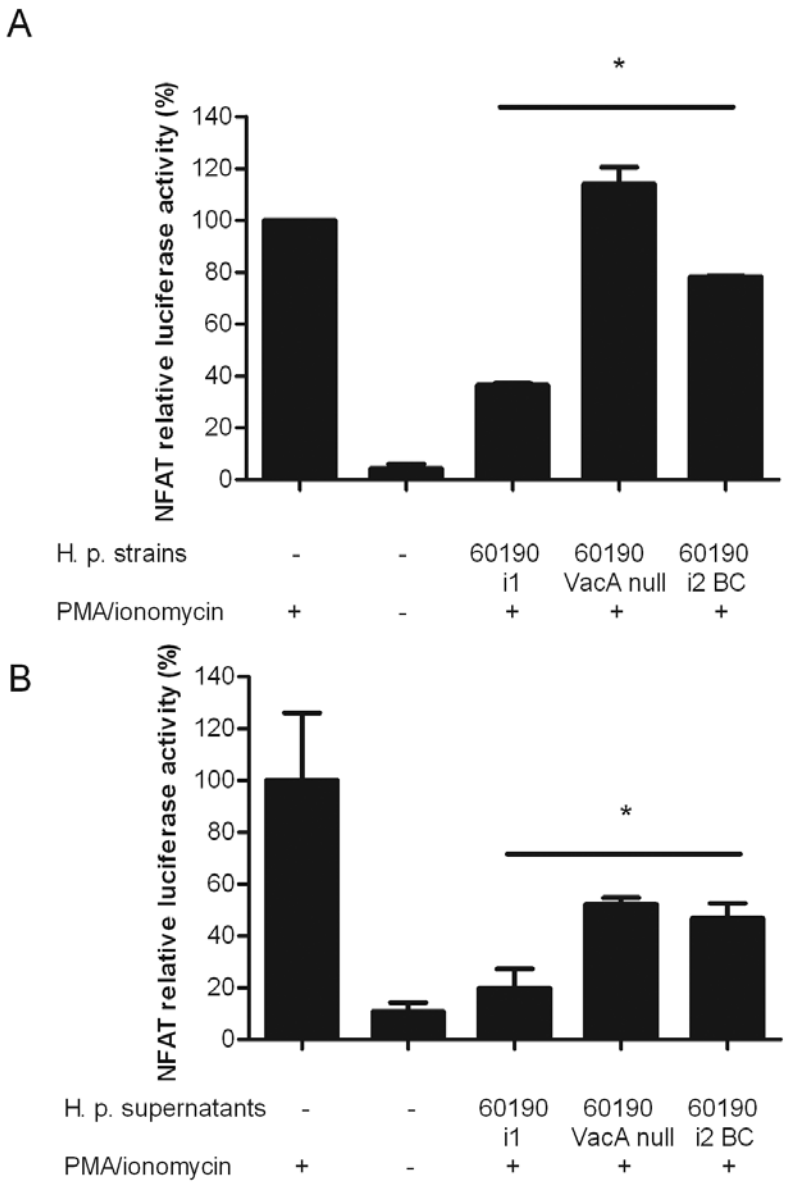

FIGURE 17: Effects of VacA proteins on NFAT activation. Jurkat cells stably expressing an NFAT luciferase reporter or a negative-control luciferase reporter were treated with viable *H. pylori* strains (WT strain 60190 [expressing i1 VacA], *vacA*-null mutant strain, or 60190 i2BC [expressing i2BC VacA]) (A) or with *H. pylori* broth culture supernatant preparations derived from these strains (B) and then activated with PMA and ionomycin. Luciferase activity was quantified by luminometry, as described in Materials and Methods. NFAT activity is expressed as relative values (luciferase activity of cells containing NFAT reporter divided by luciferase activity of cells containing the negative control reporter), and the values for control cells (stimulated with PMA-ionomycin, without VacA treatment) are assigned a relative value of 1 (or 100%). Results represent the means ± standard deviations of triplicate samples of a single experiment. Similar results were obtained in two additional experiments. *, *P* value of ≤0.05 as determined by using Student's *t* test, comparing WT strain 60190 and a strain expressing VacA i2BC (A) or culture supernatant preparations derived from these strains (B).

Analysis of VacA binding to Jurkat cells

To investigate a possible mechanism for the observed differences in activities of i1 and i2 VacA proteins, we analyzed the binding properties of VacA proteins containing type i1 or type i2 i-regions. Broth culture supernatant preparations from *H. pylori* 60190 strains expressing either i1 VacA or i2 VacA (60190 i2BC) proteins, as well as a supernatant preparation from a *vacA*-null mutant strain, were incubated with Jurkat cells for 1 h at 4°C. Cells were then washed and immunoblotted with an anti-VacA antibody to detect VacA binding. As shown in Figure 18A and 18B (top), immunoblot analysis of the supernatants in the absence of Jurkat cells indicated that the levels of VacA were similar in the normalized preparations from WT and modified strains. In comparison to i2 VacA, i1 VacA bound more avidly to the cells (Figure 18A, bottom). Additionally, we tested the binding of VacA proteins produced by *H. pylori* strain X47 (X47 WT VacA [i2] and X47 i1C). Consistent with the results obtained when analyzing VacA proteins produced by strain 60190, the WT VacA i2 protein from strain X47 exhibited decreased avidity of binding compared to the i1C VacA protein (Figure 18B, bottom).

As another approach for analyzing VacA binding, we quantified VacA binding to Jurkat cells using a flow cytometry-based assay. For these experiments, we used recombinantly expressed p33 and p55 VacA domains. We have previously shown that p33 can facilitate the binding of purified p55 to HeLa cells (*87, 201*). Therefore, in the current experiments, we labeled the recombinant VacA p55 protein with Alexa 488, as described previously (*201*), and mixed the labeled p55 protein with either unlabeled p33 i1 or unlabeled p33 i2 protein (1:1 mass ratio). These protein mixtures were incubated with Jurkat cells for 1 h at 4°C, and cells were then washed and analyzed by flow

cytometry. When combined with unlabeled p33 i1, the labeled p55 protein bound more avidly to Jurkat cells than when the labeled p55 protein alone was added to Jurkat cells (Figures 18C and 18D). The labeled p55 protein bound significantly less avidly when mixed with p33 i2 than when mixed with p33 i1 (Figures 18C and 18D). Representative histograms are presented in Figure 18C, and quantification of levels of VacA binding is shown in Figure 18D. Collectively, these experiments indicate that, compared to type i2 forms of VacA, type i1 forms of VacA bind more avidly to Jurkat cells.

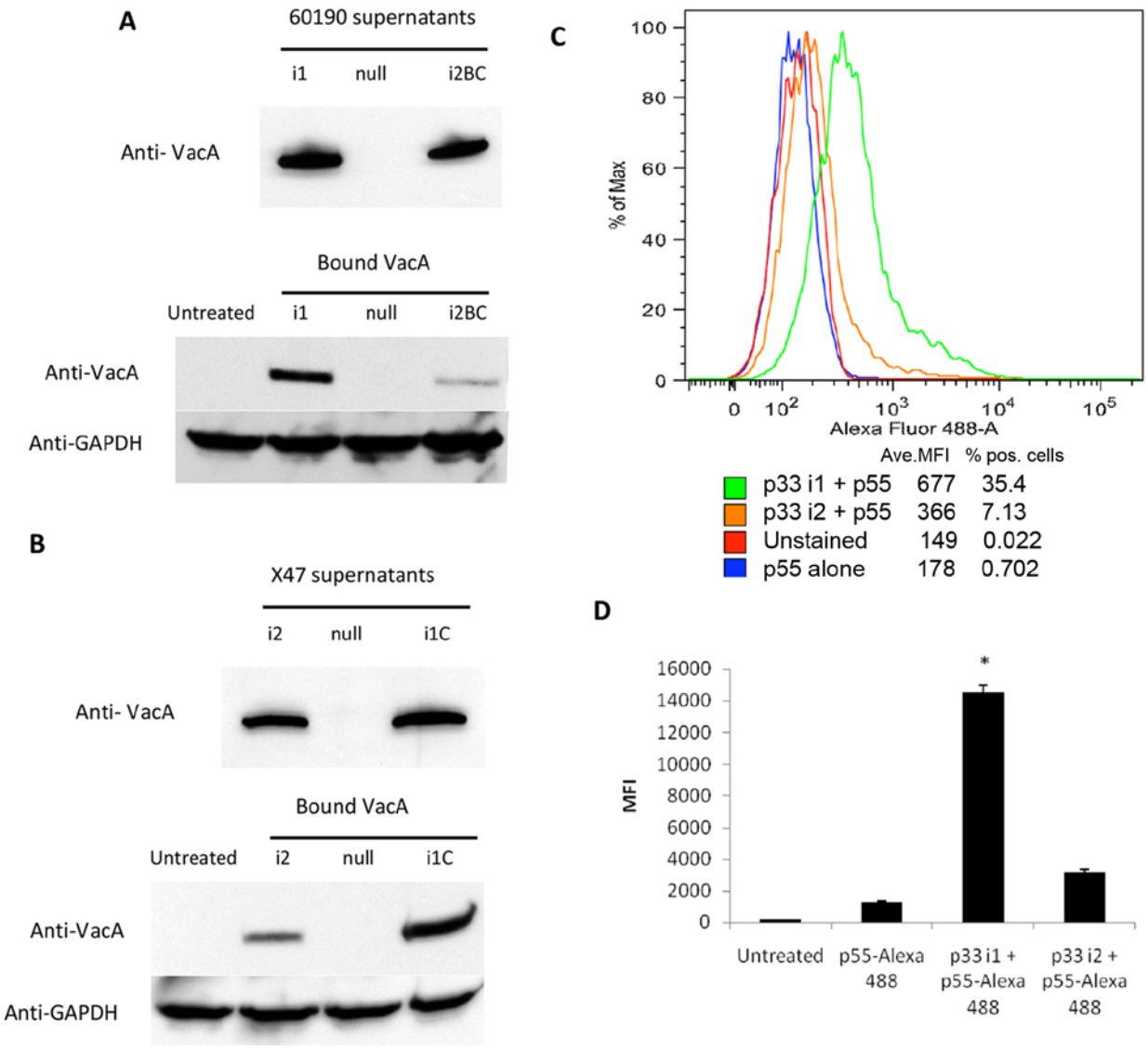
A
60190 supernatants
i1
null
i2BC
Anti- VacA
Bound VacA
Untreated
i1
null
i2BC
Anti-VacA
Anti-GAPDH
B
X47 supernatants
i2
null
i1C
Anti- VacA
Bound VacA
Untreated
i2
null
i1C
Anti-VacA
Anti-GAPDH
C
% of Max
Alexa Fluor 488-A
Ave.MFI % pos. cells
p33 i1 + p55 677 35.4
p33 i2 + p55 366 7.13
Unstained 149 0.022
p55 alone 178 0.702
D
MFI
Untreated
p55-Alexa 488
p33 i1 + p55-Alexa 488
p33 i2 + p55-Alexa 488

FIGURE 18: Binding of VacA proteins to Jurkat cells. *H. pylori* strains were cultured in broth, and culture supernatant preparations were standardized so that they contained equivalent concentrations of VacA. Jurkat cells were incubated with supernatant preparations from the indicated *H. pylori* strains for 1 h at 4°C. Cells were washed and lysed, and protein samples were then analyzed by immunoblotting using an anti-VacA antibody. (A) Analysis of WT *H. pylori* strain 60190 (expressing i1 VacA), 60190 *vacA*-null mutant strain, and 60190 i2BC (expressing i2BC VacA). (B) Analysis of WT *H. pylori* strain X47, X47 *vacA*-null mutant strain, and strain X47 i1C. Top panels (labeled "60190 supernatant" and "X47 supernatant") depict immunoblot analysis of *H. pylori* supernatant preparations prior to the addition to Jurkat cells. Bottom panels (labeled "Bound VacA") depict VacA binding to Jurkat cells. GAPDH was analyzed as a loading control. (C) Jurkat cells were treated with purified Alexa 488-labeled p55 (2.5 μg/ml) plus either purified p33 i1 or p33 i2 (2.5 μg/ml) for 1 h at 4°C. After treatment, cells were washed and analyzed by flow cytometry. Values indicate mean fluorescence intensity (MFI), based on three independent samples, and the percent positive cells (% pos. cells), defined as the proportion of cells exhibiting detectable fluorescence in comparison to control cells. Representative histograms depicting VacA binding are shown. (D) Graphical representation of VacA binding to Jurkat cells, based on flow cytometry analysis. These data are from an experiment performed on a separate day compared to the data in panel C. *, *P* value of ≤ 0.05 compared to p33 i2 and p55 Alexa 488, as determined by using Student's *t* test. Results represent the means ± standard deviations of triplicate samples from a single experiment.

Binding of type i1 and i2 VacA to β2 integrin

Previous studies have shown that β2 integrin is a receptor for VacA in T cells (*174*). We hypothesized that the observed difference in binding of i1 and i2 VacA proteins to Jurkat cells might be due to differences in the binding of these proteins to β2 integrin. To test this hypothesis, we performed an ELISA-based binding assay as described in Materials and Methods. Both VacA i1 and VacA i2 proteins bound to αMβ2 integrin in a dose-dependent manner, and no significant differences in binding avidity were detected (Figure 19). As expected, both forms of VacA bound less avidly to a control protein (αVβ3 integrin) than to αMβ2 integrin. Taken together, these results suggest that the observed difference in binding of i1 and i2 VacA proteins to Jurkat cells is not attributable to differences in VacA binding to the β2 integrin receptor.

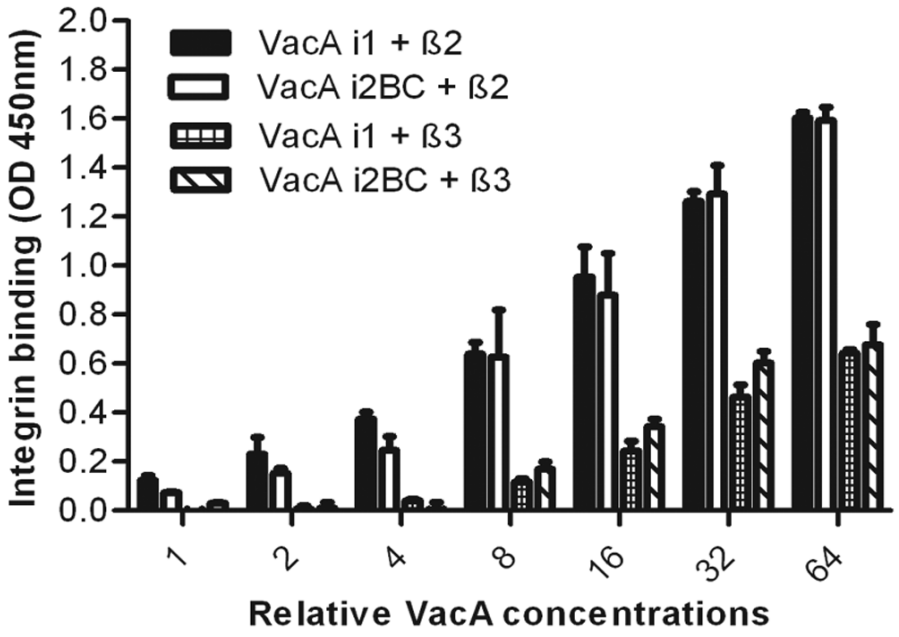

FIGURE 19: Binding of type i1 and i2 VacA proteins to β2 integrin. Wells of microtiter plates were coated with αMβ2 integrin or αVβ3 integrin as described in Materials and Methods. Serial dilutions of culture supernatants from *H. pylori* 60190 strains, containing equivalent concentrations of either WT (i1) or i2BC forms of VacA, were then added and incubated for 1 h. Unbound protein was removed, wells were washed, and VacA binding was analyzed by ELISA, as described in Materials and Methods. The background absorbance (VacA binding to wells in the absence of integrin) was subtracted from all absorbance values. Results represent the means ± standard deviations of triplicate experiments and are representative of three independent experiments.

Discussion

VacA is one of the most important virulence factors produced by *H. pylori* (*73, 202-204*). Numerous studies have shown that *H. pylori* strains containing specific *vacA* types (such as s1 or m1) are associated with a higher risk of gastric disease than are strains containing s2 or m2 *vacA* types (*205*). Correspondingly, type s1/m1 forms of VacA exhibit increased cytotoxic activity *in vitro* compared to type s2/m2 forms of VacA (*52, 90-91*). Recently, it was reported that strains containing the type i1 forms of *vacA* are associated with a higher risk of gastric disease than are strains containing type i2 forms of *vacA* (*56-62*). One study reported that the i-region is a determinant of cell-type specificity (*56*), but thus far there has been very little study of the role of the i-region in VacA activity. In the current study, we tested the hypothesis that VacA i1 and i2 proteins differ in the ability to cause functional alterations in T cells, using Jurkat cells as a model cell line.

In accordance with a previous study (*56*), we found that both i1 and i2 forms of VacA caused vacuolation of RK13 cells. Both the i1 and i2 VacA proteins inhibited IL-2 secretion and NFAT activation in Jurkat cells, but the i2 VacA proteins had a reduced potency. Type i1 VacA proteins bound more avidly than type i2 VacA proteins to Jurkat cells, and this difference in binding probably accounts, at least in part, for the observed difference in activity. Previous studies have shown that binding of VacA to epithelial cells is mediated not only by the p55 domain but also by the p33 domain (*87, 201*). The results in the current study provide additional evidence that the VacA p33 domain contributes to VacA cell-binding properties.

The observed difference in the binding properties of i1 and i2 VacA suggest that these proteins might differ in binding to a specific receptor on the surface of Jurkat cells. As shown in Figure 19, we did not detect any significant difference in the binding of type i1 and i2 VacA to β2 integrin, which is an important receptor for VacA on T cells (*174*). This result suggests that the i-region might be involved in VacA binding to alternate receptors which have not yet been characterized (*174, 176*). Various candidates for these alternate receptors include sphingomyelin, GPI-anchored proteins, or glycolipids (*174, 176*). Further studies will be required to better understand the basis for the differential binding properties of i1 and i2 forms of VacA.

Type i1 and type i2 forms of VacA differ in amino acid sequences at a relatively small number of sites within polymorphic clusters A, B, and C, and these polymorphisms account for most of the sequence variation that is observed within the VacA p33 domain (*54*). Experiments in the current study indicate that polymorphisms in cluster C are important determinants of VacA activity in a Jurkat T cell assay. Prior to the current study, a random mutagenesis study revealed that mutations in two amino acids in close proximity to this region (T210A, S246L) altered the capacity of VacA to cause vacuolation in HeLa cells (*93, 206*). Taken together, these studies highlight the functional importance of this region of the p33 domain. At present, a crystal structure is available for the p55 domain of VacA (*99*), but no structural data are available for the p33 domain. In future studies, it will be important to determine the structure of the p33 domain and to investigate the structural basis for the observed differences in activity of type i1 and i2 forms of VacA. In addition, it will be important to determine whether the VacA i-region

influences the potency of other VacA activities, including a spectrum of alterations produced by VacA in gastric epithelial cells and several types of immune cells (*73*).

It is striking that within three different regions of VacA (s-, i-, and m-regions), there is marked sequence variation among proteins expressed by different *H. pylori* strains, and analysis of each region indicates the existence of two main groups of VacA proteins categorized as type 1 (s1, i1, m1) and type 2 (s2, i2, m2) (*52, 54, 56, 207*). In each case, the sequence variations are associated with differences in VacA activity toward host cells (*52, 56, 89-91, 100-103*). It may be presumed that selective forces had an important role in the origin of these variations, as well as in the maintenance of the different allelic variants (*54*). In future studies, it will be important to determine how these different forms of VacA each provide a selective advantage to *H. pylori*.

CHAPTER 4

CRYSTALLIZATION OF THE VACA TOXIN

Introduction

The secreted pore-forming toxin known as VacA is considered one of the most important virulence factors produced by *H. pylori*. This toxin causes multiple alterations in host cells, and has been associated with *H. pylori*-related disease. The p33 domain is important for most VacA-related cellular alterations, but the structure of the p33 domain has not been determined. The availability of the p33 domain structure would provide insights into the mechanism of action of VacA, and would fill an important gap in our knowledge of the VacA toxin. In this chapter I will present experimental data describing our efforts to crystallize the VacA toxin.

Materials and Methods

Bacterial strains and growth conditions

Plasmids were propagated in *E.coli* DH5α. His-tagged recombinant proteins were expressed in *E.coli* BL21 (DE3) (supplemented with kanamycin), and maltose binding protein (MBP)-tagged recombinant proteins were expressed in *E.coli* Neb Express (supplemented with Ampicillin). *H. pylori* strains were grown as described previously (*92, 107*). Briefly, *H. pylori* 60190 strains producing WT VacA or VacA Δ6-27 were grown on Trypticase soy agar plates containing 5% sheep blood at 37°C in ambient air containing 5% CO^2. *H. pylori* mutant strains (*H. pylori ΔrdxA, H. pylori vacA::cat rdxA,*

and *H. pylori* producing VacA Δ346-347 with a strep tag) were grown on Brucella agar plates containing 10% FBS, supplemented with metronidazole (3.75 μg/ml) or chloramphenicol (5 μg/ml) when indicated. *H. pylori* liquid cultures were grown in Brucella broth supplemented with 1X cholesterol (BB-cholesterol) as described previously (*208*). Cholesterol was purchased from Gibco as a 250X solution, and a specific concentration was not given by the manufacturer.

Mutagenesis of recombinant proteins

Multiple constructs for the expression of recombinant VacA proteins were generated (see Table 1) by a mutagenesis approach as described in Chapter 3.

Purification and refolding of VacA recombinant proteins

Recombinant 6X His-tagged proteins, and an MBP/His-tagged p33 protein (containing an MBP at the N-terminus and a 6X His tag on the C-terminus, and designated as MBP-H3C-p33tail-His tag) (Table 1), were purified as described in Chapter 2. Briefly, proteins were expressed by culturing *E. coli* BL21 (DE3) (for His-tagged proteins), or *E. coli* Neb Express (MBP/His-tagged p33 protein) in TB (supplemented with kanamycin for His-tagged proteins and ampicillin for MBP/His-tagged p33 protein) at 37°C overnight with shaking. Cultures were diluted 1:100 in TB (supplemented with kanamycin for His-tagged proteins and ampicillin for MBP/His-tagged p33 protein) and grown at 37°C until they reached an A_{600} of 0.6. Cultures were induced with a final IPTG concentration of 0.5 mM and incubated at 37°C for 3 h. The proteins were purified under denaturing conditions from inclusion bodies by using Ni-affinity resin (Novagen), and were then refolded by dialysis. Finally, the proteins were purified further by gel filtration chromatography. Gel filtration was performed using

either Superdex 200 10/300 GL high-resolution resin or Superdex 200 10/300 prep grade resin, equilibrated in 55 mM Tris (pH 8.0), 21 mM NaCl, 0.88 mM KCl, 800 mM guanidine, and arginine (either 800 or 250 mM). Purification under native conditions using MBP-tagged proteins was unsuccessful. We attempted to refold MBP-tagged proteins, but the refolded protein did not bind to amylose beads.

Table 3: Recombinant VacA constructs

Constructs	Plasmid Description	Expression/ Purification	Activity
His-tagged*			
p33	Expresses a WT VacA p33 domain (amino acid 1 to 312) derived from *H. pylori* 60190 strain	Yes/Insoluble	Active w/ p55
p33 Δ6-27	Similar to p33 but contains a deletion of amino acid 6 to 27	Yes/Insoluble	D.N.° w/p33-p55
p33 Δ49-57	Similar to p33 but contains a deletion of amino acid 49 to 57	Yes/Insoluble	D.N. w/p33-p55
p33 i2C	Similar to p33 but contains an i-region in which cluster C has been changed to a type i2	Yes/Insoluble	Active w/ p55
p33 i2BC	Similar to p33 but contains an i-region in which cluster BC has been changed to a type i2	Yes/Insoluble	Active w/ p55
p33 tail	Similar to p33 but contains the C-terminus of the p55 domain (amino acids 727 to 821)	Yes/Insoluble	Active w/ p55
p33 (1-99)	Contains amino acids 1 to 99 from p33	No	
p33 (1-99) tail	Contains amino acids 1 to 99 from p33, plus the C-terminus of the p55 domain (amino acids 727 to 821)	Yes/Insoluble	N.A.ˇ w/p88 100-821
p33 (28-312)	Contains amino acids 28 to 312 from p33	No	
p33 (28-312) tail	Contains amino acids 28 to 312 from p33, plus the C-terminus of the p55 domain (amino acids 727 to 821)	Yes/Insoluble	N.A. w/p88 100-821
p33 (100-312)	Contains amino acids 100 to 312 from p33	No	
p33 (100-312) tail	Contains amino acids 100 to 312 from p33, plus the C-terminus of the p55 domain (amino acids 727 to 821)	Yes/Insoluble	N.A. w/ p88 100-821
p42 (1-478)	Expresses p33, plus a portion of the p55 domain (amino acids 313 to 478)	Yes/Insoluble	Active w/ p55
p42 12X His	Similar to p42 but contains a 12X His-tag	Yes/Insoluble	D.N. w/p33-p55
p42 Δ6-27	Similar to p42 (1-478) but contains a deletion of amino acid 6 to 27	Yes/Insoluble	D.N. w/p33-p55
p60 (1-600)	Expresses p33, plus a portion of the p55 domain (amino acids 313 to 600)	Yes/Insoluble	Active w/ p55
p88	Expresses a WT VacA p88 domain (Amino acid 1 to 821)	Yes/Insoluble	Active w/ p55
p88 100-821	Similar p88 but contains a deletion of amino acids 1 to 100	Yes/Insoluble	N.A. w/ p88 100-821
p88 Δ6-27	Similar to p88 but contains a deletion of amino acid 6 to 27	Yes/Insoluble	Not tested
p88 d2	Similar to p88 but contains a d-region type i2	Yes/Insoluble	Not tested
p88 (N-term His)	Similar to p88 but contains the His-tag in the N-terminus	No	
MBP-tagged^			
MBP p33 LL	Expresses MBP and WT VacA p33 domain (similar to p33), the linker between the MBP and p33 is 35 amino long	Yes/Insoluble	
MBP p33 tail LL	Similar to p33 LL but the p33 domain contains the C-terminus of the p55 domain (amino acids	Yes/Insoluble	

	727 to 821)	
MBP p33 ML	Similar to MBP p33 LL but contains a 7 amino acid linker	Yes/Insoluble
MBP-p33 SL	Similar to MBP p33 LL but contains a 3 amino acid linker	Yes/Insoluble
MBP p33 (1-99)	Expresses MBP and amino acids 1 to 99 from p33	Yes/Insoluble
MBP p33 (1-99) tail	Similar to MBP p33 (1-99) but contains the C-terminus of the p55 domain (amino acids 727 to 821)	Yes/Insoluble
MBP-H3C-p33 tail-His	Similar to MBP p33 tail LL but the linker is an H3C proteolytic site, and the p33 has a His tag at the C-terminus	Yes/Insoluble

*C-terminus tagged (unless otherwise stated), cloned into pET 41b, and expressed in BL21 DE3 E. coli cells
° D.N. stands for dominant negative test as described in Materials and Methods
ˇ N.A. stands for no activity
^ N-terminus tagged, cloned into pMAL, and expressed in NEB Express E. coli cells

Expression of VacA strep tag Δ346-347 in *H. pylori*

An *H. pylori* 60190 strain designated as *H. pylori* VacA strep tag Δ346-347 was constructed by a mutagenesis approach as described in Chapter 3. As a first step, we constructed a plasmid encoding a strep tag (WSHPQFEK) in VacA (amino acids 308 to 315 from *H. pylori* strain 60190), and harboring a deletion of amino acids 346 and 347 (Δ346-347). The plasmid was sequenced to ensure that unintentional mutations were not introduced. As a next step, an *H. pylori vacA::cat rdxA* strain (described in table 1 of chapter 3) was transformed with the VacA strep tag Δ346-347 plasmid, and transformants resistant to metronidazole were selected. The presence of the strep tag, and the deletion of amino acid 346 and 347, was confirmed by PCR and nucleotide sequence analysis of PCR products. VacA expression was confirmed by immunoblot analysis.

VacA expression and secretion

H. pylori strains were cultured in BB-cholesterol for 24 h (*208*). To test VacA expression, bacteria were pelleted and resuspended in SDS loading buffer. To test secretion, the culture supernatant was mixed with SDS loading buffer. The samples were then electrophoresed on a 4 to 20% gradient precast acrylamide gel (Bio-Rad) and transferred onto nitrocellulose membranes. Membranes were immunoblotted with rabbit anti-VacA serum (serum number 958, diluted 1:10,000) followed by horseradish peroxidase-conjugated secondary antibody (Promega, diluted 1:10,000). Immune complexes were revealed by using an enhanced chemiluminescence system (ECL Western Blotting Analysis System; GE Healthcare).

Purification of *H. pylori* VacA

For experiments using purified WT VacA and VacA Δ6-27, VacA oligomers were purified from *H. pylori* culture supernatants as described previously(*92, 107*). For purification of VacA strep tag Δ346-347, a modified protocol from Schmidt et al (*209*) was developed. As a first step, a seed culture of *H. pylori* VacA strep tag Δ346-347 was inoculated in BB-cholesterol and grown for 24 h. Cultures were then diluted 1:50 in BB-cholesterol, and grown for an additional 48 h. As a next step, *H. pylori* cultures were centrifuged and the supernatants were brought to a 50% saturation with ammonium sulfate. The proteins were then pelleted by centrifugation, resuspended in PBS buffer, and dialyzed into buffer A (50 mM Tris, 150 mM NaCl, 1 mM EDTA). The dialyzed proteins were incubated with Strep-Tactin resin (Quiagen), and loaded into a gravity column. Finally, the proteins were extensively washed with buffer A, and VacA was eluted with buffer B (50 mM Tris, 150 mM NaCl, 1 mM EDTA, 5 mM D-desthiobiotin).

Cell culture assays

Cell culture assays were done as described in Chapter 2. Briefly, HeLa cells were grown in minimal essential medium (modified Eagle's medium containing Earle's salts) supplemented with 10% FBS in a 5% CO_2 atmosphere at 37 °C. For vacuolating assays, HeLa cells were seeded at a density of 1.2×10^4 cells/well into 96-well plates 24 h prior to the addition of VacA proteins. To test for vacuolation activity using recombinant proteins, preparations of purified proteins (e.g. p33 plus p55 or mutant p33 proteins plus p55) were premixed in a 1:1 mass ratio (as described in Table 1). The proteins mixtures were then added to the tissue culture medium overlying HeLa cells (supplemented with 10 mM ammonium chloride) and incubated overnight at 37 °C. VacA-induced cell

vacuolation was detected by inverted light microscopy and quantified by a neutral red uptake assay. For dominant negative activity assays we tested the ability of the refolded p33Δ6−27, p33Δ49-57, p42 (1-478) Δ6-27, or VacA strep tag Δ346-347 to inhibit the activity of WT VacA. For *H. pylori* VacA strep tag Δ346-347 the proteins were acid activated by the slow addition of 200 mM HCl until a pH of 3.0 was reached, prior to addition to the cells.

Circular dichroism

H. pylori purified WT VacA and VacA strep tag Δ346-347 were diluted to 0.3 mg/ml in PBS and Buffer B (50 mM Tris, 150 mM NaCl, 1 mM EDTA, 5 mM D-desthiobiotin), respectively. Spectra were acquired with a Jasco J-810 CD spectropolarimeter at room temperature in a quartz cell with an optical path length of 0.1 cm. The spectra were recorded in the 190 to 260 nm wavelength range, using a 1 nm bandwidth and a 1 s time constant at a scan speed of 100 nm/min. The signal-to-noise ratio was improved by the accumulation of at least 5 scans.

Electron microscopy

Electron microscopy experiments were done in collaboration with the Ohi lab using a method described in Chapter 2. In summary, VacA proteins (2.5 μL of a 25 μg/mL protein solution) were spotted onto glow-discharged copper-mesh grids (EMS). The grids were then washed, and stained in 0.7% uranyl formate. Images were collected on an FEI morgagni run at 100 kV at a magnification of 36000×, and recorded on an ATM 1Kx1K CCD camera.

Crystallization and diffraction

Crystallization and diffraction was done in collaboration with the Lacy and Spiller lab. For crystallization trials using recombinant p33 proteins, we concentrated the proteins in 50 mM Tris, 21 mM NaCl, 250 mM arginine, and 800 mM guanidine buffer. We extensively attempted to reduce the amounts of guanidine and arginine in the buffer, but reducing the concentrations of these components caused the proteins to precipitate from solution. Mixtures of recombinant p33 and p55 (or the indicated mutants, see Table 2) were concentrated as described above, but the individual proteins were pre-mixed prior to concentration. For crystallization trials using *H. pylori* VacA Δ6-27, oligomeric VacA was concentrated in PBS buffer. For crystallization trials using VacA strep tag Δ346-347, the protein was concentrated in buffer B (50 mM Tris, 150 mM NaCl, 1 mM EDTA, 5 mM D-desthiobiotin). Once the protein was concentrated to at least 5 mg/ml, various commercially available (Hampton Research, QIAGEN) crystallization screens were set up using a Mosquito nanoliter dispensing high-throughput robot (see Table 2). The trays were set at 21˚C by the sitting drop method in which protein and precipitant were mixed in a 1:1 ratio. A hanging drop method was further used to optimize for VacA strep tag Δ346-347 crystals. X-ray data were collected from single crystals at 100 K on beamline 21G at the Advanced Photon Source (Argonne, IL).

Results

Crystallization trials with recombinant VacA

Chapter 2 described the development of methods to express, purify, and refold recombinant forms of the p33 domain (WT p33 and p33 Δ6-27). As an initial step to structurally characterize the p33 domain, we attempted to crystallize these proteins, but were unable to obtain crystals (Table 2). In an effort to express a soluble form of the p33 domain, we engineered multiple VacA–encoding plasmids. Surprisingly, all of our recombinant VacA proteins expressed as insoluble proteins (Table 1). Many of these proteins were purified and refolded, and caused vacuolation of HeLa cells when mixed with purified p55 (Table 1). These results suggested that the purified p55 domain could promote folding of the p33 domain. To test whether this was indeed the case, we constructed a p33 protein which contained the p33 domain plus the C terminus of the p55 domain (designated as p33tail). We purified, refolded, and set crystallization trays with the p33 tail protein, but the protein did not crystallize (Table 2). As an alternative way to test our hypothesis, we mixed refolded p33 with purified p55, refolded p33 Δ49-57 with purified p55 (non-oligomerizing mutant), and refolded p33 with purified p55 Δ346-347 (non-oligomerizing mutant), and set crystallization trays with the mixed proteins. Similar to our previous results, we were unable to obtain crystals (Table 2).

Table 4: Crystallization trials with VacA proteins

Protein source	Crystallization conditions tested	Crystals
Recombinant		
p33	Crystal Screen 1&2, Index Screen,and JCSG screen	No
p33 Δ6-27	Crystal Screen 1&2, and Index	No
p33 ACD	Crystal Screen 1&2, and Index	No
Recombinant Mixed proteins		
p33 Δ49-57 + p55	Crystal Screen 1&2, Index Screen, and JCSG screen	No
p33 + p55 Δ346-347	Crystal Screen 1&2, Index Screen, and JCSG screen	No
H.pylori		
VacA Δ6-27*	Crystal Screen 1&2, Index Screen	No

* Trays were set with protein at both neutral and low pH

Purification of *H. pylori* VacA

Our inability to crystallize recombinant VacA p33 proteins led us to explore the use of *H. pylori* purified VacA. We started these studies by trying to crystallize an oligomeric form of *H. pylori* VacA (VacA Δ6-27), but were unsuccessful (Table 2). Previous studies have shown that VacA oligomers can have multiple conformations, which can make the protein sample heterogeneous and impede protein crystallization (*107-109*). To obtain a purified non-oligomeric form of VacA, we sought to make an *H. pylori* mutant strain that encoded a non-oligomerizing VacA protein. Previous studies have shown that VacA is incapable of oligomerizing if amino acids 49-57 from the p33 domain or 346-347 from the p55 domain are deleted (*113-114*). Therefore, we deleted amino acids 346-347 and inserted a strep tag into the *H. pylori* chromosomal *vacA* gene (see Materials and Methods). A schematic of the construct is shown in Figure 20A. To ensure that the presence of the strep tag and the deletion of amino acids 346-347 did not alter protein stability or impair VacA secretion, we tested protein expression and secretion by immunoblotting, as described in Materials and Methods. As expected, WT VacA was efficiently expressed and secreted, while a VacA null strain did not express or secrete VacA (Figures 20B and 20C). The VacA strep tag 346-347 was efficiently expressed and secreted (Figures 20B and 20C).

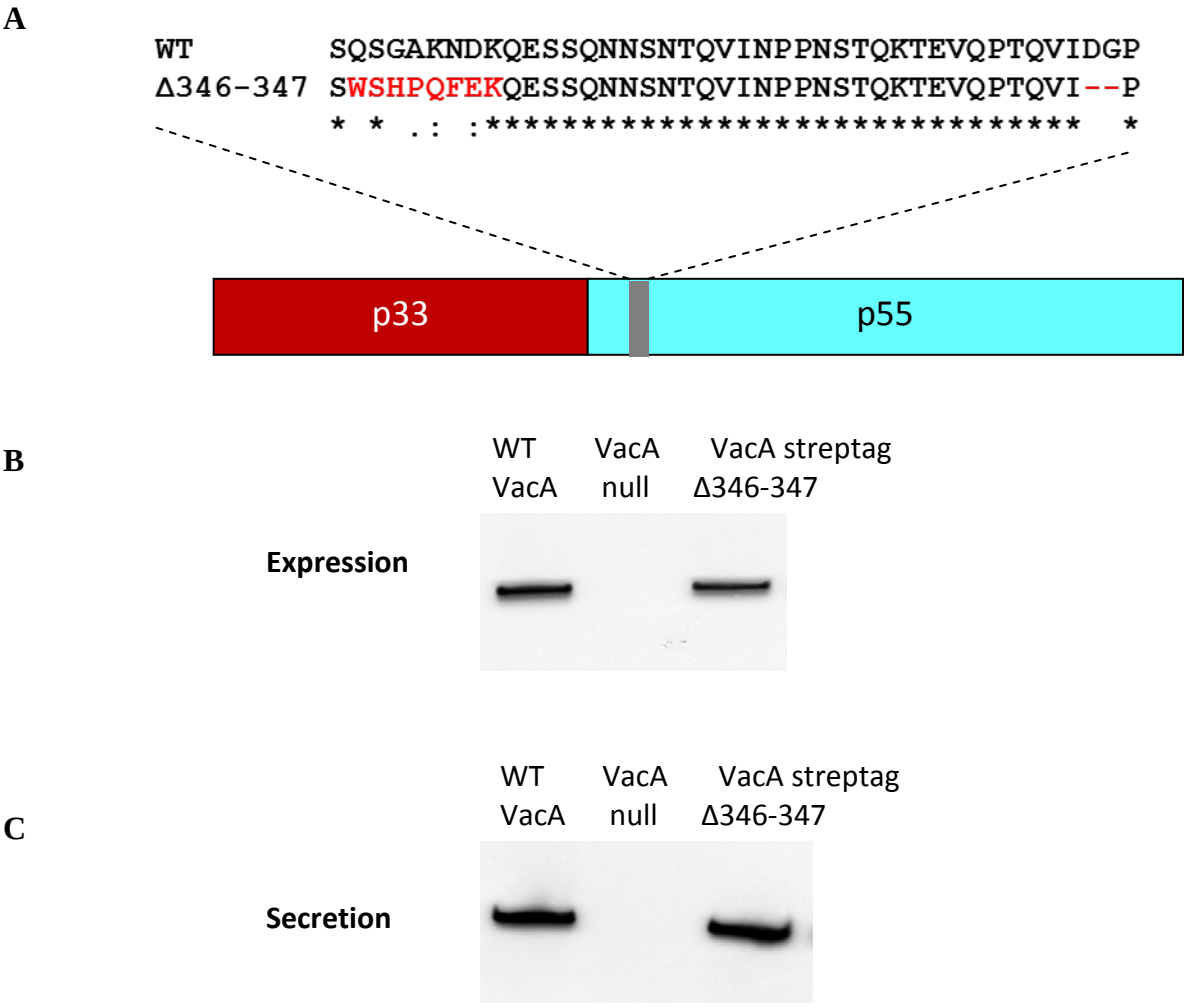

Figure 20: *H. pylori* VacA strep tag Δ346-347 construction. (A) A mutagenesis approach was used to insert a strep tag (amino acids 308-315) and delete amino acids 346 and 347 (Δ346-347) as described in Materials and Methods. The figure is a representation of the secreted p88 VacA containing the p33 and p55 domains, and the approximate location of the strep tag and Δ346-347. A comparison of the amino acids in the WT and strep tag Δ346-347 *H. pylori* strains is also shown. The strep tag and Δ346-347 are highlighted in red. (B) Immunoblot analysis of VacA (B) expression and (C) secretion in *H. pylori* producing WT VacA, VacA null, or *H. pylori* producing VacA strep tag Δ346-347.

Purification of *H. pylori* VacA strep tag Δ346-347

Previous analyses of non-oligomerizing VacA mutants have mainly been done using *H. pylori* culture supernatants, and previous efforts to purify such proteins were unsuccessful (*113-114*). Therefore, as a first step in trying to structurally analyze the VacA strep tag Δ346-347, we developed a purification system as described in Materials and Methods. Using this method, we were able to purify the VacA strep tag Δ346-347 as an approximate 88 kDa protein with minimal p33 and p55 breakdown (Figure 21A). Protein purification was confirmed by immunoblotting with anti-VacA and anti-strep tag antibodies (data not shown). We performed gel filtration chromatography experiments, but were unable to recover the protein (data not shown). To ensure that the protein did not aggregate or oligomerize, we analyzed the purified VacA strep tag Δ346-347 by electron microscopy. The VacA strep tag Δ346-347 had a rod-shaped appearance (Figure 21B). Previous studies have shown that *H. pylori* VacA assembles into flower shaped oligomers, and that acid treatment causes VacA oligomers to disassemble into possible monomers (*107*). To compare the macromolecular structure of VacA strep tag Δ346-347 with WT VacA, we performed electron microscopy on the oligomeric and acid-treated VacA (data not shown and Figure 21C). When compared, the VacA strep tag Δ346-347 had a similar appearance to the acid treated WT VacA (Figures 21B and 21C).

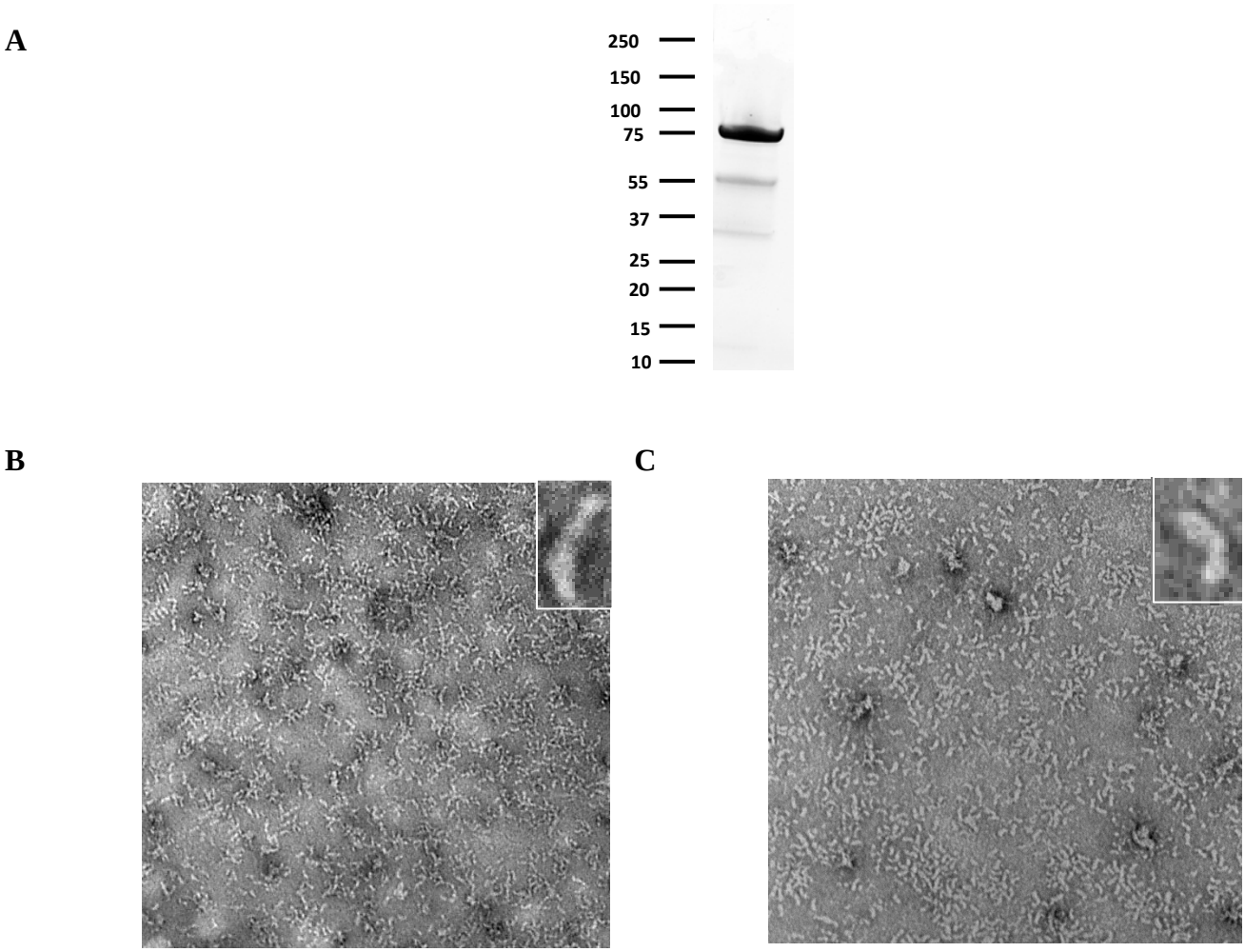

Figure 21: Purification of *H. pylori* VacA strep tag Δ346-347. (A) SDS-PAGE and Coomasie blue staining of the purified VacA strep tag Δ346-347. Electron microscopy analysis of purified (A) VacA streptag Δ346-347 and (B) acid treated WT VacA. Insets show a closeup of the grid.

Inhibitory activity of *H. pylori* VacA strep tag Δ346-347

A previous study by Ivie et al (*114*) demonstrated that deleting amino acids 346 and 347 caused the toxin to be inactive in a cell vacuolation assay. Furthermore, it was demonstrated that mixing supernatants from *H. pylori* strains expressing WT VacA and Δ346-347 resulted in inhibition of the activity of WT VacA (*114*). Therefore, the VacA Δ346-347 was categorized as a dominant negative mutant (*114*). To test whether our purified VacA strep tag Δ346-347 had a similar phenotype, we mixed purified WT VacA with purified VacA strep tag Δ346-347, and tested for vacuolating activity. As expected, adding purified WT VacA alone to HeLa cells caused extensive vacuolation, while adding the VacA strep tag Δ346-347 alone did not cause any detectable vacuolation (Figure 22). Consistent with results from by Ivie et al (*114*), we observed that mixing purified WT VacA with purified VacA strep tag Δ346-347 caused an inhibition in the activity of the WT VacA protein (Figure 22). These results suggest that the VacA strep tag Δ346-347 can interact with WT VacA.

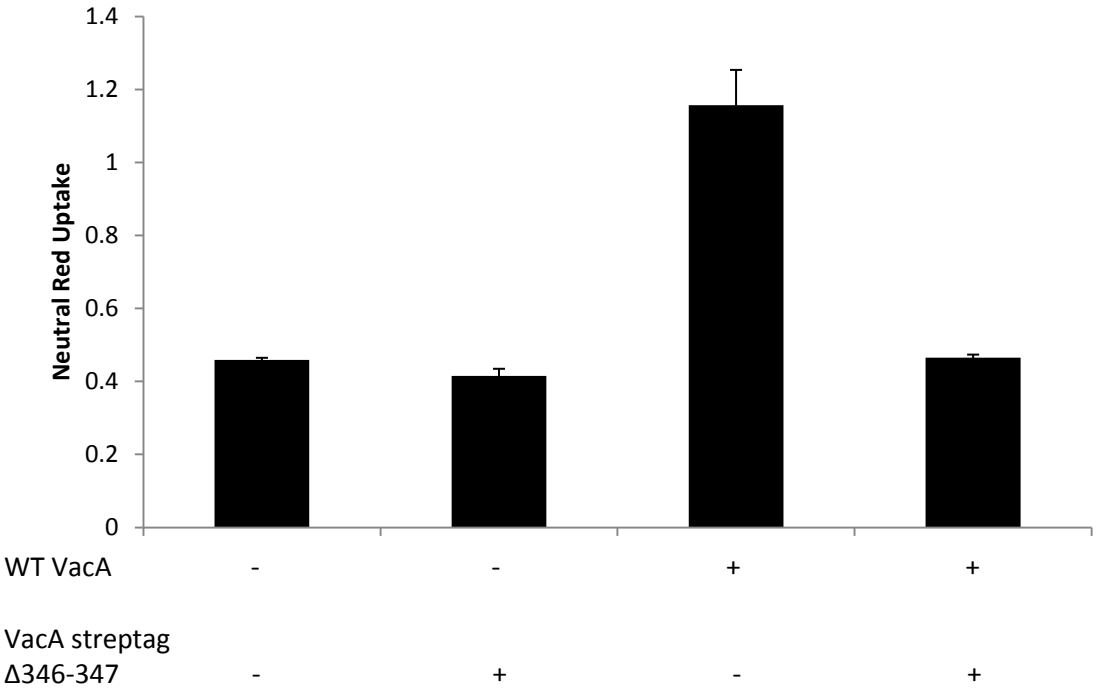

Figure 22: Inhibitory activity of *H. pylori* VacA strep tag Δ346-347. Purified VacA strep tag Δ346-347 (10 μg/ml) was mixed with WT VacA (2.5 μg/ml), and HeLa cells were then incubated with the indicated VacA proteins (either individually or in a mixture) for 9 h at 37°C. Cell vacuolation was quantified by the neutral red uptake assay.

Folding of the *H. pylori* VacA strep tag Δ346-347 protein

The observed expression, secretion, and dominant negative activity of VacA strep tag Δ346-347 all suggested that the protein is folded. To directly demonstrate proper folding, we performed circular dichroism experiments as described in Materials and Methods. We first obtained the spectra for oligomeric purified WT VacA. In agreement with a previous studies (*113*), the WT VacA had a negative band at around 220nm (Figure 23A). We then tested VacA strep tag Δ346-347 and obtained a spectra that was identical to the WT VacA (Figure 23B). Our results suggest that the VacA strep tag Δ346-347 protein is folded.

A

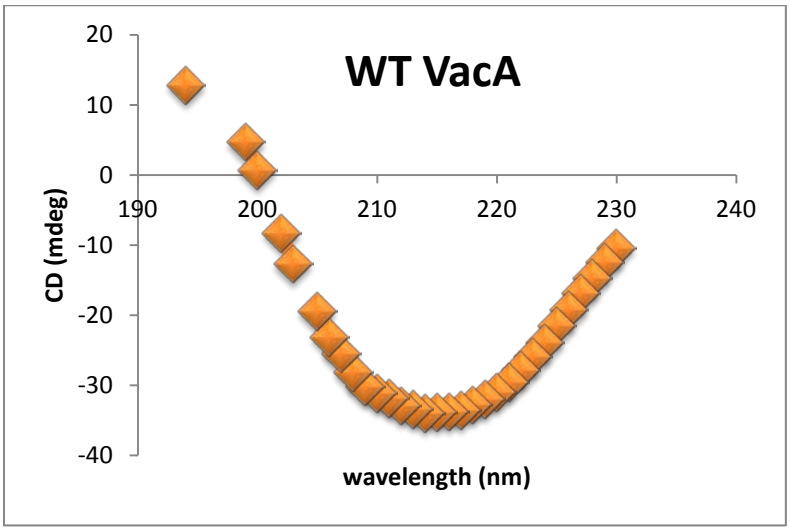

B

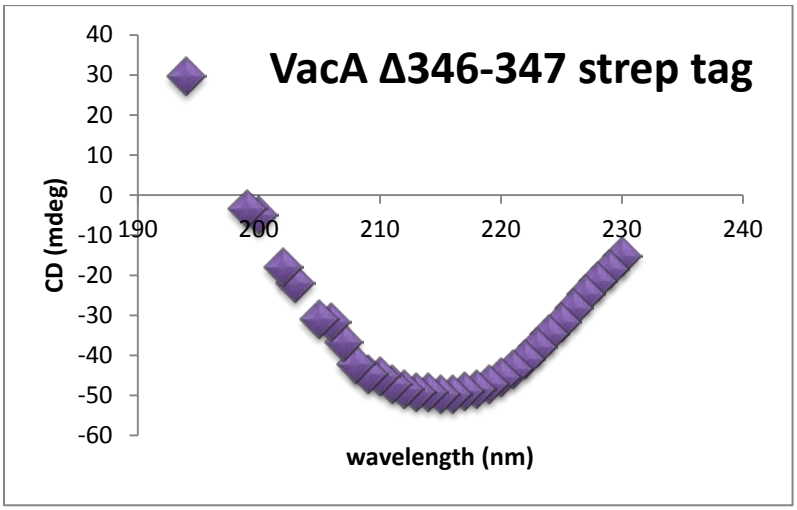

Figure 23: Folding of *H. pylori* VacA strep tag Δ346-347. Purified (A) WT VacA and (B) VacA strep tag Δ346-347 were diluted to 0.3 mg/ml and the spectra for the proteins were obtained as described in Materials and Methods

Crystallization of VacA strep tag Δ346-347

We then set out to crystallize the VacA strep tag Δ346-347, in collaboration with the Lacy lab. Our initial screen was done by the sitting drop method as described in Materials and Methods, and we tested over 1000 crystallization conditions. After 7 days we observed cube-form crystals in 4 conditions (condition 1, 1M Ammonuim sulfate/ 5% Isopropanol; condition 2, 1.5M Sodium chloride/ 10% Ethanol; condition 3, 1M Ammonium phosphate/ 100mM Sodium Citrate pH 5; and condition 4, 1M Sodium chloride/ 100mM Sodium acetate pH 4.6). To optimize and obtain larger crystals, we then set crystallization trays by the hanging drop method as described in Materials and Methods. From the 4 conditions that yielded crystals by sitting method, we were able to reproduce "condition 3" and "condition 4" using the hanging drop method. After further optimization of "condition 4", we obtained larger crystals, which diffracted to 4.5 A (Figure 24A and 24B). All the diffraction data were indexed, integrated, scaled, and merged with HKL2000 (Figure 24 B and Table 1). The crystals were spacegroup I23 with an a=b=c=330.7 Å cell edge. Molecular replacement using the 2.4 Å p55 domain of VacA (*99*) as our search model revealed a solution where each asymmetric unit has two monomers (Figure 24C). A packing arrangement of two monomers per asymmetric unit in a 330 $Å^3$ cubic I23 spacegroup indicates that the crystals are 88% solvent. While this is high, we observe a full array of crystal packing contacts that allow for the formation of the cubic spacegroup (Figure 24C), and we have not been able to identify convincing molecular replacement solutions that contain additional monomers. The resulting electron density map suggests that the β-helical structure of the p55 domain will extend into the C-terminal portion of p33 (Figure 24D).

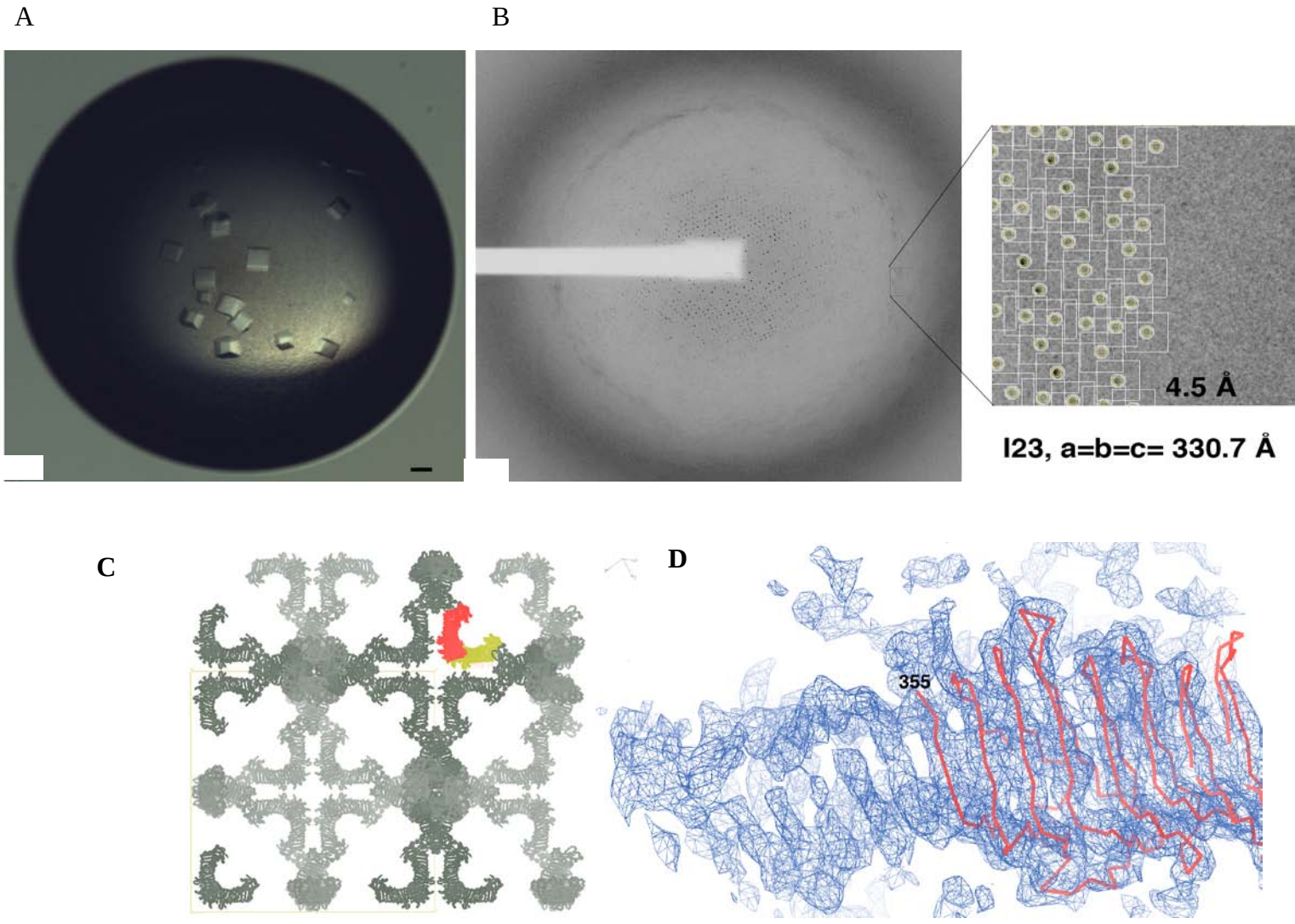

Figure 24: *H. pylori* VacA strep tag Δ346-347 crystallization. Purified VacA strep tag Δ346-347 was concentrated and crystallization trays were set as described in Materials and Methods.(a) Crystals of the VacA strep tag Δ346-347 can grow reproducibly in hanging drops within 3 days in 0.9-1.5 M sodium chloride and 0.1 mM sodium acetate pH 4.6 - 5. (b) The crystals diffract to 4.5 Å resolution at the synchrotron X-ray source. Molecular replacement using the 2.4 Å p55 domain [104] structure shows the (a) orientation of the protein in the crystals and (b) the density map for the p33-p55 junction.

Table 5: X-ray data collection statistics

Data Collection	VacA44
Unit Cell	330.7, 330.7, 330.7, 90, 90, 90
Resolution (outer shell), Å	50.0-4.5 (4.58-4.50)
R_{merge}*, %	10.9 (52.1)
Mean I/σI	10.4 (2.75)
Completeness, %	99.7 (97.8)
Redundancy	7.4 (6.6)
Unique observations	35776 (1747)

Outer resolution bin statistics are given in parentheses.

*$R_{merge} = \Sigma_{hkl}(\Sigma_i | I_{hkl,i} - \langle I_{hkl} \rangle)) / \Sigma_{hkl,i} \langle I_{hkli} \rangle$, where $I_{hkl,i,}$ is the intensity of an individual measurement of the reflection with Miller indices h, k and l, and $\langle I_{hkl} \rangle$ is the mean intensity of that reflection.

Discussion

Structural characterization of a protein requires its efficient purification and crystallization. Previously, the crystal structure of the VacA p55 domain was determined (*99*). In this study, our objective was to crystallize the p33 domain. In Chapter 2 we performed an extensive analysis of the VacA p33 domain, and were able to purify and refold a recombinant form of the p33 domain. As a first logical step we attempted to crystallize the refolded p33 domain (as described in Chapter 2), but were unsuccessful. One possible explanation is that the high concentrations of guanidine and arginine in the buffer could interfere with protein crystallization. We tried to reduce the amounts of guanidine and arginine in the buffer, but reducing the concentration of any of these components caused the protein to precipitate from solution. To avoid the refolding step, we preceded our studies by making and expressing various mutant forms of the p33 domain (Table 1). Many of these mutant proteins were engineered to contain fragments of the p55 domain. Our hypothesis was that these fragments could help improve solubility. However, we show that when tested for expression, none of the proteins were expressed in the soluble fraction (Table 3).

Interestingly, we were able to purify and refold mutant forms of the p33 domain and found that most of the proteins were active in a cell culture assay, only when mixed with purified p55. This was a rather unexpected finding, because when mixed together, some of the proteins (i.e. p33 tail, p42, and p60 [see Table 3]) had an overlap of at least 100 amino acids within the p55 domain. These experiments demonstrate that VacA toxin activity can be reconstituted in the presence of overlapping segments. Further experiments will be needed to determine the oligomeric arrangement and molecular

events that occur during the VacA reconstitution process. The fact that refolded p33 proteins were only active when mixed with purified p55 suggests that the purified p55 may be promoting the folding of a partially refolded p33 protein. To test this hypothesis we tried to crystallize p33-p55 mixtures, but were unsuccessful.

Recombinant proteins are a widely use tool in structural biology. However, based on our inability to express a soluble form of the p33 domain or crystallize the p33-p55 recombinant mixtures, we decided to test *H. pylori* purified VacA. The p88 VacA protein is typically purified in an oligomeric form from the *H. pylori* broth culture supernatant, and monomeric forms of p88 VacA have been relatively difficult to purify (*113-114*). Previous studies have shown that VacA can form many types of oligomers, which can make a VacA sample extremely heterogeneous (*107-109*). In fact many activity assays require the disassembly of VacA oligomers by the slow addition of acid (*107*). Therefore, we tried to crystallize both an oligomeric form of VacA and an acid treated purified VacA, but were unsuccessful. We found that in the VacA acid treated sample, the pH was raised in several of the crystallization conditions, which may have caused the protein to re-oligomerize or aggregate.

As an alternative approach to crystallize *H. pylori* purified VacA toxin, we were interested in analyzing non-oligomerizing forms of the VacA toxin. Thus far, it has been shown that deleting either amino acids 49 to 57 from the p33 domain or amino acids 346 to 347 from the p55 domain yields a non-oligomerizing VacA protein (*113-114*). These studies were mainly done using *H. pylori* broth culture supernatants (*113-114*). Therefore, in this study we developed a system for the purification of non-oligomerizing VacA mutants. Specifically, we manipulated the *H. pylori* chromosome using a method

described in Chapter 3, and inserted a strep tag into a *vacA* gene encoding a Δ346-347. We performed an extensive analysis of the purified protein and showed that the protein was efficiently expressed and secreted, had an inhibitory effect when mixed with WT VacA, and was correctly folded. We performed crystallization trials and for the first time we were able to crystallize a full length VacA toxin which contained a WT p33 domain. Furthermore, the VacA crystals diffracted to a 4.5 Å resolution. Further experiments will be necessary to obtain a high resolution structure of the VacA toxin.

A very high priority is to optimize our existing crystals for higher resolution diffraction (< 4 Å). Our preliminary experience in analyzing the diffraction properties of these crystals at the synchrotron indicates that the resolution improves as the size of the crystals increases. We will try a variety of techniques aimed at growing larger crystals. These include, but are not limited to, seeding, the incorporation of additives, adjustments in protein concentration and temperature, and moving from a hanging drop vapor diffusion experiment to sitting drop conditions and crystallization under oil. Datasets will be collected for all crystals that diffract better than 4.5 Å. The dataset that reflects a combination of high-resolution diffraction intensities with excellent scaling statistics (low R_{merge}, high signal-to-noise, high completeness and redundancy) will be used for structure determination.

CHAPTER 5

CONCLUSIONS

Summary and Conclusions

One of the most important virulence factors produced by *H. pylori* is the secreted toxin known as VacA. The toxin causes multiple alterations in host cells, and is considered a multifunctional toxin. VacA is secreted as an 88 kDa protein containing two domains designated as p33 and p55. The p55 domain has been shown to be important for binding to cells, and the crystal structure of this domain has been determined. When I initiated my studies of the VacA toxin, very few studies had directly analyzed the p33 domain, and the structure of the p33 domain had not been determined. The overall objective of my thesis work was to structurally and functionally analyze the p33 domain, in order to provide a better understanding of the mechanism of action of the VacA toxin.

In Chapter II, we expressed and purified a recombinant form of p33 under denaturing conditions and optimized conditions for the refolding of the soluble protein. We showed that refolded p33 could be added to purified p55 in trans to cause vacuolation of HeLa cells and inhibition of IL-2 production by Jurkat cells, effects identical to those produced by the p88 toxin from *H. pylori*. The p33 protein markedly enhanced the cell binding properties of p55. Size exclusion chromatography experiments suggested that p33 and p55 assembled into complexes consistent with the size of a p88 monomer. Electron microscopy of these p33/p55 complexes revealed small rod-shaped structures that converted into oligomeric flower-shaped structures in the presence of detergent. This

study was the first report of the purification of an active form of the VacA p33 domain. Our data highlighted the importance of the p33 domain in VacA activity and binding to cells, and showed that p33 contributes to the assembly of VacA oligomers.

In Chapter III, we compared the ability of i1 and i2 forms of VacA to cause functional alterations in Jurkat cells. To do this, we manipulated the chromosomal *vacA* gene in two *H. pylori* strains to introduce alterations in the region encoding the VacA i-region. We did not detect any differences in the capacity of i1 and i2 forms of VacA to cause vacuolation of RK13 cells. In comparison to i1 forms of VacA, i2 forms of VacA had a diminished capacity to inhibit NFAT and suppress IL-2 production. Correspondingly, i2 forms of VacA bound to Jurkat cells less avidly than did i1 forms of VacA. Our results indicated that the VacA p33 i-region is an important determinant of VacA effects on human T cell function, and specifically highlighted the importance of the p33 domain in VacA activity and binding.

In Chapter IV, we developed a method for the purification of a non-oligomeric *H. pylori* secreted VacA, which we designated as VacA strep tag Δ346-347. Immunoblot analysis showed that the VacA strep tag Δ346-347 was efficiently expressed and secreted. Electron microscopy revealed that the purified protein adopted a rod-shape form, which was similar to acid treated WT VacA. In agreement with results of a previous publication (*114*), the VacA strep tag Δ346-347 inhibited the activity of WT VacA in a cell vacuolation assay. Circular dichroism demonstrated that the protein was correctly folded, and crystallization trials were performed. The VacA strep tag Δ346-347 formed cube-like crystals that diffracted to 4.5 Å, and molecular replacement showed that a portion of the density map was consistent with the previously determined structure of

the p55 domain. These results provide a structural basis for the determination of a high resolution p88 VacA structure, which includes the p33 domain.

Collectively, my thesis work has provided important insights into the structure and function of the p33 domain. Functionally, my work has demonstrated the importance of the p33 domain in VacA activity and binding to epithelial and T cells. Structurally, my work has demonstrated the importance of the p33 domain in the formation of VacA oligomers, and has provided important structural data which will serve as a platform to determine a high resolution structure of the VacA toxin. Overall, our work has helped fill important knowledge gaps in the VacA toxin field. However, as expected with any scientific field, many questions remain unanswered. In my next section, I will discuss ongoing and future efforts to further understand the VacA toxin.

Future Directions

Analyze the mechanism by which VacA causes alterations in T cells:

VacA is considered an imumomodulatory protein, and in my thesis work I have shown that the p33 domain is important for VacA alterations in T cells. However, many important questions related to VacA-T cell interactions remain unanswered.

What is factor X? A previous study showed that integrin β2 is a receptor for VacA on T cells [180]. In the same report, the authors proposed that VacA could also bind to another receptor designated as factor X. In our analysis of the i-region, we observed differential binding of i1 and i2 VacA proteins to Jurkat cells, but our binding experiments showed that these differences were not β2 integrin dependent. On the other hand, sphingomyelin has recently been identified as a receptor for VacA in epithelial

cells (*121-122*), and a previous study showed that another pore forming toxin is capable of binding to sphingomyelin in Jurkat cells (*210-211*). Therefore, we hypothesize that the factor X in T cells is sphingomyelin. To test our hypothesis, we performed a pilot experiment using a flow cytometry binding assay. Specifically, we added VacA toxin to Jurkat cells that had been pretreated with sphingomyelinase. Then, we performed a binding assay as described in Chapter III. Compared to cells treated with buffer alone, we observed that pretreatment with sphingomyelinase caused VacA to bind less avidly to Jurkat cells. These preliminary results suggest that sphingomyelin is important for VacA binding to cells. As a followup to these studies, we could potentially knockdown a gene that is required for sphingomyelin synthesis, and test VacA binding. One candidate gene could be sphingomyelin synthase 1, which in a previous study was shown to be important for sphingomyelin production in Jurkat cells (*210*). As an alternative approach, we could perform a competition binding assay using a sphingomyelin binding protein (such as lysenin) and VacA (*210-213*).

Alternatively, it is possible that sphingomyelin is not factor X. As another approach to identify factor X, we could perform crosslinking, pulldown, and mass spectrometry experiments. Specifically, we would insert a strep tag into the WT VacA protein by a mutagenesis approach. We would then purify the tagged protein, add VacA to Jurkat cells, chemically crosslink the proteins, lyse the cells containing complexes, and analyze these complexes by mass spectrometry.

Does the i-region affect human T cells? We have been able to study the effect of the p33 i-region in Jurkat cells. The use of Jurkat cells presents certain drawbacks because these cells do not precisely mimic naturally occurring T cells. As another

approach to study VacA-T cell interactions, we began a collaboration with the Kalams lab, and our main objective was to analyze the effects of VacA on human T cells. We began this work by performing a pilot experiment which tested the effect of the i-region on IL-2 production by human T cells. Our preliminary results show that, similar to the Jurkat cell system, the i1 VacA was able to inhibit IL-2 production more efficiently than i2 VacA in human cells. Further experiments will be needed to confirm these results and optimize the assay. Once this assay is optimized and we are certain about our results, we could potentially analyze the effect of the i-region on T cell proliferation, NFAT activation, and VacA binding, using i1 and i2 VacA proteins. Additionally, we could test the activation of other cytokines, and test specific pathways that lead to this activation in human T cells.

To analyze the role of VacA in vivo, it would be necessary to use an animal model system; however, previous studies have shown that mouse T cells are not VacA sensitive (*175*). Another animal model system which has not been explored for VacA studies is the gerbil model. Unlike mice, gerbils develop gastric cancer when infected with *H. pylori* (*214-216*). In an effort to use the gerbil model for VacA studies, we isolated T cells from gerbil spleens, and attempted to stimulate cell proliferation using various compounds. None of the tested compounds stimulated gerbil T cells to proliferate, and this complicated efforts to assess effects of VacA on these cells. As one way to move forward, we could infect gerbils with *H. pylori* strains expressing various VacA forms (i.e. s1/i1/m1 or s2/i2/m2). This would permit us to test colonization, and various T cell markers (such as IL-2) by real time PCR.

What are specific VacA targets in T-cells? Previous studies have shown that VacA interacts with mitochondria in epithelial cells (*73, 118-120*). The effect of the VacA toxin on T cell mitochondria has not been analyzed in detail. To evaluate this, we could use a recombinant p33 protein tagged with a specific epitope; once tagged, we could add VacA to cells, allow for internalization, and perform pulldown experiments. This would allow us to identify specific intracellular VacA targets. Alternatively, we could perform confocal microscopy and assess colocalization with labeled mitochondrial proteins that have been shown to be important for VacA interactions in epithelial cells.

Analyze trafficking of the VacA toxin

What is the molecular mechanism for VacA trafficking in T cells and gastric cells? As a first step in VacA intoxication, the toxin binds to a receptor and is then internalized (*73*). VacA can potentially enter cells through various routes and localize in multiple sites (*73, 118-120*). Currently, the exact molecular mechanism for VacA trafficking has not been determined. Some studies propose that both the p33 and p55 interact with mitochondria (*154*). In contrast, other studies propose that the p33 is the only domain necessary for VacA-mitochondria interactions (*97-98*). Most of these studies have been done in gastric cells, and it will be necessary to establish if the same patterns of trafficking occur in T cells.

As a first step in trying to understand VacA trafficking, it will be necessary to test whether VacA breaks down into p33 and p55 within specific intracellular organelles. These studies could potentially be done by isolating cellular organelles from VacA-infected cells, and analyzing VacA breakdown by immunoblotting. As a next step, the

routes through which VacA travels could be tested. As a classical way to study trafficking, we could potentially perform immunofluorescence microscopy. As a pilot experiment to test whether this system would work with purified p33 and p55 proteins, we performed immunofluorescence microscopy using a mitochondrial labeling compound (Mitotracker) and a mixture of refolded p33 with Alexa488-labeled p55. Our results suggest that there is minimal colocalization of labeled p55 with mitochondria (Figure 25). These studies can be continued by monitoring colocalization of the p33 domain with mitochondria. Alternatively, we could label various intracellular targets, and monitor trafficking of the p33 and p55 domains. This system could then be adapted for use in T cells.

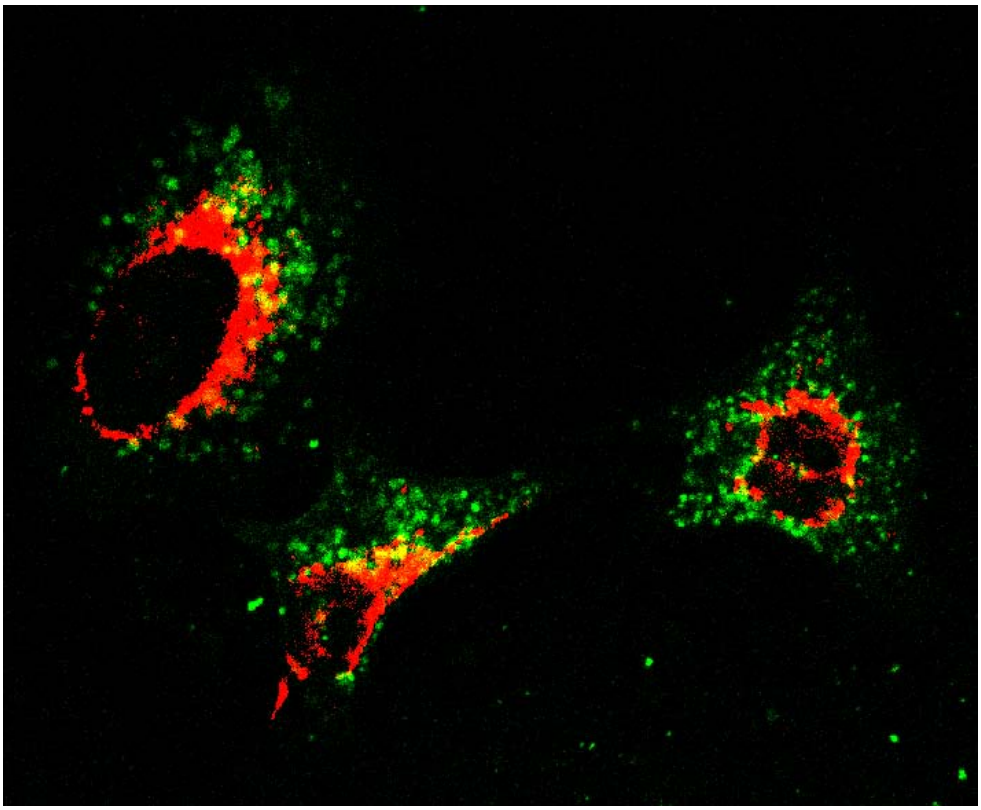

FIGURE 25: Analysis of VacA localization by immunofluorescence microscopy. Mitochondria from HeLa cells were labeled with Mitotracker (red). A mixture of purified p33 plus Alexa48-labeled p55 (green) was then added to cells, and after internalization, the sample was analyzed by microscopy.

Evaluate structural properties of the VacA toxin

What is the structure of the p33 domain? Given our recent success in crystallizing VacA, we expect that it will be feasible to determine a high resolution structure of the toxin. To accomplish this, I am optimizing crystallization conditions to obtain larger crystals that will diffract to a higher resolution. As an alternate approach, I have been generating *H. pylori* strains that secrete other non-oligomeric VacA mutant proteins. These mutants will contain a strep tag and will be purified as described in Chapter IV. Crystallization trials will then be conducted.

Assuming that we can determine a high resolution structure of the VacA toxin, an immediate followup could be to try to crystallize other VacA variants. These variants include the s2, i2, and m2 VacA forms. For these experiments, we would purify *H. pylori* secreted toxins as described in Chapter IV. In future studies it will also be of interest to try to co-crystallize VacA with candidate receptors, including sphingomyelin. Recently, the crystal structure of lysenin bound to sphingomyelin was determined (*211*), and the methodology in this report could be used as a platform for this type of study.

The availability of the VacA crystal structure could help us understand structural features of the p33 domain that are relevant for VacA function. Previous mutagenesis studies have identified specific amino acids within the p33 domain that are important for VacA activity (*92-94*). With the VacA structure available, we could map the sites of these mutations and deduce how the corresponding residues contribute to VacA function. On the other hand, the availability of the VacA structure could help explain whether structural differences within the i-region are responsible for the observed differences in activity (described in Chapter 3).

VacA is considered a pore-forming toxin, and the p33 domain is thought to be the pore forming domain (*118-119*). The membrane-inserting portions of pore-forming toxins are structurally categorized as β-barrel or α-helical, and these (*183-185, 217*)[214-217][214-217]structural features determine the specific mechanism of action (*183-185, 217*). Therefore, the VacA structure would provide insights into the mechanism by which VacA inserts into membranes to form pores.

Evaluate VacA oligomerization

Recently the Ohi, Lacy, and Cover lab performed an electron microscopy analysis of the VacA toxin (*218*). These studies were done by a negative stain microscopy method. Importantly, the crystal structure of the p55 domain was modeled into VacA oligomers, and we observed that the p33 domain was localized to the central core of the oligomer (Figure 26A and 26B).

Further electron microscopy experiments could analyze VacA insertion into membranes. Specifically, we could analyze VacA oligomerization in the presence of lipids. This type of analysis could elucidate quaternary conformational changes that are important for membrane insertion. Other EM studies include testing whether different forms of VacA (s2, i2, and m2) differ in their oligomeric structures when compared to VacA type s1/i1/m1. One drawback of our current electron microscopy approach is that there are limits of the resolution at which a structure can be determined. As an alternative approach, we could perform cryo-EM analysis of the VacA toxin. These studies are currently been performed in collaboration with the Ohi lab, and we are hopeful that they

will provide insight into VacA oligomeric structure. In all of these studies, valuable insights will emerge by comparing the VacA crystal structure with EM structures.

A

B

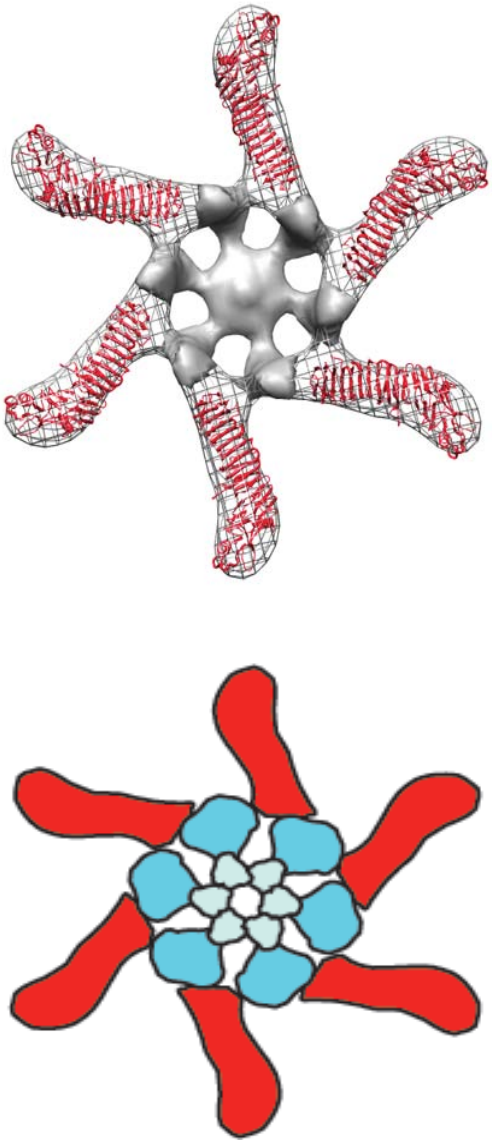

FIGURE 26: Electron microscopy analysis of the VacA toxin. (a) The 2.4-Å crystal structure of p55 was modeled into an oligomeric VacA structure, and the domain fit into the straight "arms" of the EM map of the oligomer (b) Cartoon representation of (a). Blue domains are the p33, and red domain is the p55 domain.

APPENDIX

List of publications

González-Rivera, C.*, Gangwer K.A.*, McClain M.S., Eli, I.M., Chambers, M.G., Ohi, M.D., Lacy, D.B., and Cover, T.L. Reconstitution of *Helicobacter pylori* VacA toxin from purified components. *Biochemistry* 2010; 49; 5743–5752

Radin, J.N., **González-Rivera, C.**, Ivie, S.E., McClain M.S., and Cover, T.L. *Helicobacter pylori* induces programmed necrosis in gastric epithelial cells. *Infection and Immunity* 2011; 79; 2535–2543

González-Rivera, C., Algood, H.M., Radin, J.N., McClain M.S., and Cover, T.L. The intermediate region of *Helicobacter pylori* VacA is a determinant of toxin potency in a Jurkat T cell assay. *Infection and Immunity* 2012; 80; 2578–2588

Chambers, M.G.*, Pyburn, T.M.*, **González-Rivera, C.**, Collier, S.E., Eli, I.M., Yip, C.K., Takizawa, Y., Lacy, D.B., Cover, T.L., and Ohi, M.D. Structural analysis of the oligomeric states of *Helicobacter pylori* VacA toxin. *Journal of Molecular Biology* 2013; 425; 524-535

Radin, J.N.*, Gaddy, J.A.*, **González-Rivera, C.**, Loh, J.T., Algood, H.M., and Cover, T.L. Flagellar localization of a *Helicobacter pylori* autotransporter protein. *MBio* 2013 (In press)

*Contributed equally to authorship

BIBLIOGRAPHY

1. Marshall, B. J., and Warren, J. R. (1984) Unidentified curved bacilli in the stomach of patients with gastritis and peptic ulceration, *Lancet 1*, 1311-1315.
2. Cover, T. L., and Blaser, M. J. (2009) Helicobacter pylori in health and disease, *Gastroenterology 136*, 1863-1873.
3. Varbanova, M., Schulz, C., and Malfertheiner, P. (2011) Helicobacter pylori and other gastric bacteria, *Dig Dis 29*, 562-569.
4. Rowland, M., Daly, L., Vaughan, M., Higgins, A., Bourke, B., and Drumm, B. (2006) Age-specific incidence of Helicobacter pylori, *Gastroenterology 130*, 65-72; quiz 211.
5. Velazquez, M., and Feirtag, J. M. (1999) Helicobacter pylori: characteristics, pathogenicity, detection methods and mode of transmission implicating foods and water, *Int J Food Microbiol 53*, 95-104.
6. Suerbaum, S., and Michetti, P. (2002) Helicobacter pylori infection, *N Engl J Med 347*, 1175-1186.
7. Atherton, J. C. (2006) The pathogenesis of Helicobacter pylori-induced gastro-duodenal diseases, *Annu Rev Pathol 1*, 63-96.
8. Peek, R. M., Jr., and Crabtree, J. E. (2006) Helicobacter infection and gastric neoplasia, *J Pathol 208*, 233-248.
9. Malfertheiner, P., Chan, F. K., and McColl, K. E. (2009) Peptic ulcer disease, *Lancet 374*, 1449-1461.
10. Parkin, D. M., Bray, F., Ferlay, J., and Pisani, P. (2005) Global cancer statistics, 2002, *CA Cancer J Clin 55*, 74-108.
11. Polk, D. B., and Peek, R. M., Jr. (2010) Helicobacter pylori: gastric cancer and beyond, *Nat Rev Cancer 10*, 403-414.
12. Osato, M. S., Reddy, R., Reddy, S. G., Penland, R. L., Malaty, H. M., and Graham, D. Y. (2001) Pattern of primary resistance of Helicobacter pylori to metronidazole or clarithromycin in the United States, *Arch Intern Med 161*, 1217-1220.
13. Nahar, S., Mukhopadhyay, A. K., Khan, R., Ahmad, M. M., Datta, S., Chattopadhyay, S., Dhar, S. C., Sarker, S. A., Engstrand, L., Berg, D. E., Nair, G. B., and Rahman, M. (2004) Antimicrobial susceptibility of Helicobacter pylori strains isolated in Bangladesh, *J Clin Microbiol 42*, 4856-4858.
14. Megraud, F. (2004) H pylori antibiotic resistance: prevalence, importance, and advances in testing, *Gut 53*, 1374-1384.
15. Rimbara, E., Noguchi, N., Tanabe, M., Kawai, T., Matsumoto, Y., and Sasatsu, M. (2005) Susceptibilities to clarithromycin, amoxycillin and metronidazole of Helicobacter pylori isolates from the antrum and corpus in Tokyo, Japan, 1995-2001, *Clin Microbiol Infect 11*, 307-311.
16. Hazell, S. L., Lee, A., Brady, L., and Hennessy, W. (1986) Campylobacter pyloridis and gastritis: association with intercellular spaces and adaptation to an environment of mucus as important factors in colonization of the gastric epithelium, *J Infect Dis 153*, 658-663.

17. Eaton, K. A., Suerbaum, S., Josenhans, C., and Krakowka, S. (1996) Colonization of gnotobiotic piglets by Helicobacter pylori deficient in two flagellin genes, *Infect Immun 64*, 2445-2448.
18. Magariyama, Y., and Kudo, S. (2002) A mathematical explanation of an increase in bacterial swimming speed with viscosity in linear-polymer solutions, *Biophys J 83*, 733-739.
19. Lertsethtakarn, P., Ottemann, K. M., and Hendrixson, D. R. (2011) Motility and chemotaxis in Campylobacter and Helicobacter, *Annu Rev Microbiol 65*, 389-410.
20. Ferrero, R. L., and Lee, A. (1988) Motility of Campylobacter jejuni in a viscous environment: comparison with conventional rod-shaped bacteria, *J Gen Microbiol 134*, 53-59.
21. Worku, M. L., Sidebotham, R. L., Baron, J. H., Misiewicz, J. J., Logan, R. P., Keshavarz, T., and Karim, Q. N. (1999) Motility of Helicobacter pylori in a viscous environment, *Eur J Gastroenterol Hepatol 11*, 1143-1150.
22. Bauerfeind, P., Garner, R., Dunn, B. E., and Mobley, H. L. (1997) Synthesis and activity of Helicobacter pylori urease and catalase at low pH, *Gut 40*, 25-30.
23. Scott, D. R., Marcus, E. A., Weeks, D. L., and Sachs, G. (2002) Mechanisms of acid resistance due to the urease system of Helicobacter pylori, *Gastroenterology 123*, 187-195.
24. Sachs, G., Scott, D. R., and Wen, Y. (2011) Gastric infection by Helicobacter pylori, *Curr Gastroenterol Rep 13*, 540-546.
25. Alm, R. A., Ling, L. S., Moir, D. T., King, B. L., Brown, E. D., Doig, P. C., Smith, D. R., Noonan, B., Guild, B. C., deJonge, B. L., Carmel, G., Tummino, P. J., Caruso, A., Uria-Nickelsen, M., Mills, D. M., Ives, C., Gibson, R., Merberg, D., Mills, S. D., Jiang, Q., Taylor, D. E., Vovis, G. F., and Trust, T. J. (1999) Genomic-sequence comparison of two unrelated isolates of the human gastric pathogen Helicobacter pylori, *Nature 397*, 176-180.
26. Oh, J. D., Kling-Backhed, H., Giannakis, M., Xu, J., Fulton, R. S., Fulton, L. A., Cordum, H. S., Wang, C., Elliott, G., Edwards, J., Mardis, E. R., Engstrand, L. G., and Gordon, J. I. (2006) The complete genome sequence of a chronic atrophic gastritis Helicobacter pylori strain: evolution during disease progression, *Proc Natl Acad Sci U S A 103*, 9999-10004.
27. Tomb, J. F., White, O., Kerlavage, A. R., Clayton, R. A., Sutton, G. G., Fleischmann, R. D., Ketchum, K. A., Klenk, H. P., Gill, S., Dougherty, B. A., Nelson, K., Quackenbush, J., Zhou, L., Kirkness, E. F., Peterson, S., Loftus, B., Richardson, D., Dodson, R., Khalak, H. G., Glodek, A., McKenney, K., Fitzegerald, L. M., Lee, N., Adams, M. D., Hickey, E. K., Berg, D. E., Gocayne, J. D., Utterback, T. R., Peterson, J. D., Kelley, J. M., Cotton, M. D., Weidman, J. M., Fujii, C., Bowman, C., Watthey, L., Wallin, E., Hayes, W. S., Borodovsky, M., Karp, P. D., Smith, H. O., Fraser, C. M., and Venter, J. C. (1997) The complete genome sequence of the gastric pathogen Helicobacter pylori, *Nature 388*, 539-547.
28. Baltrus, D. A., Amieva, M. R., Covacci, A., Lowe, T. M., Merrell, D. S., Ottemann, K. M., Stein, M., Salama, N. R., and Guillemin, K. (2009) The complete genome sequence of Helicobacter pylori strain G27, *J Bacteriol 191*, 447-448.

29. Baltrus, D. A., Blaser, M. J., and Guillemin, K. (2009) Helicobacter pylori Genome Plasticity, *Genome Dyn 6*, 75-90.
30. McClain, M. S., Shaffer, C. L., Israel, D. A., Peek, R. M., Jr., and Cover, T. L. (2009) Genome sequence analysis of Helicobacter pylori strains associated with gastric ulceration and gastric cancer, *BMC Genomics 10*, 3.
31. Yamaoka, Y., Ojo, O., Fujimoto, S., Odenbreit, S., Haas, R., Gutierrez, O., El-Zimaity, H. M., Reddy, R., Arnqvist, A., and Graham, D. Y. (2006) Helicobacter pylori outer membrane proteins and gastroduodenal disease, *Gut 55*, 775-781.
32. Boren, T., Falk, P., Roth, K. A., Larson, G., and Normark, S. (1993) Attachment of Helicobacter pylori to human gastric epithelium mediated by blood group antigens, *Science 262*, 1892-1895.
33. Gerhard, M., Lehn, N., Neumayer, N., Boren, T., Rad, R., Schepp, W., Miehlke, S., Classen, M., and Prinz, C. (1999) Clinical relevance of the Helicobacter pylori gene for blood-group antigen-binding adhesin, *Proc Natl Acad Sci U S A 96*, 12778-12783.
34. Ilver, D., Arnqvist, A., Ogren, J., Frick, I. M., Kersulyte, D., Incecik, E. T., Berg, D. E., Covacci, A., Engstrand, L., and Boren, T. (1998) Helicobacter pylori adhesin binding fucosylated histo-blood group antigens revealed by retagging, *Science 279*, 373-377.
35. Backert, S., and Selbach, M. (2008) Role of type IV secretion in Helicobacter pylori pathogenesis, *Cell Microbiol 10*, 1573-1581.
36. Johnson, E. M., Gaddy, J. A., and Cover, T. L. (2012) Alterations in Helicobacter pylori Triggered by Contact with Gastric Epithelial Cells, *Front Cell Infect Microbiol 2*, 17.
37. Kwok, T., Zabler, D., Urman, S., Rohde, M., Hartig, R., Wessler, S., Misselwitz, R., Berger, J., Sewald, N., Konig, W., and Backert, S. (2007) Helicobacter exploits integrin for type IV secretion and kinase activation, *Nature 449*, 862-866.
38. Terradot, L., and Waksman, G. (2011) Architecture of the Helicobacter pylori Cag-type IV secretion system, *FEBS J 278*, 1213-1222.
39. Kaplan-Turkoz, B., Jimenez-Soto, L. F., Dian, C., Ertl, C., Remaut, H., Louche, A., Tosi, T., Haas, R., and Terradot, L. (2012) Structural insights into Helicobacter pylori oncoprotein CagA interaction with beta1 integrin, *Proc Natl Acad Sci U S A 109*, 14640-14645.
40. Jimenez-Soto, L. F., Kutter, S., Sewald, X., Ertl, C., Weiss, E., Kapp, U., Rohde, M., Pirch, T., Jung, K., Retta, S. F., Terradot, L., Fischer, W., and Haas, R. (2009) Helicobacter pylori type IV secretion apparatus exploits beta1 integrin in a novel RGD-independent manner, *PLoS Pathog 5*, e1000684.
41. Odenbreit, S., Puls, J., Sedlmaier, B., Gerland, E., Fischer, W., and Haas, R. (2000) Translocation of Helicobacter pylori CagA into gastric epithelial cells by type IV secretion, *Science 287*, 1497-1500.
42. Shaffer, C. L., Gaddy, J. A., Loh, J. T., Johnson, E. M., Hill, S., Hennig, E. E., McClain, M. S., McDonald, W. H., and Cover, T. L. (2011) Helicobacter pylori exploits a unique repertoire of type IV secretion system components for pilus assembly at the bacteria-host cell interface, *PLoS Pathog 7*, e1002237.
43. Backert, S., Moese, S., Selbach, M., Brinkmann, V., and Meyer, T. F. (2001) Phosphorylation of tyrosine 972 of the Helicobacter pylori CagA protein is

essential for induction of a scattering phenotype in gastric epithelial cells, *Mol Microbiol 42*, 631-644.
44. Poppe, M., Feller, S. M., Romer, G., and Wessler, S. (2007) Phosphorylation of Helicobacter pylori CagA by c-Abl leads to cell motility, *Oncogene 26*, 3462-3472.
45. Hatakeyama, M. (2004) Oncogenic mechanisms of the Helicobacter pylori CagA protein, *Nat Rev Cancer 4*, 688-694.
46. Backert, S., Tegtmeyer, N., and Selbach, M. (2010) The versatility of Helicobacter pylori CagA effector protein functions: The master key hypothesis, *Helicobacter 15*, 163-176.
47. Murata-Kamiya, N., Kurashima, Y., Teishikata, Y., Yamahashi, Y., Saito, Y., Higashi, H., Aburatani, H., Akiyama, T., Peek, R. M., Jr., Azuma, T., and Hatakeyama, M. (2007) Helicobacter pylori CagA interacts with E-cadherin and deregulates the beta-catenin signal that promotes intestinal transdifferentiation in gastric epithelial cells, *Oncogene 26*, 4617-4626.
48. Nesic, D., Miller, M. C., Quinkert, Z. T., Stein, M., Chait, B. T., and Stebbins, C. E. (2010) Helicobacter pylori CagA inhibits PAR1-MARK family kinases by mimicking host substrates, *Nat Struct Mol Biol 17*, 130-132.
49. Hayashi, T., Senda, M., Morohashi, H., Higashi, H., Horio, M., Kashiba, Y., Nagase, L., Sasaya, D., Shimizu, T., Venugopalan, N., Kumeta, H., Noda, N. N., Inagaki, F., Senda, T., and Hatakeyama, M. (2012) Tertiary structure-function analysis reveals the pathogenic signaling potentiation mechanism of Helicobacter pylori oncogenic effector CagA, *Cell Host Microbe 12*, 20-33.
50. Leunk, R. D., Johnson, P. T., David, B. C., Kraft, W. G., and Morgan, D. R. (1988) Cytotoxic activity in broth-culture filtrates of Campylobacter pylori, *J Med Microbiol 26*, 93-99.
51. Cover, T. L., and Blaser, M. J. (1992) Purification and characterization of the vacuolating toxin from Helicobacter pylori, *J Biol Chem 267*, 10570-10575.
52. Atherton, J. C., Cao, P., Peek, R. M., Jr., Tummuru, M. K., Blaser, M. J., and Cover, T. L. (1995) Mosaicism in vacuolating cytotoxin alleles of Helicobacter pylori. Association of specific vacA types with cytotoxin production and peptic ulceration, *J Biol Chem 270*, 17771-17777.
53. Atherton, J. C., and Blaser, M. J. (2009) Coadaptation of Helicobacter pylori and humans: ancient history, modern implications, *J Clin Invest 119*, 2475-2487.
54. Gangwer, K. A., Shaffer, C. L., Suerbaum, S., Lacy, D. B., Cover, T. L., and Bordenstein, S. R. (2010) Molecular evolution of the Helicobacter pylori vacuolating toxin gene vacA, *J Bacteriol 192*, 6126-6135.
55. Van Doorn, L. J., Figueiredo, C., Megraud, F., Pena, S., Midolo, P., Queiroz, D. M., Carneiro, F., Vanderborght, B., Pegado, M. D., Sanna, R., De Boer, W., Schneeberger, P. M., Correa, P., Ng, E. K., Atherton, J., Blaser, M. J., and Quint, W. G. (1999) Geographic distribution of vacA allelic types of Helicobacter pylori, *Gastroenterology 116*, 823-830.
56. Rhead, J. L., Letley, D. P., Mohammadi, M., Hussein, N., Mohagheghi, M. A., Eshagh Hosseini, M., and Atherton, J. C. (2007) A new Helicobacter pylori vacuolating cytotoxin determinant, the intermediate region, is associated with gastric cancer, *Gastroenterology 133*, 926-936.

57. Basso, D., Zambon, C. F., Letley, D. P., Stranges, A., Marchet, A., Rhead, J. L., Schiavon, S., Guariso, G., Ceroti, M., Nitti, D., Rugge, M., Plebani, M., and Atherton, J. C. (2008) Clinical relevance of Helicobacter pylori cagA and vacA gene polymorphisms, *Gastroenterology 135*, 91-99.
58. Chung, C., Olivares, A., Torres, E., Yilmaz, O., Cohen, H., and Perez-Perez, G. (2010) Diversity of VacA intermediate region among Helicobacter pylori strains from several regions of the world, *J Clin Microbiol 48*, 690-696.
59. Douraghi, M., Talebkhan, Y., Zeraati, H., Ebrahimzadeh, F., Nahvijoo, A., Morakabati, A., Ghafarpour, M., Esmaili, M., Bababeik, M., Oghalaie, A., Rakhshani, N., Hosseini, M. E., Mohagheghi, M. A., and Mohammadi, M. (2009) Multiple gene status in Helicobacter pylori strains and risk of gastric cancer development, *Digestion 80*, 200-207.
60. Hussein, N. R., Mohammadi, M., Talebkhan, Y., Doraghi, M., Letley, D. P., Muhammad, M. K., Argent, R. H., and Atherton, J. C. (2008) Differences in virulence markers between Helicobacter pylori strains from Iraq and those from Iran: potential importance of regional differences in H. pylori-associated disease, *J Clin Microbiol 46*, 1774-1779.
61. Jones, K. R., Jang, S., Chang, J. Y., Kim, J., Chung, I. S., Olsen, C. H., Merrell, D. S., and Cha, J. H. (2010) Polymorphisms in the Intermediate Region of VacA Impact Helicobacter pylori - Induced Disease Development, *J Clin Microbiol*.
62. Sheu, S. M., Hung, K. H., Sheu, B. S., Yang, H. B., and Wu, J. J. (2009) Association of nonsynonymous substitutions in the intermediate region of the vacA gene of Helicobacter pylori with gastric diseases in Taiwan, *J Clin Microbiol 47*, 249-251.
63. Yordanov, D., Boyanova, L., Markovska, R., Gergova, G., and Mitov, I. (2012) Significance of Helicobacter pylori vacA intermediate region genotyping-a Bulgarian study, *Diagn Microbiol Infect Dis*.
64. Tuncel, I. E., Hussein, N. R., Bolek, B. K., Arikan, S., and Salih, B. A. (2010) Helicobacter pylori virulence factors and their role in peptic ulcer diseases in Turkey, *Acta Gastroenterol Belg 73*, 235-238.
65. Ogiwara, H., Sugimoto, M., Ohno, T., Vilaichone, R. K., Mahachai, V., Graham, D. Y., and Yamaoka, Y. (2009) Role of deletion located between the intermediate and middle regions of the Helicobacter pylori vacA gene in cases of gastroduodenal diseases, *J Clin Microbiol 47*, 3493-3500.
66. Forsyth, M. H., and Cover, T. L. (1999) Mutational analysis of the vacA promoter provides insight into gene transcription in Helicobacter pylori, *J Bacteriol 181*, 2261-2266.
67. Merrell, D. S., Thompson, L. J., Kim, C. C., Mitchell, H., Tompkins, L. S., Lee, A., and Falkow, S. (2003) Growth phase-dependent response of Helicobacter pylori to iron starvation, *Infect Immun 71*, 6510-6525.
68. Keenan, J. I., and Allardyce, R. A. (2000) Iron influences the expression of Helicobacter pylori outer membrane vesicle-associated virulence factors, *Eur J Gastroenterol Hepatol 12*, 1267-1273.
69. Szczebara, F., Dhaenens, L., Armand, S., and Husson, M. O. (1999) Regulation of the transcription of genes encoding different virulence factors in Helicobacter pylori by free iron, *FEMS Microbiol Lett 175*, 165-170.

70. Cover, T. L., Tummuru, M. K., Cao, P., Thompson, S. A., and Blaser, M. J. (1994) Divergence of genetic sequences for the vacuolating cytotoxin among Helicobacter pylori strains, *J Biol Chem 269*, 10566-10573.
71. Telford, J. L., Ghiara, P., Dell'Orco, M., Comanducci, M., Burroni, D., Bugnoli, M., Tecce, M. F., Censini, S., Covacci, A., Xiang, Z., and et al. (1994) Gene structure of the Helicobacter pylori cytotoxin and evidence of its key role in gastric disease, *J Exp Med 179*, 1653-1658.
72. Schmitt, W., and Haas, R. (1994) Genetic analysis of the Helicobacter pylori vacuolating cytotoxin: structural similarities with the IgA protease type of exported protein, *Mol Microbiol 12*, 307-319.
73. Cover, T. L., and Blanke, S. R. (2005) Helicobacter pylori VacA, a paradigm for toxin multifunctionality, *Nat Rev Microbiol 3*, 320-332.
74. Ilver, D., Barone, S., Mercati, D., Lupetti, P., and Telford, J. L. (2004) Helicobacter pylori toxin VacA is transferred to host cells via a novel contact-dependent mechanism, *Cell Microbiol 6*, 167-174.
75. Dautin, N., and Bernstein, H. D. (2007) Protein secretion in gram-negative bacteria via the autotransporter pathway, *Annu Rev Microbiol 61*, 89-112.
76. Leyton, D. L., Rossiter, A. E., and Henderson, I. R. (2012) From self sufficiency to dependence: mechanisms and factors important for autotransporter biogenesis, *Nat Rev Microbiol 10*, 213-225.
77. Fischer, W., Buhrdorf, R., Gerland, E., and Haas, R. (2001) Outer membrane targeting of passenger proteins by the vacuolating cytotoxin autotransporter of Helicobacter pylori, *Infect Immun 69*, 6769-6775.
78. Junker, M., Schuster, C. C., McDonnell, A. V., Sorg, K. A., Finn, M. C., Berger, B., and Clark, P. L. (2006) Pertactin beta-helix folding mechanism suggests common themes for the secretion and folding of autotransporter proteins, *Proc Natl Acad Sci U S A 103*, 4918-4923.
79. Nguyen, V. Q., Caprioli, R. M., and Cover, T. L. (2001) Carboxy-terminal proteolytic processing of Helicobacter pylori vacuolating toxin, *Infect Immun 69*, 543-546.
80. Wang, H. J., Chang, P. C., Kuo, C. H., Tzeng, C. S., and Wang, W. C. (1998) Characterization of the C-terminal domain of Helicobacter pylori vacuolating toxin and its relationship with extracellular toxin production, *Biochem Biophys Res Commun 250*, 397-402.
81. Genevrois, S., Steeghs, L., Roholl, P., Letesson, J. J., and van der Ley, P. (2003) The Omp85 protein of Neisseria meningitidis is required for lipid export to the outer membrane, *EMBO J 22*, 1780-1789.
82. Ricci, D. P., and Silhavy, T. J. (2012) The Bam machine: A molecular cooper, *Biochim Biophys Acta 1818*, 1067-1084.
83. Voulhoux, R., Bos, M. P., Geurtsen, J., Mols, M., and Tommassen, J. (2003) Role of a highly conserved bacterial protein in outer membrane protein assembly, *Science 299*, 262-265.
84. Wu, T., Malinverni, J., Ruiz, N., Kim, S., Silhavy, T. J., and Kahne, D. (2005) Identification of a multicomponent complex required for outer membrane biogenesis in Escherichia coli, *Cell 121*, 235-245.

85. Webb, C. T., Heinz, E., and Lithgow, T. (2012) Evolution of the beta-barrel assembly machinery, *Trends Microbiol*.
86. Marin, E., Bodelon, G., and Fernandez, L. A. (2010) Comparative analysis of the biochemical and functional properties of C-terminal domains of autotransporters, *J Bacteriol 192*, 5588-5602.
87. Torres, V. J., Ivie, S. E., McClain, M. S., and Cover, T. L. (2005) Functional properties of the p33 and p55 domains of the Helicobacter pylori vacuolating cytotoxin, *J Biol Chem 280*, 21107-21114.
88. Torres, V. J., McClain, M. S., and Cover, T. L. (2004) Interactions between p-33 and p-55 domains of the Helicobacter pylori vacuolating cytotoxin (VacA), *J Biol Chem 279*, 2324-2331.
89. Forsyth, M. H., Atherton, J. C., Blaser, M. J., and Cover, T. L. (1998) Heterogeneity in levels of vacuolating cytotoxin gene (vacA) transcription among Helicobacter pylori strains, *Infect Immun 66*, 3088-3094.
90. Letley, D. P., Rhead, J. L., Twells, R. J., Dove, B., and Atherton, J. C. (2003) Determinants of non-toxicity in the gastric pathogen Helicobacter pylori, *J Biol Chem 278*, 26734-26741.
91. McClain, M. S., Cao, P., Iwamoto, H., Vinion-Dubiel, A. D., Szabo, G., Shao, Z., and Cover, T. L. (2001) A 12-amino-acid segment, present in type s2 but not type s1 Helicobacter pylori VacA proteins, abolishes cytotoxin activity and alters membrane channel formation, *J Bacteriol 183*, 6499-6508.
92. Vinion-Dubiel, A. D., McClain, M. S., Czajkowsky, D. M., Iwamoto, H., Ye, D., Cao, P., Schraw, W., Szabo, G., Blanke, S. R., Shao, Z., and Cover, T. L. (1999) A dominant negative mutant of Helicobacter pylori vacuolating toxin (VacA) inhibits VacA-induced cell vacuolation, *J Biol Chem 274*, 37736-37742.
93. McClain, M. S., Iwamoto, H., Cao, P., Vinion-Dubiel, A. D., Li, Y., Szabo, G., Shao, Z., and Cover, T. L. (2003) Essential role of a GXXXG motif for membrane channel formation by Helicobacter pylori vacuolating toxin, *J Biol Chem 278*, 12101-12108.
94. McClain, M. S., Cao, P., and Cover, T. L. (2001) Amino-terminal hydrophobic region of Helicobacter pylori vacuolating cytotoxin (VacA) mediates transmembrane protein dimerization, *Infect Immun 69*, 1181-1184.
95. McClain, M. S., Czajkowsky, D. M., Torres, V. J., Szabo, G., Shao, Z., and Cover, T. L. (2006) Random mutagenesis of Helicobacter pylori vacA to identify amino acids essential for vacuolating cytotoxic activity, *Infect Immun 74*, 6188-6195.
96. Ye, D., Willhite, D. C., and Blanke, S. R. (1999) Identification of the minimal intracellular vacuolating domain of the Helicobacter pylori vacuolating toxin, *J Biol Chem 274*, 9277-9282.
97. Galmiche, A., Rassow, J., Doye, A., Cagnol, S., Chambard, J. C., Contamin, S., de Thillot, V., Just, I., Ricci, V., Solcia, E., Van Obberghen, E., and Boquet, P. (2000) The N-terminal 34 kDa fragment of Helicobacter pylori vacuolating cytotoxin targets mitochondria and induces cytochrome c release, *EMBO J 19*, 6361-6370.
98. Domanska, G., Motz, C., Meinecke, M., Harsman, A., Papatheodorou, P., Reljic, B., Dian-Lothrop, E. A., Galmiche, A., Kepp, O., Becker, L., Gunnewig, K.,

Wagner, R., and Rassow, J. (2010) Helicobacter pylori VacA toxin/subunit p34: targeting of an anion channel to the inner mitochondrial membrane, *PLoS Pathog 6*, e1000878.

99. Gangwer, K. A., Mushrush, D. J., Stauff, D. L., Spiller, B., McClain, M. S., Cover, T. L., and Lacy, D. B. (2007) Crystal structure of the Helicobacter pylori vacuolating toxin p55 domain, *Proc Natl Acad Sci U S A 104*, 16293-16298.
100. Ji, X., Fernandez, T., Burroni, D., Pagliaccia, C., Atherton, J. C., Reyrat, J. M., Rappuoli, R., and Telford, J. L. (2000) Cell specificity of Helicobacter pylori cytotoxin is determined by a short region in the polymorphic midregion, *Infect Immun 68*, 3754-3757.
101. Pagliaccia, C., de Bernard, M., Lupetti, P., Ji, X., Burroni, D., Cover, T. L., Papini, E., Rappuoli, R., Telford, J. L., and Reyrat, J. M. (1998) The m2 form of the Helicobacter pylori cytotoxin has cell type-specific vacuolating activity, *Proc Natl Acad Sci U S A 95*, 10212-10217.
102. Skibinski, D. A., Genisset, C., Barone, S., and Telford, J. L. (2006) The cell-specific phenotype of the polymorphic vacA midregion is independent of the appearance of the cell surface receptor protein tyrosine phosphatase beta, *Infect Immun 74*, 49-55.
103. Wang, W. C., Wang, H. J., and Kuo, C. H. (2001) Two distinctive cell binding patterns by vacuolating toxin fused with glutathione S-transferase: one high-affinity m1-specific binding and the other lower-affinity binding for variant m forms, *Biochemistry 40*, 11887-11896.
104. Kuhnel, K., and Diezmann, D. (2011) Crystal structure of the autochaperone region from the Shigella flexneri autotransporter IcsA, *J Bacteriol 193*, 2042-2045.
105. Soprova, Z., Sauri, A., van Ulsen, P., Tame, J. R., den Blaauwen, T., Jong, W. S., and Luirink, J. (2010) A conserved aromatic residue in the autochaperone domain of the autotransporter Hbp is critical for initiation of outer membrane translocation, *J Biol Chem 285*, 38224-38233.
106. Ivie, S. E., McClain, M. S., Algood, H. M., Lacy, D. B., and Cover, T. L. (2010) Analysis of a beta-helical region in the p55 domain of Helicobacter pylori vacuolating toxin, *BMC Microbiol 10*, 60.
107. Cover, T. L., Hanson, P. I., and Heuser, J. E. (1997) Acid-induced dissociation of VacA, the Helicobacter pylori vacuolating cytotoxin, reveals its pattern of assembly, *J Cell Biol 138*, 759-769.
108. El-Bez, C., Adrian, M., Dubochet, J., and Cover, T. L. (2005) High resolution structural analysis of Helicobacter pylori VacA toxin oligomers by cryo-negative staining electron microscopy, *J Struct Biol 151*, 215-228.
109. Adrian, M., Cover, T. L., Dubochet, J., and Heuser, J. E. (2002) Multiple oligomeric states of the Helicobacter pylori vacuolating toxin demonstrated by cryo-electron microscopy, *J Mol Biol 318*, 121-133.
110. Czajkowsky, D. M., Iwamoto, H., Cover, T. L., and Shao, Z. (1999) The vacuolating toxin from Helicobacter pylori forms hexameric pores in lipid bilayers at low pH, *Proc Natl Acad Sci U S A 96*, 2001-2006.

111. Geisse, N. A., Cover, T. L., Henderson, R. M., and Edwardson, J. M. (2004) Targeting of Helicobacter pylori vacuolating toxin to lipid raft membrane domains analysed by atomic force microscopy, *Biochem J 381*, 911-917.
112. Wang, X., Wattiez, R., Paggliacia, C., Telford, J. L., Ruysschaert, J., and Cabiaux, V. (2000) Membrane topology of VacA cytotoxin from H. pylori, *FEBS Lett 481*, 96-100.
113. Genisset, C., Galeotti, C. L., Lupetti, P., Mercati, D., Skibinski, D. A., Barone, S., Battistutta, R., de Bernard, M., and Telford, J. L. (2006) A Helicobacter pylori vacuolating toxin mutant that fails to oligomerize has a dominant negative phenotype, *Infect Immun 74*, 1786-1794.
114. Ivie, S. E., McClain, M. S., Torres, V. J., Algood, H. M., Lacy, D. B., Yang, R., Blanke, S. R., and Cover, T. L. (2008) Helicobacter pylori VacA subdomain required for intracellular toxin activity and assembly of functional oligomeric complexes, *Infect Immun 76*, 2843-2851.
115. Torres, V. J., McClain, M. S., and Cover, T. L. (2006) Mapping of a domain required for protein-protein interactions and inhibitory activity of a Helicobacter pylori dominant-negative VacA mutant protein, *Infect Immun 74*, 2093-2101.
116. de Bernard, M., Papini, E., de Filippis, V., Gottardi, E., Telford, J., Manetti, R., Fontana, A., Rappuoli, R., and Montecucco, C. (1995) Low pH activates the vacuolating toxin of Helicobacter pylori, which becomes acid and pepsin resistant, *J Biol Chem 270*, 23937-23940.
117. Palframan, S. L., Kwok, T., and Gabriel, K. (2012) Vacuolating cytotoxin A (VacA), a key toxin for Helicobacter pylori pathogenesis, *Front Cell Infect Microbiol 2*, 92.
118. Rassow, J., and Meinecke, M. (2012) Helicobacter pylori VacA: a new perspective on an invasive chloride channel, *Microbes Infect 14*, 1026-1033.
119. Boquet, P., and Ricci, V. (2012) Intoxication strategy of Helicobacter pylori VacA toxin, *Trends Microbiol 20*, 165-174.
120. Kim, I. J., and Blanke, S. R. (2012) Remodeling the host environment: modulation of the gastric epithelium by the Helicobacter pylori vacuolating toxin (VacA), *Front Cell Infect Microbiol 2*, 37.
121. Gupta, V. R., Patel, H. K., Kostolansky, S. S., Ballivian, R. A., Eichberg, J., and Blanke, S. R. (2008) Sphingomyelin functions as a novel receptor for Helicobacter pylori VacA, *PLoS Pathog 4*, e1000073.
122. Gupta, V. R., Wilson, B. A., and Blanke, S. R. (2010) Sphingomyelin is important for the cellular entry and intracellular localization of Helicobacter pylori VacA, *Cell Microbiol 12*, 1517-1533.
123. Yahiro, K., Niidome, T., Kimura, M., Hatakeyama, T., Aoyagi, H., Kurazono, H., Imagawa, K., Wada, A., Moss, J., and Hirayama, T. (1999) Activation of Helicobacter pylori VacA toxin by alkaline or acid conditions increases its binding to a 250-kDa receptor protein-tyrosine phosphatase beta, *J Biol Chem 274*, 36693-36699.
124. Yahiro, K., Wada, A., Nakayama, M., Kimura, T., Ogushi, K., Niidome, T., Aoyagi, H., Yoshino, K., Yonezawa, K., Moss, J., and Hirayama, T. (2003) Protein-tyrosine phosphatase alpha, RPTP alpha, is a Helicobacter pylori VacA receptor, *J Biol Chem 278*, 19183-19189.

125. Seto, K., Hayashi-Kuwabara, Y., Yoneta, T., Suda, H., and Tamaki, H. (1998) Vacuolation induced by cytotoxin from Helicobacter pylori is mediated by the EGF receptor in HeLa cells, *FEBS Lett 431*, 347-350.
126. Utt, M., Danielsson, B., and Wadstrom, T. (2001) Helicobacter pylori vacuolating cytotoxin binding to a putative cell surface receptor, heparan sulfate, studied by surface plasmon resonance, *FEMS Immunol Med Microbiol 30*, 109-113.
127. Roche, N., Ilver, D., Angstrom, J., Barone, S., Telford, J. L., and Teneberg, S. (2007) Human gastric glycosphingolipids recognized by Helicobacter pylori vacuolating cytotoxin VacA, *Microbes Infect 9*, 605-614.
128. Ricci, V., Galmiche, A., Doye, A., Necchi, V., Solcia, E., and Boquet, P. (2000) High cell sensitivity to Helicobacter pylori VacA toxin depends on a GPI-anchored protein and is not blocked by inhibition of the clathrin-mediated pathway of endocytosis, *Mol Biol Cell 11*, 3897-3909.
129. Gauthier, N. C., Ricci, V., Gounon, P., Doye, A., Tauc, M., Poujeol, P., and Boquet, P. (2004) Glycosylphosphatidylinositol-anchored proteins and actin cytoskeleton modulate chloride transport by channels formed by the Helicobacter pylori vacuolating cytotoxin VacA in HeLa cells, *J Biol Chem 279*, 9481-9489.
130. Yahiro, K., Satoh, M., Nakano, M., Hisatsune, J., Isomoto, H., Sap, J., Suzuki, H., Nomura, F., Noda, M., Moss, J., and Hirayama, T. (2012) Low-density Lipoprotein Receptor-related Protein-1 (LRP1) Mediates Autophagy and Apoptosis Caused by Helicobacter pylori VacA, *J Biol Chem 287*, 31104-31115.
131. Schraw, W., Li, Y., McClain, M. S., van der Goot, F. G., and Cover, T. L. (2002) Association of Helicobacter pylori vacuolating toxin (VacA) with lipid rafts, *J Biol Chem 277*, 34642-34650.
132. Kuo, C. H., and Wang, W. C. (2003) Binding and internalization of Helicobacter pylori VacA via cellular lipid rafts in epithelial cells, *Biochem Biophys Res Commun 303*, 640-644.
133. Nakayama, M., Kimura, M., Wada, A., Yahiro, K., Ogushi, K., Niidome, T., Fujikawa, A., Shirasaka, D., Aoyama, N., Kurazono, H., Noda, M., Moss, J., and Hirayama, T. (2004) Helicobacter pylori VacA activates the p38/activating transcription factor 2-mediated signal pathway in AZ-521 cells, *J Biol Chem 279*, 7024-7028.
134. Hisatsune, J., Yamasaki, E., Nakayama, M., Shirasaka, D., Kurazono, H., Katagata, Y., Inoue, H., Han, J., Sap, J., Yahiro, K., Moss, J., and Hirayama, T. (2007) Helicobacter pylori VacA enhances prostaglandin E2 production through induction of cyclooxygenase 2 expression via a p38 mitogen-activated protein kinase/activating transcription factor 2 cascade in AZ-521 cells, *Infect Immun 75*, 4472-4481.
135. Fujikawa, A., Shirasaka, D., Yamamoto, S., Ota, H., Yahiro, K., Fukada, M., Shintani, T., Wada, A., Aoyama, N., Hirayama, T., Fukamachi, H., and Noda, M. (2003) Mice deficient in protein tyrosine phosphatase receptor type Z are resistant to gastric ulcer induction by VacA of Helicobacter pylori, *Nat Genet 33*, 375-381.
136. Papini, E., Satin, B., Norais, N., de Bernard, M., Telford, J. L., Rappuoli, R., and Montecucco, C. (1998) Selective increase of the permeability of polarized epithelial cell monolayers by Helicobacter pylori vacuolating toxin, *J Clin Invest 102*, 813-820.

137. Tombola, F., Morbiato, L., Del Giudice, G., Rappuoli, R., Zoratti, M., and Papini, E. (2001) The Helicobacter pylori VacA toxin is a urea permease that promotes urea diffusion across epithelia, *J Clin Invest 108*, 929-937.
138. Debellis, L., Papini, E., Caroppo, R., Montecucco, C., and Curci, S. (2001) Helicobacter pylori cytotoxin VacA increases alkaline secretion in gastric epithelial cells, *Am J Physiol Gastrointest Liver Physiol 281*, G1440-1448.
139. Guarino, A., Bisceglia, M., Canani, R. B., Boccia, M. C., Mallardo, G., Bruzzese, E., Massari, P., Rappuoli, R., and Telford, J. (1998) Enterotoxic effect of the vacuolating toxin produced by Helicobacter pylori in Caco-2 cells, *J Infect Dis 178*, 1373-1378.
140. Ge, R., and Sun, X. (2012) Iron trafficking system in Helicobacter pylori, *Biometals 25*, 247-258.
141. Garner, J. A., and Cover, T. L. (1996) Binding and internalization of the Helicobacter pylori vacuolating cytotoxin by epithelial cells, *Infect Immun 64*, 4197-4203.
142. McClain, M. S., Schraw, W., Ricci, V., Boquet, P., and Cover, T. L. (2000) Acid activation of Helicobacter pylori vacuolating cytotoxin (VacA) results in toxin internalization by eukaryotic cells, *Mol Microbiol 37*, 433-442.
143. Patel, H. K., Willhite, D. C., Patel, R. M., Ye, D., Williams, C. L., Torres, E. M., Marty, K. B., MacDonald, R. A., and Blanke, S. R. (2002) Plasma membrane cholesterol modulates cellular vacuolation induced by the Helicobacter pylori vacuolating cytotoxin, *Infect Immun 70*, 4112-4123.
144. Gauthier, N. C., Monzo, P., Kaddai, V., Doye, A., Ricci, V., and Boquet, P. (2005) Helicobacter pylori VacA cytotoxin: a probe for a clathrin-independent and Cdc42-dependent pinocytic pathway routed to late endosomes, *Mol Biol Cell 16*, 4852-4866.
145. Gauthier, N. C., Monzo, P., Gonzalez, T., Doye, A., Oldani, A., Gounon, P., Ricci, V., Cormont, M., and Boquet, P. (2007) Early endosomes associated with dynamic F-actin structures are required for late trafficking of H. pylori VacA toxin, *J Cell Biol 177*, 343-354.
146. Li, Y., Wandinger-Ness, A., Goldenring, J. R., and Cover, T. L. (2004) Clustering and redistribution of late endocytic compartments in response to Helicobacter pylori vacuolating toxin, *Mol Biol Cell 15*, 1946-1959.
147. Howes, M. T., Kirkham, M., Riches, J., Cortese, K., Walser, P. J., Simpson, F., Hill, M. M., Jones, A., Lundmark, R., Lindsay, M. R., Hernandez-Deviez, D. J., Hadzic, G., McCluskey, A., Bashir, R., Liu, L., Pilch, P., McMahon, H., Robinson, P. J., Hancock, J. F., Mayor, S., and Parton, R. G. (2010) Clathrin-independent carriers form a high capacity endocytic sorting system at the leading edge of migrating cells, *J Cell Biol 190*, 675-691.
148. Genisset, C., Puhar, A., Calore, F., de Bernard, M., Dell'Antone, P., and Montecucco, C. (2007) The concerted action of the Helicobacter pylori cytotoxin VacA and of the v-ATPase proton pump induces swelling of isolated endosomes, *Cell Microbiol 9*, 1481-1490.
149. Papini, E., Gottardi, E., Satin, B., de Bernard, M., Massari, P., Telford, J., Rappuoli, R., Sato, S. B., and Montecucco, C. (1996) The vacuolar ATPase

proton pump is present on intracellular vacuoles induced by Helicobacter pylori, *J Med Microbiol 45*, 84-89.
150. Cover, T. L., Vaughn, S. G., Cao, P., and Blaser, M. J. (1992) Potentiation of Helicobacter pylori vacuolating toxin activity by nicotine and other weak bases, *J Infect Dis 166*, 1073-1078.
151. Papini, E., de Bernard, M., Milia, E., Bugnoli, M., Zerial, M., Rappuoli, R., and Montecucco, C. (1994) Cellular vacuoles induced by Helicobacter pylori originate from late endosomal compartments, *Proc Natl Acad Sci U S A 91*, 9720-9724.
152. Molinari, M., Galli, C., Norais, N., Telford, J. L., Rappuoli, R., Luzio, J. P., and Montecucco, C. (1997) Vacuoles induced by Helicobacter pylori toxin contain both late endosomal and lysosomal markers, *J Biol Chem 272*, 25339-25344.
153. Calore, F., Genisset, C., Casellato, A., Rossato, M., Codolo, G., Esposti, M. D., Scorrano, L., and de Bernard, M. (2010) Endosome-mitochondria juxtaposition during apoptosis induced by H. pylori VacA, *Cell Death Differ 17*, 1707-1716.
154. Foo, J. H., Culvenor, J. G., Ferrero, R. L., Kwok, T., Lithgow, T., and Gabriel, K. (2010) Both the p33 and p55 subunits of the Helicobacter pylori VacA toxin are targeted to mammalian mitochondria, *J Mol Biol 401*, 792-798.
155. Willhite, D. C., and Blanke, S. R. (2004) Helicobacter pylori vacuolating cytotoxin enters cells, localizes to the mitochondria, and induces mitochondrial membrane permeability changes correlated to toxin channel activity, *Cell Microbiol 6*, 143-154.
156. Manente, L., Perna, A., Buommino, E., Altucci, L., Lucariello, A., Citro, G., Baldi, A., Iaquinto, G., Tufano, M. A., and De Luca, A. (2008) The Helicobacter pylori's protein VacA has direct effects on the regulation of cell cycle and apoptosis in gastric epithelial cells, *J Cell Physiol 214*, 582-587.
157. Radin, J. N., Gonzalez-Rivera, C., Ivie, S. E., McClain, M. S., and Cover, T. L. (2011) Helicobacter pylori VacA induces programmed necrosis in gastric epithelial cells, *Infect Immun 79*, 2535-2543.
158. Jain, P., Luo, Z. Q., and Blanke, S. R. (2011) Helicobacter pylori vacuolating cytotoxin A (VacA) engages the mitochondrial fission machinery to induce host cell death, *Proc Natl Acad Sci U S A 108*, 16032-16037.
159. Yamasaki, E., Wada, A., Kumatori, A., Nakagawa, I., Funao, J., Nakayama, M., Hisatsune, J., Kimura, M., Moss, J., and Hirayama, T. (2006) Helicobacter pylori vacuolating cytotoxin induces activation of the proapoptotic proteins Bax and Bak, leading to cytochrome c release and cell death, independent of vacuolation, *J Biol Chem 281*, 11250-11259.
160. Ashktorab, H., Frank, S., Khaled, A. R., Durum, S. K., Kifle, B., and Smoot, D. T. (2004) Bax translocation and mitochondrial fragmentation induced by Helicobacter pylori, *Gut 53*, 805-813.
161. Rassow, J. (2011) Helicobacter pylori vacuolating toxin A and apoptosis, *Cell Commun Signal 9*, 26.
162. Cover, T. L., Krishna, U. S., Israel, D. A., and Peek, R. M., Jr. (2003) Induction of gastric epithelial cell apoptosis by Helicobacter pylori vacuolating cytotoxin, *Cancer Res 63*, 951-957.

163. Kuck, D., Kolmerer, B., Iking-Konert, C., Krammer, P. H., Stremmel, W., and Rudi, J. (2001) Vacuolating cytotoxin of Helicobacter pylori induces apoptosis in the human gastric epithelial cell line AGS, *Infect Immun 69*, 5080-5087.
164. Cho, S. J., Kang, N. S., Park, S. Y., Kim, B. O., Rhee, D. K., and Pyo, S. (2003) Induction of apoptosis and expression of apoptosis related genes in human epithelial carcinoma cells by Helicobacter pylori VacA toxin, *Toxicon 42*, 601-611.
165. Terebiznik, M. R., Raju, D., Vazquez, C. L., Torbricki, K., Kulkarni, R., Blanke, S. R., Yoshimori, T., Colombo, M. I., and Jones, N. L. (2009) Effect of Helicobacter pylori's vacuolating cytotoxin on the autophagy pathway in gastric epithelial cells, *Autophagy 5*, 370-379.
166. Raju, D., and Jones, N. L. (2010) Methods to monitor autophagy in H. pylori vacuolating cytotoxin A (VacA)-treated cells, *Autophagy 6*, 138-143.
167. Raju, D., Hussey, S., Ang, M., Terebiznik, M. R., Sibony, M., Galindo-Mata, E., Gupta, V., Blanke, S. R., Delgado, A., Romero-Gallo, J., Ramjeet, M. S., Mascarenhas, H., Peek, R. M., Correa, P., Streutker, C., Hold, G., Kunstmann, E., Yoshimori, T., Silverberg, M. S., Girardin, S. E., Philpott, D. J., El Omar, E., and Jones, N. L. (2012) Vacuolating cytotoxin and variants in Atg16L1 that disrupt autophagy promote Helicobacter pylori infection in humans, *Gastroenterology 142*, 1160-1171.
168. Boncristiano, M., Paccani, S. R., Barone, S., Ulivieri, C., Patrussi, L., Ilver, D., Amedei, A., D'Elios, M. M., Telford, J. L., and Baldari, C. T. (2003) The Helicobacter pylori vacuolating toxin inhibits T cell activation by two independent mechanisms, *J Exp Med 198*, 1887-1897.
169. Gebert, B., Fischer, W., Weiss, E., Hoffmann, R., and Haas, R. (2003) Helicobacter pylori vacuolating cytotoxin inhibits T lymphocyte activation, *Science 301*, 1099-1102.
170. Sundrud, M. S., Torres, V. J., Unutmaz, D., and Cover, T. L. (2004) Inhibition of primary human T cell proliferation by Helicobacter pylori vacuolating toxin (VacA) is independent of VacA effects on IL-2 secretion, *Proc Natl Acad Sci U S A 101*, 7727-7732.
171. Zheng, P. Y., and Jones, N. L. (2003) Helicobacter pylori strains expressing the vacuolating cytotoxin interrupt phagosome maturation in macrophages by recruiting and retaining TACO (coronin 1) protein, *Cell Microbiol 5*, 25-40.
172. Molinari, M., Salio, M., Galli, C., Norais, N., Rappuoli, R., Lanzavecchia, A., and Montecucco, C. (1998) Selective inhibition of Ii-dependent antigen presentation by Helicobacter pylori toxin VacA, *J Exp Med 187*, 135-140.
173. Supajatura, V., Ushio, H., Wada, A., Yahiro, K., Okumura, K., Ogawa, H., Hirayama, T., and Ra, C. (2002) Cutting edge: VacA, a vacuolating cytotoxin of Helicobacter pylori, directly activates mast cells for migration and production of proinflammatory cytokines, *J Immunol 168*, 2603-2607.
174. Sewald, X., Gebert-Vogl, B., Prassl, S., Barwig, I., Weiss, E., Fabbri, M., Osicka, R., Schiemann, M., Busch, D. H., Semmrich, M., Holzmann, B., Sebo, P., and Haas, R. (2008) Integrin subunit CD18 Is the T-lymphocyte receptor for the Helicobacter pylori vacuolating cytotoxin, *Cell Host Microbe 3*, 20-29.

175. Algood, H. M., Torres, V. J., Unutmaz, D., and Cover, T. L. (2007) Resistance of primary murine CD4+ T cells to Helicobacter pylori vacuolating cytotoxin, *Infect Immun 75*, 334-341.
176. Sewald, X., Jimenez-Soto, L., and Haas, R. (2011) PKC-dependent endocytosis of the Helicobacter pylori vacuolating cytotoxin in primary T lymphocytes, *Cell Microbiol 13*, 482-496.
177. Torres, V. J., VanCompernolle, S. E., Sundrud, M. S., Unutmaz, D., and Cover, T. L. (2007) Helicobacter pylori vacuolating cytotoxin inhibits activation-induced proliferation of human T and B lymphocyte subsets, *J Immunol 179*, 5433-5440.
178. Eaton, K. A., Cover, T. L., Tummuru, M. K., Blaser, M. J., and Krakowka, S. (1997) Role of vacuolating cytotoxin in gastritis due to Helicobacter pylori in gnotobiotic piglets, *Infect Immun 65*, 3462-3464.
179. Wirth, H. P., Beins, M. H., Yang, M., Tham, K. T., and Blaser, M. J. (1998) Experimental infection of Mongolian gerbils with wild-type and mutant Helicobacter pylori strains, *Infect Immun 66*, 4856-4866.
180. Ogura, K., Maeda, S., Nakao, M., Watanabe, T., Tada, M., Kyutoku, T., Yoshida, H., Shiratori, Y., and Omata, M. (2000) Virulence factors of Helicobacter pylori responsible for gastric diseases in Mongolian gerbil, *J Exp Med 192*, 1601-1610.
181. Salama, N. R., Otto, G., Tompkins, L., and Falkow, S. (2001) Vacuolating cytotoxin of Helicobacter pylori plays a role during colonization in a mouse model of infection, *Infect Immun 69*, 730-736.
182. Guo, B. P., and Mekalanos, J. J. (2002) Rapid genetic analysis of Helicobacter pylori gastric mucosal colonization in suckling mice, *Proc Natl Acad Sci U S A 99*, 8354-8359.
183. Gonzalez, M. R., Bischofberger, M., Pernot, L., van der Goot, F. G., and Freche, B. (2008) Bacterial pore-forming toxins: the (w)hole story?, *Cell Mol Life Sci 65*, 493-507.
184. Rossjohn, J., Feil, S. C., McKinstry, W. J., Tsernoglou, D., van der Goot, G., Buckley, J. T., and Parker, M. W. (1998) Aerolysin--a paradigm for membrane insertion of beta-sheet protein toxins?, *J Struct Biol 121*, 92-100.
185. Parker, M. W., and Feil, S. C. (2005) Pore-forming protein toxins: from structure to function, *Prog Biophys Mol Biol 88*, 91-142.
186. Middelberg, A. P. (2002) Preparative protein refolding, *Trends Biotechnol 20*, 437-443.
187. Cover, T. L., Puryear, W., Perez-Perez, G. I., and Blaser, M. J. (1991) Effect of urease on HeLa cell vacuolation induced by Helicobacter pylori cytotoxin, *Infect Immun 59*, 1264-1270.
188. Ohi, M., Li, Y., Cheng, Y., and Walz, T. (2004) Negative Staining and Image Classification - Powerful Tools in Modern Electron Microscopy, *Biol Proced Online 6*, 23-34.
189. Hawrylik, S. J., Wasilko, D. J., Haskell, S. L., Gootz, T. D., and Lee, S. E. (1994) Bisulfite or sulfite inhibits growth of Helicobacter pylori, *J Clin Microbiol 32*, 790-792.
190. Ludtke, S. J., Baldwin, P. R., and Chiu, W. (1999) EMAN: semiautomated software for high-resolution single-particle reconstructions, *J Struct Biol 128*, 82-97.

191. Frank, J., Radermacher, M., Penczek, P., Zhu, J., Li, Y., Ladjadj, M., and Leith, A. (1996) SPIDER and WEB: processing and visualization of images in 3D electron microscopy and related fields, *J Struct Biol 116*, 190-199.
192. Reyrat, J. M., Lanzavecchia, S., Lupetti, P., de Bernard, M., Pagliaccia, C., Pelicic, V., Charrel, M., Ulivieri, C., Norais, N., Ji, X., Cabiaux, V., Papini, E., Rappuoli, R., and Telford, J. L. (1999) 3D imaging of the 58 kDa cell binding subunit of the Helicobacter pylori cytotoxin, *J Mol Biol 290*, 459-470.
193. Wang, H. J., and Wang, W. C. (2000) Expression and binding analysis of GST-VacA fusions reveals that the C-terminal approximately 100-residue segment of exotoxin is crucial for binding in HeLa cells, *Biochem Biophys Res Commun 278*, 449-454.
194. Lupetti, P., Heuser, J. E., Manetti, R., Massari, P., Lanzavecchia, S., Bellon, P. L., Dallai, R., Rappuoli, R., and Telford, J. L. (1996) Oligomeric and subunit structure of the Helicobacter pylori vacuolating cytotoxin, *J Cell Biol 133*, 801-807.
195. Ye, D., and Blanke, S. R. (2002) Functional complementation reveals the importance of intermolecular monomer interactions for Helicobacter pylori VacA vacuolating activity, *Mol Microbiol 43*, 1243-1253.
196. Szabo, I., Brutsche, S., Tombola, F., Moschioni, M., Satin, B., Telford, J. L., Rappuoli, R., Montecucco, C., Papini, E., and Zoratti, M. (1999) Formation of anion-selective channels in the cell plasma membrane by the toxin VacA of Helicobacter pylori is required for its biological activity, *EMBO J 18*, 5517-5527.
197. Tombola, F., Oregna, F., Brutsche, S., Szabo, I., Del Giudice, G., Rappuoli, R., Montecucco, C., Papini, E., and Zoratti, M. (1999) Inhibition of the vacuolating and anion channel activities of the VacA toxin of Helicobacter pylori, *FEBS Lett 460*, 221-225.
198. Molinari, M., Galli, C., de Bernard, M., Norais, N., Ruysschaert, J. M., Rappuoli, R., and Montecucco, C. (1998) The acid activation of Helicobacter pylori toxin VacA: structural and membrane binding studies, *Biochem Biophys Res Commun 248*, 334-340.
199. Loh, J. T., Shaffer, C. L., Piazuelo, M. B., Bravo, L. E., McClain, M. S., Correa, P., and Cover, T. L. (2011) Analysis of cagA in Helicobacter pylori Strains from Colombian Populations with Contrasting Gastric Cancer Risk Reveals a Biomarker for Disease Severity, *Cancer Epidemiol Biomarkers Prev*.
200. Handt, L. K., Fox, J. G., Stalis, I. H., Rufo, R., Lee, G., Linn, J., Li, X., and Kleanthous, H. (1995) Characterization of feline Helicobacter pylori strains and associated gastritis in a colony of domestic cats, *J Clin Microbiol 33*, 2280-2289.
201. Gonzalez-Rivera, C., Gangwer, K. A., McClain, M. S., Eli, I. M., Chambers, M. G., Ohi, M. D., Lacy, D. B., and Cover, T. L. (2010) Reconstitution of Helicobacter pylori VacA toxin from purified components, *Biochemistry 49*, 5743-5752.
202. de Bernard, M., Cappon, A., Del Giudice, G., Rappuoli, R., and Montecucco, C. (2004) The multiple cellular activities of the VacA cytotoxin of Helicobacter pylori, *Int J Med Microbiol 293*, 589-597.

203. Fischer, W., Prassl, S., and Haas, R. (2009) Virulence mechanisms and persistence strategies of the human gastric pathogen Helicobacter pylori, *Curr Top Microbiol Immunol 337*, 129-171.
204. Jones, K. R., Whitmire, J. M., and Merrell, D. S. (2010) A Tale of Two Toxins: Helicobacter Pylori CagA and VacA Modulate Host Pathways that Impact Disease, *Front Microbiol 1*, 115.
205. Strobel, S., Bereswill, S., Balig, P., Allgaier, P., Sonntag, H. G., and Kist, M. (1998) Identification and analysis of a new vacA genotype variant of Helicobacter pylori in different patient groups in Germany, *J Clin Microbiol 36*, 1285-1289.
206. McClain, M. S., and Cover, T. L. (2003) Expression of Helicobacter pylori vacuolating toxin in Escherichia coli, *Infect Immun 71*, 2266-2271.
207. Atherton, J. C., Peek, R. M., Jr., Tham, K. T., Cover, T. L., and Blaser, M. J. (1997) Clinical and pathological importance of heterogeneity in vacA, the vacuolating cytotoxin gene of Helicobacter pylori, *Gastroenterology 112*, 92-99.
208. Jimenez-Soto, L. F., Rohrer, S., Jain, U., Ertl, C., Sewald, X., and Haas, R. (2012) Effects of cholesterol on Helicobacter pylori growth and virulence properties in vitro, *Helicobacter 17*, 133-139.
209. Schmidt, T. G., and Skerra, A. (2007) The Strep-tag system for one-step purification and high-affinity detection or capturing of proteins, *Nat Protoc 2*, 1528-1535.
210. Jin, Z. X., Huang, C. R., Dong, L., Goda, S., Kawanami, T., Sawaki, T., Sakai, T., Tong, X. P., Masaki, Y., Fukushima, T., Tanaka, M., Mimori, T., Tojo, H., Bloom, E. T., Okazaki, T., and Umehara, H. (2008) Impaired TCR signaling through dysfunction of lipid rafts in sphingomyelin synthase 1 (SMS1)-knockdown T cells, *Int Immunol 20*, 1427-1437.
211. De Colibus, L., Sonnen, A. F., Morris, K. J., Siebert, C. A., Abrusci, P., Plitzko, J., Hodnik, V., Leippe, M., Volpi, E., Anderluh, G., and Gilbert, R. J. (2012) Structures of lysenin reveal a shared evolutionary origin for pore-forming proteins and its mode of sphingomyelin recognition, *Structure 20*, 1498-1507.
212. Yamaji, A., Sekizawa, Y., Emoto, K., Sakuraba, H., Inoue, K., Kobayashi, H., and Umeda, M. (1998) Lysenin, a novel sphingomyelin-specific binding protein, *J Biol Chem 273*, 5300-5306.
213. Yamaji-Hasegawa, A., Makino, A., Baba, T., Senoh, Y., Kimura-Suda, H., Sato, S. B., Terada, N., Ohno, S., Kiyokawa, E., Umeda, M., and Kobayashi, T. (2003) Oligomerization and pore formation of a sphingomyelin-specific toxin, lysenin, *J Biol Chem 278*, 22762-22770.
214. Watanabe, T., Tada, M., Nagai, H., Sasaki, S., and Nakao, M. (1998) Helicobacter pylori infection induces gastric cancer in mongolian gerbils, *Gastroenterology 115*, 642-648.
215. Tsukamoto, T., Toyoda, T., Mizoshita, T., and Tatematsu, M. (2012) Helicobacter pylori infection and gastric carcinogenesis in rodent models, *Semin Immunopathol*.
216. Noto, J. M., Gaddy, J. A., Lee, J. Y., Piazuelo, M. B., Friedman, D. B., Colvin, D. C., Romero-Gallo, J., Suarez, G., Loh, J., Slaughter, J. C., Tan, S., Morgan, D. R., Wilson, K. T., Bravo, L. E., Correa, P., Cover, T. L., Amieva, M. R., and Peek, R.

M., Jr. (2013) Iron deficiency accelerates Helicobacter pylori-induced carcinogenesis in rodents and humans, *J Clin Invest 123*, 479-492.
217. Tilley, S. J., and Saibil, H. R. (2006) The mechanism of pore formation by bacterial toxins, *Curr Opin Struct Biol 16*, 230-236.
218. Chambers, M. G., Pyburn, T. M., Gonzalez-Rivera, C., Collier, S. E., Eli, I., Yip, C. K., Takizawa, Y., Lacy, D. B., Cover, T. L., and Ohi, M. D. (2012) Structural Analysis of the Oligomeric States of Helicobacter pylori VacA Toxin, *J Mol Biol*.